QUALITATIVE AND QUANTITATIVE INFRARED SPECTROSCOPY OF SELECTED NEW MEXICO COAL

by

John H. Dooley

Submitted in Partial Fulfillment
of the Requirements for the Degree of
Master of Science in Geoscience

New Mexico Institute of Mining and Technology

Socorro, New Mexico
December, 1983

ABSTRACT

Seven whole coals, principally New Mexico coals, have been qualitatively and quantitatively characterized by dispersive infrared spectroscopy. The position of certain characteristic absorption band maxima shifts by as much as 20 cm^{-1}. In addition systematic variations in band shape occur with rank changes. The seven whole coals have been chemically demineralized in order to determine qualitatively the effects mineral species have on the absorption bands of the seven whole coals.

Plotting absorptivity at a particular frequency as a function of various physio-chemical parameters reveals systematic variations in absorptivity generally parallel changes in rank. Linear relationships between absorptivity and various physio-chemical parameters characterize significant variations in the substituents that occur as a function of rank in whole coals. Absorption bands ascribed to aliphatic, alicyclic, and aromatic hydrogen functionalities generally are a complex function of the hydrogen content. Some of the relationships with high correlations (r ranging from ± 0.995 to 0.864) for the whole coals heretofore have never been reported in the literature.

Plots of absorptivity at a particular frequency as a function of absorptivity at a different frequency reveal many modes vary in a systematic fashion with rank suggesting much of the data are not independent but related in some fashion. Commercially important

properties of whole coals can be rapidly characterized from the chemical and structural information provided by qualtitative and quantitative analyses of infrared spectra of whole coals, thus permitting optimum utilization of each coal.

Table of Contents

List of Tables

List of Figures

ACKNOWLEDGEMENT

The author expresses gratitude to Dr. Frederick J. Kuellmer for his supervision of this study. David E. Tabet, Stephen J. Frost, and Dr. Kuellmer kindly provided the coal samples used in this study. A feeling of sincere appreciation is also extended to Dr. Jacques Renault and the New Mexico Bureau of Mines and Mineral Resources for providing the cryogenic grinder, hydraulic press, and laboratory facilities. Dr. Kay R. Brower of the Chemistry Department graciously allowed the author to use the infrared spectrophotometer and laboratory facilities. James Brannen is gratefully acknowledged for his assistance with the drafting. Finally, the author dearly thanks his family for their endless encouragement, understanding, support, and love. This study was supported by a grant (G1124125) from the State Mining and Mineral Resources Research Institute.

INTRODUCTION

There has been a growing and sustained interest in coals since the OPEC (Oil Producing and Exporting Countries) oil embargoes in 1973. Coals have a high relative abundance and wide geographical distribution thus making coals attractive as a preferred feedstock for the production of synthetic fuels.

Dispersive infrared spectroscopy has traditionally been an important tool in fuel characterization since most organic and mineral components absorb in the infrared region. Quantitative infrared spectroscopy offers valuable information on the chemical composition of coal. Quantitative use of the spectra provides a sort of functional group analysis of complex organic material, such as coal. The principal advantages of quantitative infrared spectroscopy are that the coal can be characterized as a whole, without destructive treatment, and that a very small amount of coal is sufficient for the analysis.

The work reported here qualitatively and quantitatively characterizes the structure of seven selected whole coals, principally New Mexico coals, covering a range of rank. Information concerning the structure of the seven whole coals as a function of rank includes a qualitative determination of the molecular types of hydrocarbons present, i.e. alipahtic and aromatic, and the type and distribution of specific functional groups, e.g. aliphatic C-H, phenolic OH, and

carbonyl modes. With these data it is possible to establish an evolutionary sequence for the functionalities in the selected high volatile and medium volatile bituminous whole coals studied. Oxygen-containing functionalities influence the behavior of whole coals during gasification, liquefaction, coke production, and carbonization processes (Durie, 1982; Rouxhet et al., 1980). Infrared spectra offer a valuable tool for investigating the molecular type and distribution of oxygen-containing functionalities in whole coals. Coal-structure characterization using infrared spectroscopy can be useful for evaluating the hydrocarbon potential of the corresponding sediment (Rouxhet et al., 1980).

FUNDAMENTALS OF INFRARED SPECTROSCOPY

Introduction

Detailed accounts of theoretical and applied infrared spectroscopy are numerous in the literature (Smith, 1979; Conley, 1972; Alpert et al., 1970; and Potts Jr., 1963). Infrared spectroscopy is similar to other absorption measurements in that a specimen thin enough to be highly transparent to the incident radiation is immersed in an infrared beam. The infrared beam is absorbed at certain wavelengths as a function of the properties of the chemical bonds and the numbers of those bonding types. The infrared region used for this study lies in the 2.5 to 20 micron wavelength range. For this paper the common convention of expressing the radiant energy in terms of wavenumber rather than wavelength will be followed. Wavenumber is the reciprocal of wavelength and commonly expressed in units of cm^{-1}.

Selective absorption at certain frequencies in the electromagnetic spectrum is displayed by most organic and many inorganic substances. These absorption bands occur because quanta of energy are absorbed when the atoms of a molecule show any relative movement that is accompanied by an electrical dipole moment change. The frequencies proportional to the energy of radiation corresponding to the quanta of energy absorbed in molecular vibration or rotation lie in the infrared region of the electromagnetic spectrum. The precise frequencies are a function of the

masses of the constituent atoms, the strength of the binding forces, and the geometrical configuration of the molecule in space. Any vibration that involves a change in the relative positions of the positive and negative centers of molecules with respect to the molecular center of gravity will cause a change in the dipole moment of the molecule as it vibrates.

The magnitude of the absorption due to a given species is directly related to the concentration of that species and on the change in electric moment associated with the vibration in question. The intensity of the corresponding infrared absorption band is proportional to the square of the rate of change of electrical dipole moment during the vibration. Thus absorption intensity is proportional to the amount of a given constituent present in the sample.

Qualitative Spectrophotometry

Absorption bands occurring at certain frequencies can be correlated with specific groupings of atoms which are common in molecules by comparing spectra of large numbers of pure compounds. The absence of a particular absorption band in the unmodified sample permits the definite conclusion that this group is either not present or is present only in such a small concentration that it cannot be observed. This feature and the possibility of detecting structural differences has led to the use of infrared spectra as a means of attacking problems of molecular

structure.

Bouguer-Beer Law

The Bouguer-Beer law is used in practically all absorption analysis. The Bouguer-Beer law is stated in the following ways:

$$A = \log I_o/I = -\log T = \log (1/T) = abc \quad (1)$$

where A is the absorbance; I_o represents the total radiant energy of the incident beam; I is the transmitted radiant energy after passage through the sample; T is transmittance; a is the absorption coefficient in cm^2/mg; b is the optical path length (or pellet thickness) of the sample in centimeters; and c is the concentration of the absorbing species in mg/cm^3. Figure 1 shows a comparison of absorbance and transmission scales.

In this study it is recognized that absorbance is not merely a factor of the variables in equation 1 but is related to the concentration of coal in the pellet. Therefore, equation 1 can be written as:

$$A = a\ b\ c_s c_c \quad (2)$$

where A is the absorbance; a is the absorption coefficient; b is the optical path length; c_s is the concentration of the absorbing species;

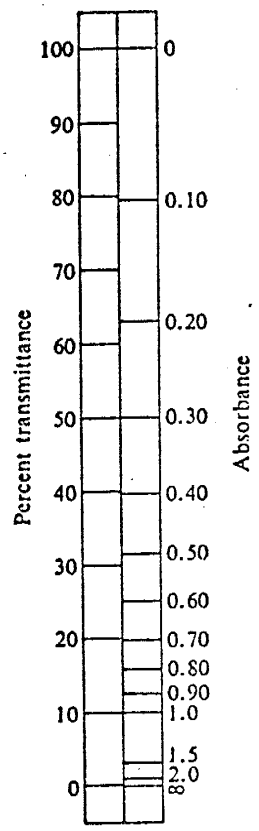

Figure 1. Comparison of absorbance and transmission scales.
(From: Conley, 1972)

and c_c is the concentration of the coal in the pellet. Absorbance, optical path length (pellet thickness), and concentration of coal in the pellet are measured values while the absorption coefficient and concentration of the absorbing species remain as unknowns. Henceforth the product of the absorption coefficient and concentration of absorbing species, i.e. ac_s, shall be simply referred to as absorptivity (a) in this study.

Presently it is not possible to effectively evaluate the effects of changing the absorption coefficient, or the concentration of absorbing species, or both over a range of rank. For example, if the absorption coefficient is not constant over a range of rank, then a change in the absorption coefficient produces a change in the absorbance without changing the concentration of the absorbing species. Currently, there is no satisfactory means to determine the nature of these changes.

Infrared Spectra of Complex Organic Solids

The infrared spectra of complex organic solids show a limited number of rather broad bands which are due to well-known chemical groups. These broad bands can be correlated by comparison with the spectra of numerous simple substances (Rouxhet et al., 1980).

Coals have the same types of bonds as kerogens, humic substances, chars, and other natural polymers. For this reason the possibility of having a fingerprint, or unique set of absorption bands, doesn't occur. The real utility of infrared spectroscopy of complex organic solids rests in the fact that the spectra differ from each other by the intensity of the various bands. For example, the spectra of coals change regularly in absorption intensity according to rank and reflect the major chemical modifications occurring as coalification proceeds (Rouxhet et al., 1980).

MATERIALS

Seven coals, listed in Table 1, of various ages and locality were studied. Five of the seven coals are from New Mexico, one coal is from Illinois (Herrin 6), and one coal is from Nova Scotia. The coal samples from Illinois and Nova Scotia were chosen as reference samples. The age of the coals from Illinois and Nova Scotia is Pennsylvanian and those of New Mexico are Cretaceous. All the coals studied are typical of humic coals of North America, that is rich in vitrinite.

Proximate-analysis data on an as received basis are reported in Table 2. The ultimate analysis on an as received and dry, ash-free (daf) basis (or inorganic-matter-free basis) are indicated in Tables 3I and 3II, respectively. Proximate and ultimate analyses of Coals 1, 2, 3 and 7 were performed by the Commercial Testing and Engineering (CTE) Company. Proximate and ultimate analyses of Coal 4 were performed by the United States Geological Survey (USGS), and for Coals 5 and 6 by Hazen Research, Inc.

The seven coals were selected for this study on the basis of the range in composition among the coals available to us (see Tables 2 and 3). The coal rank ranges from sub-bituminous B (DT 47772) to low volatile bituminous (DT 46772).

TABLE 1

Geologic Data and Sample Locality of Specimens Studied

Sample: Coal 1

Specimen number: DT 47772

Locality: Sandoval County, New Mexico

Geologic formation: Mesaverde Group

Geologic age: Upper Cretaceous

Kind of sample: channel sample

Specimen location: unnamed coal bed, Una del Gato Field SW, NW, Sec. 17, T.13N., R.6E., New Mexico.

Sample: Coal 2

Specimen number: DT 42771

Locality: Bernalillo County, New Mexico

Geologic formation: Mesaverde Group

Geologic age: Upper Cretaceous

Kind of sample: channel sample

Specimen location: upper seam, Canoncito Mine SE, SW, NE, Sec. 8, T.10N., R.2W., New Mexico.

Sample: Coal 3

Specimen number: DT 418771-A

Locality: McKinley County, New Mexico

Geologic formation: Crevasse Canyon Formation

Geologic age: Upper Cretaceous

Kind of sample: channel samples

Specimen location: Green Seam, Gibson member, McKinley Mine SW, NW, Sec.6, T.16N., R.20W., New Mexico.

Sample: Coal 4

Specimen number: Nm-Tm

Locality: Bernalillo County, New Mexico

Geologic formation: Crevasse Canyon Formation

Geologic age: Upper Cretaceous

Kind of sample: grab sample

Specimen location: unnamed coal bed, Tijeras Coal Field, Tocco Mine, New Mexico.

Sample: Coal 5

Specimen number: C-80

Locality: Illinois

Geologic formation: ??

Geologic age: Pennsylvanian

Kind of sample: composite sample

Sample location: Herrin 6, Eagle Surface Mine, Illinois.

Sample: Coal 6

Specimen number: C-16

Locality: Nova Scotia

Geologic formation: ??

Geologic age: Pennsylvanian (Westphalian D)

Kind of sample: abandoned stockpile

Sample location: Hub Seam, Prince Mine, Nova Scotia.

Sample: Coal 7

Specimen number: DT 46772

Locality: Sierra County, New Mexico

Geologic formation: Mesaverde Group

Geologic age: Upper Cretaceous

Kind of sample: abandoned stockpile

Sample location: south of Engle Field, mine working, NE, NW, SE, Sec. 12, T.14S., R.4W., New Mexico.

TABLE 2

Proximate Analysis of Coal Specimens Studied on as Received Basis

Sample Number	Specimen Number	Fixed Carbon	Volatile Matter	Moisture	Ash	Calorific Value (BTU/lb)
Coal 1	DT 47772	40.16%	39.23%	9.47%	11.14%	8257
Coal 2	DT 42771	46.46%	38.46%	7.28%	7.80%	9361
Coal 3	DT 418771-A	50.20%	38.16%	3.99%	7.65%	11918
Coal 4	Nm-Tm	51.2%	26.3%	1.1%	21.4%	11469
Coal 5	C-80	53.65%	37.81%	1.51%	7.03%	13783
Coal 6	C-16	58.30%	34.01%	3.77%	3.92%	13220
Coal 7	DT 46772	66.15%	13.35%	0.63%	19.87%	11825

TABLE 3I

Ultimate Analysis on As Received Basis of the Coals Studied

Sample Number	Specimen Number	Carbon	Hydrogen	Nitrogen	Sulfur	Chlorine	Oxygen*
Coal 1	DT 47772	54.29%	3.25%	1.25%	0.36%	0.09%	20.15%
Coal 2	DT 42771	59.97%	3.83%	1.21%	0.78%	0.06%	19.07%
Coal 3	DT 418771-A	68.13%	4.82%	1.16%	0.42%	0.04%	13.73%
Coal 4	Nm-Tm	64.9%	4.5%	1.1%	0.5%	n.d.	6.5%
Coal 5	C-80	76.62%	5.31%	1.41%	1.95%	n.d.	6.17%
Coal 6	C-16	74.58%	4.97%	1.48%	2.33%	n.d.	8.95%
Coal 7	DT-46772	68.19%	3.46%	0.88%	0.52%	0.06%	6.39%

* oxygen determined by difference.

n.d. = not determined.

TABLE 3II

Ultimate Analysis on Dry, Ash-Free Basis of the Coals Studied

Sample Number	Specimen Number	Carbon	Hydrogen	Nitrogen	Sulfur	Chlorine	Oxygen*
Coal 1	DT 47772	68.39%	4.09%	1.57%	0.46%	0.11%	25.38%
Coal 2	DT 47771	70.62%	4.51%	1.42%	0.92%	0.07%	22.46%
Coal 3	DT 418771-A	77.10%	5.46%	1.32%	0.47%	0.04%	15.61%
Coal 4	Nm-Tm	83.7%	5.8%	1.4%	0.7%	n.d.	8.4%
Coal 5	C-80	83.77%	5.80%	1.55%	2.13%	n.d.	6.75%
Coal 6	C-16	80.79%	5.38%	1.60%	2.53%	n.d.	9.70%
Coal 7	DT 46772	85.77%	4.35%	1.11%	0.66%	0.06%	8.05%

* oxygen determined by difference.

n.d. = not determined.

METHODS

Individual bulk coal samples are gently crushed with a steel, impact mortar until all the material passes a 20-mesh screen (0.850 mm opening). The nest of sieves used for size fractionation of the individual coals is used exclusively for coals. Cone-and-quartering of the less than 20-mesh material is employed to obtain a 5 gram aliquot of the material.

The 5 gram aliquot is placed in a cryogenic grinder (SPEX Freezer/Mill) with a small, steel grinding rod. The sealed grinding unit is then immersed in a liquid nitrogen (boiling pt. -195.8°C) bath. Several minutes of waiting are required to lower the temperature of the coal sample to that of the liquid nitrogen. Then the coal sample is pulverized to a fine powder by the percussive action of the small, steel grinding rod. A six minute grinding time is used for each 5 gram aliquot. Solomon and Mains (1977) discuss the advantages cryocrushing of coal has over conventional grinding processes.

The finely pulverized coal sample is placed in a silica-gel-filled desiccator to dry at room temperature for two days. The dried, pulverized coal sample is sieved using a 325-mesh (0.045 mm opening) screen and pan. The material passing the 325-mesh screen is stored in a silica-gel-filled desiccator at room temperature for five days.

Twenty grams of potassium bromide (KBr) is ground with an agate pestle in a hand-operated agate mortar until a coarse KBr powder is attained. The coarsely ground KBr is stored in a silica-gel-filled desiccator to dry at room temperature for seven days.

An aliquot of the finely pulverized, dry coal is added to approximately five times (by weight) the amount of coarsely ground, dry KBr powder, and the two components are ground together in a hand-operated agate mortar. Further addition of coarsely ground, dry KBr is made in fractional amounts to the finely ground material already in the agate mortar. For each coarsely ground, dried KBr addition to the mixture, the mixture must be finely ground before another fraction is added. This insures a homogeneous distribution of coal in the KBr. Coal concentration in KBr is characteristically on the order of one weight percent (see Appendix 1).

The finely powdered mixture of coal and KBr is again dried in the silica-gel-filled desiccator at room temperature for six days. Approximately 0.100 gram aliquot of the finely pulverized, dried coal-KBr mixture is added to a stainless-steel evacuable die and pressed into a pellet. The coal-KBr mixture aliquot is pressed at 6804 kg/cm^2 (1.50×10^4 lbs/cm^2) under vacuum for 5 minutes. The resultant pellet is 13 mm in diameter. Two pellets are pressed from the finely pulverized, dried coal-KBr mixture for each coal sample with the only exception being Coal DT 46772 in which three pellets are pressed. The

pellets are dried in a silica-gel-filled glass desiccator at room temperature for seven days. Robin and Rouxhet (1976) suggest that storing the pellets in a desiccator for one week is useful as a standard drying procedure, particularly when optimum quantitative data are desired.

The dried coal-KBr pellets are weighed on an analytical balance just prior to recording the infrared spectra on a Perkin-Elmer 421 double-beam infrared grating spectrophotometer which is calibrated with a polystyrene film. The dried pellets are scanned every five days on the Perkin-Elmer 421 spectrophotometer to obtain three infrared spectra for each pellet of each coal. The infrared spectra are recorded in transmittance (%T) and converted to absorbance (A).

Consistent instrumental conditions were used for all spectral analyses. The following instrumental conditions are employed for recording infrared spectra:

Scan time ≈ 11 minutes

Suppression = 6

Expansion = 1X

Attenuator speed = 1100

Amplifier gain ≈ 5.9

Slit program = 1000

Source current = 0.3 amp

Scan range = 4000 cm^{-1} to approx. 550 cm^{-1}.

These spectrograph conditions are set to yield undeformed spectra allowing computation of band intensities.

The thickness (b) of each coal-KBr pellet is measured using a metric micrometer having 0.001mm precision subsequent to the recording of the spectra. Data for the whole coal-KBr pellets are reported in Appendix 1.

CHEMICAL DEMINERALIZATION PROCEDURES

Chemical demineralization of coal was accomplished by using HF-HCl acids. Presumably, dissolution of many mineral phases in coal occurs upon HF-HCl acid treatments while modifications in the chemical composition of the coal are held to a minimum (Durand and Nicaise, 1980).

An aliquot of finely pulverized (<325 mesh) coal sample is placed in a polymethylpentene (PMP) beaker. To the beaker 4N HCl is added so that the coal is totally immersed in the HCl solution. The HCl-coal mixture is heated for about 2 hours at 70° C. Carefully decant off the HCl liquor. Add enough 4N HCl-40% HF solution in proportion 1:2 to completely immerse the coal sample in the beaker, and react this mixture for about 2 hours at 70°C. Decant off the 4N HCl-40% HF liquor. The coal sample is submitted to repeated treatments at 70°C by 4N HCl and subsequently by a mixture of 4N HCl-40% HF in proportion 1:2 until no apparent reaction occurs. The procedure was repeated 4 to 5 times dependent on the amount of mineral matter in the coal. The coal sample is washed thoroughly by distilled water. The coal sample is dried for 1 hour at 100°C.

Demineralized coal-KBr pellets are pressed and dried according to the procedures described above. The demineralized coal-KBr pellets are scanned using the same instrumental conditions used for the whole

coal-KBr pellet scans. Data for the demineralized coal-KBr pellets are indicated in Appendix 2.

Chemical demineralization of four coals is used qualitatively to determine the contribution mineral matter has on infrared spectral features observed in our selected whole coal samples. The utility of chemical demineralization of the coals in this study is that a greater amount of confidence is gained in the band assignments, particularly in regions where mineral matter absorptions interfere with absorptions attributable to organic functionalities, e.g. the 1100-1000 cm^{-1} region.

METHOD USED TO MEASURE ABSORPTION ON INFRARED SPECTRA

A general method employing peak heights for quantitative determination of absorbance is referred to as the baseline method. This method yields a value for the absorbance directly.

The baseline method consists simply of sketching an arbitrarily chosen line to represent the base line of the absorption band. The choice of a baseline, Figure 2, depends on the absorption characteristics of other components in the coal. In all cases the baseline drawn is chosen on the basis of the relative reproducibility of the points from which the baseline is constructed from among the spectra being compared (Conley, p. 228, 1972). Though the baseline selection procedures are arbitrary they permit comparisons among coal samples. The sample standard deviation of the absorptivities measured for a given band of a given sample is on the order of a few percent (see Appendix 4), which indicates a satisfactory reproducibility of the measurements.

The absorbance of the OH stretching band centered around 3300 cm^{-1} is determined by drawing the baseline from 3700 cm^{-1} to the apex at approximately 3000 cm^{-1} adjacent to the CH stretching band, shown in Figure 3. Henceforth this baseline selection procedure for the OH stretching region will be referred to as the 3700-3000 cm^{-1} method. An alternative method, described by Robin and Rouxhet (1976), draws the baseline over the broad spectral range between 3700 cm^{-1} to 2500 cm^{-1}.

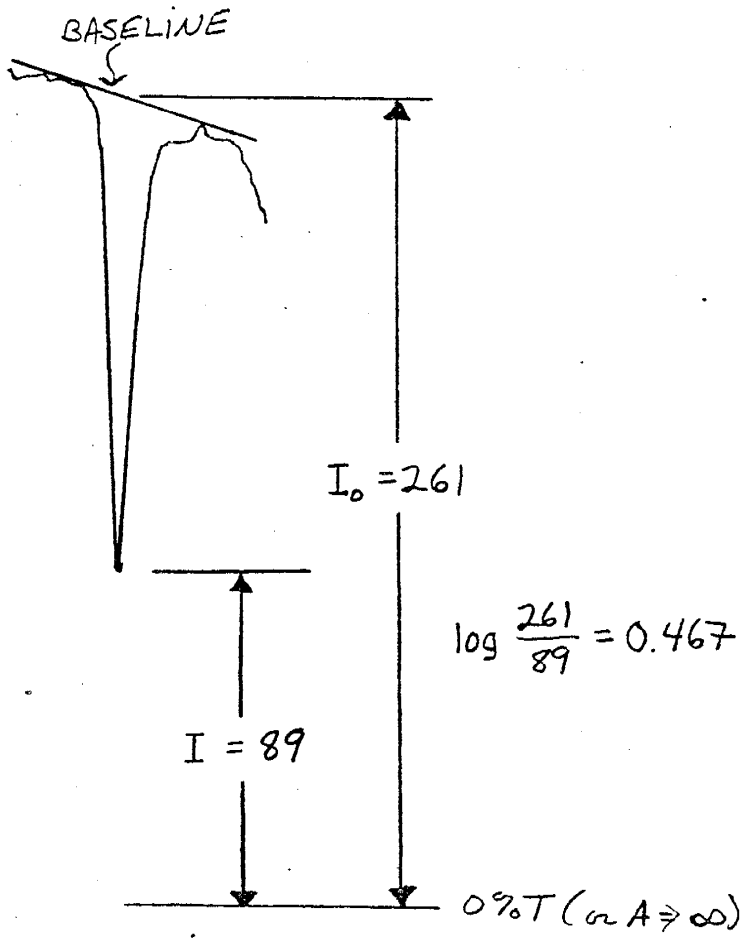

Figure 2. Baseline and absorbance measurement technique employed in this study. I_o is the radiant energy incident upon the sample and I represents the radiant energy transmitted by the sample, equation 1.

Fig 3

page 24

Henceforth this alternative baseline selection method will be referred to as the Robin-Rouxhet method. For each method the absorbance is measured at the band height maximum occurring around 3400 cm^{-1}.

ABSORBANCE MEASUREMENT PROCEDURE

The absorbance of an absorption band is determined after the baseline is established. The absorption band measurement procedure adopted for this study is illustrated in Figure 2. The vertical distance from the baseline through the absorption band maximum to the 0% T point on the spectrogram is measured using a millimeter scale. This value, I_o , represents the radiant energy incident upon the sample. The vertical distance from the absorption band maximum to the 0% T point on the spectrogram is measured using a millimeter scale, and this value, I, represents the radiant energy transmitted by the sample. The absorbance is then calculated by employing equation (1).

It is well established that the baseline of coal absorption spectra ascends from low wavenumber to the high, particularly from 2000 to 4000 cm^{-1} (see Fig. 3). This phenomenon is attributed to increased scattering of the radiation as the radiation wavelength approaches the particle size. The slope of the baseline also increases as rank increases. These baseline slope variations resulting from unspecific background absorption need be considered when the measured absorption band of one coal of a particular rank is compared to the same measured absorption band of a coal of different rank. In order to overcome these baseline variations the measured absorbance values are normalized to a common reference baseline, arbitrarily set at I_o = 354 units on a metric scale, which corresponds to 90.4% T (or A of background = 0.044).

Normalizing the measured absorption band intensities to a standard baseline (in this case 90.4% T) facilitates the comparison of magnitudes of absorption band intensities within one particular coal or among various coals or both.

It is well established that grinding KBr, a hygroscopic substance, promotes the adsorption of water on to the surface of the pulverized KBr. This adsorbed water ubiquitous in KBr pellets dried at room temperature absorbs infrared radiation and thus contributes to the 3400 and 1600 cm^{-1} absorption bands. The contribution of OH absorptions from the adsorbed water in the KBr pellets must be subtracted from the measured total absorbance near 3400 and 1600 cm^{-1}. Subtracting the absorption that results from the adsorbed water in the KBr pell ets from the measured total absorbance yields the absorbance from the whole coal.

Briefly, the procedure followed to correct for this adsorbed water in the KBr pellets is described below. An aliquot of the finely pulverized, desiccator-dried KBr was pressed into six pellets consisting entirely of KBr. The six KBr pellets, each having a different thickness and hence concentration, were dried according to the procedure described above. Employing the instrumental conditions described in the preceeding section, each pellet was scanned twice from 4000 to approximately 550 cm^{-1}. Each KBr pellet was stored in a desiccator at room temperature for 5 days between spectral scans. The absorbances near 3400 and 1600 cm^{-1} were measured and normalized to the reference

baseline as described above. Figure 4 shows the result of plotting the normalized measured absorbance (Acorr) at 3400 cm^{-1} as a function of the pellet thickness (b) in centimeters and KBr concentration (c) in gm/cm^3. The slope of the linear correlation line in Figure 4 defines the absorptivity coefficient (a = 0.1950 cm^2/mg) at 3400 cm^{-1} of the KBr. Given the weight of KBr in a whole coal-$K_3Fe(CN)_6$-KBr pellet, the total pellet weight (see Appendix 1), and the density of the KBr (ρ = 2.717 gm/cm^3), the product of thickness (b) multiplied by KBr concentration (c) of a given pellet consisting entirely of KBr can be readily calculated. The normalized absorbance (Acorr) at 3400 cm^{-1} resulting from the water adsorbed on the KBr in the whole coal-$K_3Fe(CN)_6$-KBr pellet then can be calculated using: $Acorr = 0.1950\ (b_{KBr})(c_{KBr})$. Knowing the contribution water adsorbed on the KBr has on the measured total absorbance of the whole coal-$K_3Fe(CN)_6$-KBr pellet allows one to substract this contribution from the measured total absorbance thus leaving the absorbance resulting from the coal. The same procedure was followed to correct for water (OH) absorptions near 1600 cm^{-1}. The normalized absorbance near 1600 cm^{-1} resulting from OH absorptions associated with the KBr was calculated using: $Acorr = 0.1010\ (b_{KBr})(c_{KBr})$. All the absorptivity values for 3400 and 1590 cm^{-1} listed in Appendices 3 and 4 and plotted at 3400 and 1590 cm^{-1} have been corrected for this OH absorbance.

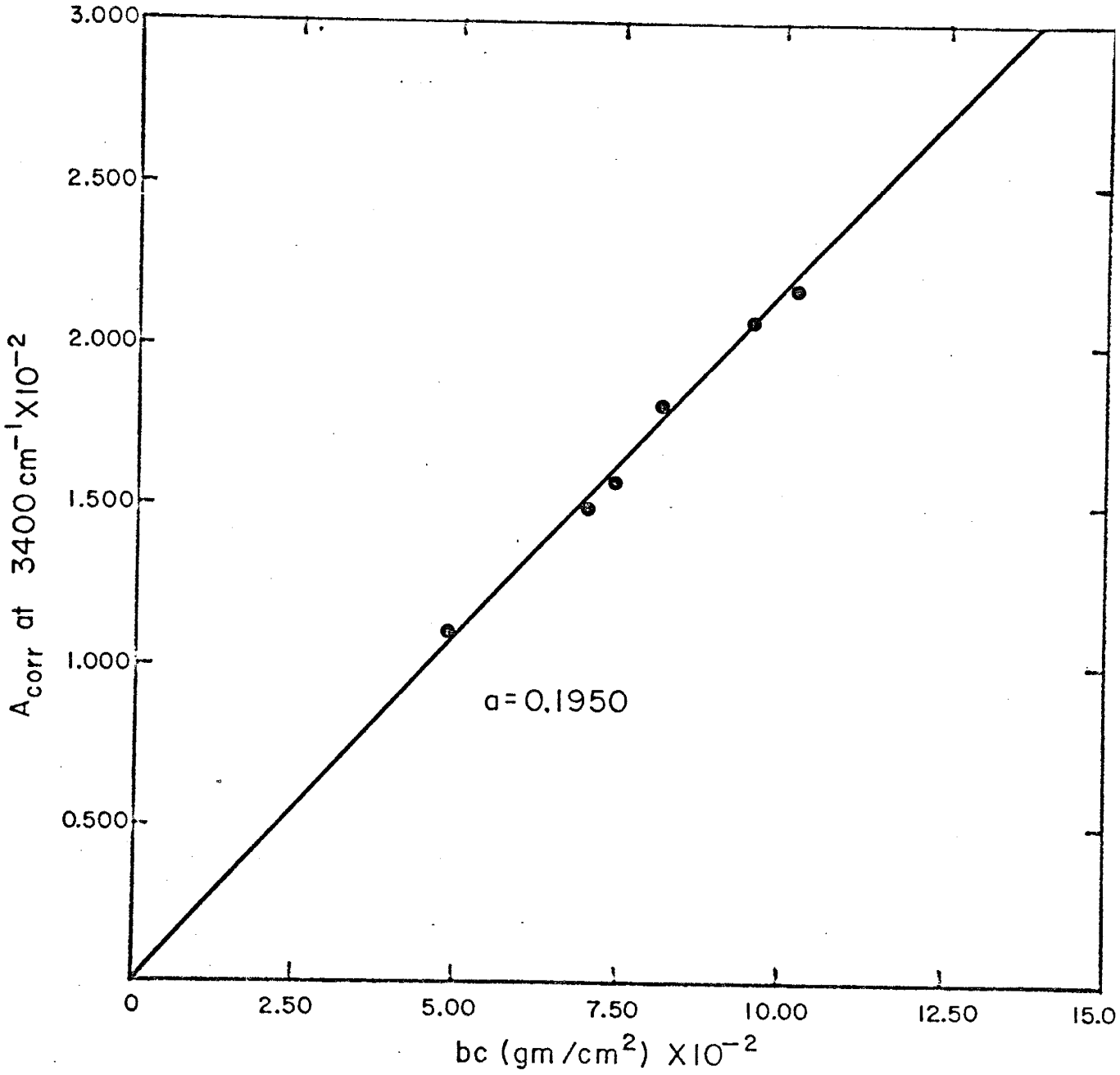

Figure 4. Absorbance (Acorr) at 3400 cm-1 of pellets consisting entirely of KBr normalized to a common baseline, described on page , as a function of the product of pellet thickness (b) and KBr concentration (c). Absorptivity (a) at 3400 cm-1 for the KBr pellets studied is 0.1950 cm^2/mg.

Potassium ferricyanide ($K_3Fe(CN)_6$) was used as an internal standard to calibrate the position of the absorption bands in the infrared spectra of the whole coals only. The well resolved absorption peak at 2117 cm^{-1} in Figure 3 results from C≡N deformational modes characteristic of the cyanide component of the potassium ferricyanide. Calibration of the infrared spectrophotometer with a polystyrene film in addition to the constant position of the C≡N absorption peak at 2117 cm^{-1} permits a precise measurement of the position of each absorption band in the spectra of the whole coals studied.

QUALITATIVE ANALYSIS OF WHOLE COAL INFRARED SPECTROGRAMS

Introduction

Qualitative applications of infrared spectroscopy arise from the observation that many atomic groupings, such as

$$>O\text{-}H, \qquad >C{=}O, \qquad -\overset{\overset{H}{|}}{\underset{\underset{H}{|}}{C}}-$$

and larger groups, exhibit absorption bands at positions mainly independent of the rest of the molecule; these absorption bands are referred to as the characteristic frequencies of the group, or simply group frequencies. Group frequencies are vibrations that are associated with certain structural units. This concept of group frequencies may appear to be in conflict with the concept concerning vibrations of molecules, that is, a molecule vibrates as a unit and the vibration of one part of the molecule cannot be considered to be isolated from the vibrations of other parts. Nevertheless, the approximate constancy of position of group frequencies has been well established and forms the basis for the structural analysis of compounds (Alpert et al., 1970). The appearance and analysis of absorption spectra can often be used to determine or verify the spatial configuration of the atoms within a molecule (Friedel and Queiser, 1966).

Infrared spectra of coals have absorption bands characteristic of well defined molecular groups and chemical bonds. In Table 4, a survey of the positions of characteristic infrared absorption bands and their assignments by various authors is presented.

A qualitative description of discernible absorption band characteristics, such as band shape, position, intensity, and occurrence in a particular coal, is presented for each coal in the following pages.

The terms resolution, distinct, strong, medium, and weak are used to describe absorption band character qualitatively. Each descriptive term is defined below.

Resolution is a qualitative term describing the physical appearance and development of absorption bands. Generally, sharp absorption bands, i.e. absorption peaks, are referred to as being well resolved, whereas broader, more dispersed absorption bands (as opposed to absorption peaks) are referred to as moderately resolved or poorly resolved. Resolution implies nothing about absorption band symmetry.

Distinct refers to an absorption band that is clearly separated from other absorption bands in the vicinity. The term distinct is used when there is no doubt an absorption band exists.

The terms strong, medium, and weak, used to describe absorption band intensity, are qualitative statements of the absorption magnitude.

TABLE 4

Survey of the Positions of Characteristic Infrared Absorption Bands and Their Assignments.

Band Position (cm^{-1})	Assignment	References
3700	Kaolin, minerals	Murchison (1966); Farmer (1974); Van der Marel and Beutelspacher (1976); Solomon and Miknis (1980).
3600	a) minerals	a) Solomon and Miknis (1980).
	b) -OH str. (free water)	b) Robin and Rouxhet (1976); Durand (1980).
3400	a) -NH str. (N-H....N)	a) Brown (1955).
	b) -OH str. (hydroperoxide)	b) Friedel and Queiser (1956).
	c) -OH str. (phenolic -OH....O, alcoholic, carboxylic -OH)	c) Cannon and Sutherland (1945); Orchin et al. (1951); Cannon (1953); Brown (1955); van Vucht et al. (1955); Friedel and Queiser (1956); Roy (1957); Rao et al. (1962); Osawa and Shih (1971); Robin and Rouxhet (1976); Rouxhet et al. (1979); Painter et al. (1981b).
3100 to 3000	ar. -CH str.	Cannon and Sutherland (1945); Cannon (1953) Brown (1955); van Vucht et al. (1955); Friedel and Queiser (1956); Roy (1957).
2978 (sh)	$-CH_3$ str.	Durand (1980).
2955 to	$-CH_3$ str.,	Cannon and Sutherland (1945); Cannon

2855	$>CH_2$ str., al. $-CH$ str.	(1953); Brown (1955); van Vucht et al. (1955); Friedel and Queiser (1956); Roy (1957); Murchison (1976); Painter and Coleman (1979); Rouxhet et al. (1979); Durand (1980); Painter et al. (1981a,b).
1700	$>C = O$ str.	Orchin et al. (1951); Cannon (1953); Friedel and Queiser (1956); Roy (1957); Rao et al. (1962); Lowry (1963); Rao (1963); Colthump (1964); Murchison (1966); Dorrence (1974); Painter et al. (1981a,b).
1630	a) -OH def (molecular water)	a) Murray (1972); Robin and Rouxhet (1976); Painter and Coleman (1979).
	b) conjugated (hydrogen bonded carbonyls; conjugated chelated carbonyl. $>C=O....HO-$	b) Friedel (1958); Robin and Rouxhet (1976); Painter and Coleman (1979); Painter et al. (1981a,b).
	c) graphitic structures ($>C=C<$)	c) Friedel and Carlson (1972).
1600	a) -OH def. (molecular water)	a) Durie et al. (1967).
	b) $>C = O....HO-$	b) Brown (1955); Friedel and Queiser (1956); Roy (1957); Rao et al. (1962); Fujii (1963); Fujii and Tsuboi (1966); Friedel et al. (1967); Fujii et al. (1970); Painter and Coleman (1979); Painter et al. (1981a,b).
	c) ar. $>C=C<$ str.	c) Cannon and Sutherland (1945); Orchin et al. (1951); Brown (1955); van Vucht et al. (1955); Elofson (1957); Roy (1957); Pierron et al. (1959); Rao et al. (1962);

		Czuchajowski and Lawson (1963); de Ruiter and Tschamler (1966); Oberlin et al. (1974); Painter and Coleman (1979); Painter et al. (1981a,b).
1540 and 1660	a) ar. acids with hydroxyl substitution and/or quinonic groups.	a) Durand (1980).
	b) ar. $>C=C<$ str.	b) Lowry (1963).
1500	a) ar. $>C=C<$ str. with non-cyclic substituents.	a) Elofson (1957); Roy (1957); Rouxhet et al. (1979); Durand (1980); Painter et al. (1981a,b).
	b) carbonates (minerals)	b) Solomon and Miknis (1980).
1455	a) $-CH_3$ asym def, $>CH_2$ scissor.	a) Cannon and Sutherland (1945); Brown (1955); Friedel and Queiser (1956); Elofson (1957); Roy (1957); Bent et al. (1964); Osawa and Shih (1971); Durand (1980); Painter et al. (1981b).
	b) ar. $>C=C<$ str.	b) Brown (1955); Painter et al. (1981b).
1375	$-CH_3$ sym def.	Cannon and Sutherland (1945); Orchin et al. (1951); Brown (1955); van Vucht et al. (1955); Friedel and Queiser (1956); Elofson (1957); Roy (1957); Colthump et al. (1964); Durand (1980); Painter et al. (1981b).
1300 to 975	a) -C-O- str. (phenols) -OH def.	a) Brown (1955); Elofson (1957); Friedel (1958); Colthump et al. (1964); Osawa and Shih (1971); Siskov and Petrova (1974); Murchison (1976); Durand (1980); Painter et al. (1981b).

	b) C-O- str. (alcohols)	b) Brown (1955); Siskov and Petrova (1974); Durand (1980); Painter et al. (1981b).
	c) Cal-O-Cal str.	c) Brown (1955); Roy (1957); Rao (1963); Painter et al. (1981b).
	d) Car-O-Cal str.	d) Brown (1955); Friedel and Queiser (1956); Friedel (1958); Colthump et al. (1964).
	e) Car-O-Car str.	e) Cannon and Sutherland (1945); Brown (1955); Friedel and Queiser (1956); Roy (1957); Friedel (1958); Colthump et al. (1964); Osawa and Shih (1971); Durand (1980); Painter et al. (1981b).
	f) silicates carbonates (minerals)	f) Bent and Brown (1961); Murchison (1966); Farmer (1974); Van der Marel and Beutelspacher (1976).
900 to 700	a) ar C-H op def. ar skeletal vibes	a) Orchin et al. (1951); Gordon et al. (1952); Cannon (1953); Brown (1955); van Vucht et al. (1955); Friedel and Queiser (1956); Roy (1957); Friedel (1958); Colthump et al. (1964); Rouxhet et al. (1979); Durand (1980); Painter et al. (1981b).
	b) silicate minerals, carbonate minerals.	b) Farmer (1974); Van der Marel and Beutelspacher (1976); Solomon and Miknis (1980); Elliott (1981).
	c) al. $>CH_2$ rock	c) Drushel et al. (1968); Painter et al. (1981b); Kuehn et al. (1982).
720	al. $>CH_2$ def. $(CH2)_n$ $n \geq 4$	Rao (1962); Tissot and Welte (1978); Durand (1980).

al. = aliphatic; ar. = aromatic; def. = deformation; op = out of plane bending; rock = rocking mode; and str. = stretching mode. sh = shoulder -- a shoulder occurs as a prominent point of inflexion on a more intense absorption band. Absorption band is defined as a region of the absorption spectrum in which the absorbance passes through a maximum (Conley, 1972).

The 3400 cm^{-1} Band Range

This absorption band is present in all seven coal samples. The absorption band occurs as a very broad band extending from approximately 3650 cm^{-1} to 2700 cm^{-1} with an absorption maximum occurring at approximately 3380 cm^{-1}. In all seven coals, the absorption band appears to be skewed toward the low wavenumber (low frequency) side of the absorption maximum. Coals 2-6 have absorption bands of moderate skewness relative to Coal 1 which is slightly skewed, and Coal 7 which is rather strongly skewed toward the low wavenumber side of the absorption maximum. This information suggests that stronger and more extensive hydrogen-bonded groups (hydrogen-bonded phenolic-hydroxyl groups) occur with increasing rank based on reported carbon values (Colthump et al., 1964; Bellamy, 1958; Friedel, 1953).

The absorption maximum at approximately 3380 cm^{-1} decreases regularly in absorption intensity with Coal 1 having a moderately strong absorption intensity and progressively decreasing with increasing rank to a very weak absorption in Coal 7. These data suggest that at approximately 86% carbon (daf) the 3380 cm^{-1} absorption maximum becomes extremely difficult or impossible to distinguish from the background characteristic of this region.

Qualitative analysis of the spectral information for this series of coals suggests that stronger, more extensive hydrogen-bonding and decrease in phenolic-hydroxyl group content of coals attend increasing rank.

3040 cm^{-1} Band

This absorption band is a weak absorption band superposed on the low wavenumber side of the 3400 cm^{-1} band in Coals 4-7. Coals 1-3 do not show a distinct absorption band here but this does not preclude the existence of absorption due to the stretching of aryl (Ar) CH groups for these coals. Three possible explanations for the lack of a distinct absorption band in Coals 1-3 are: 1) Coals 1-3 may have very few aromatic components in their structure, i.e. largely derived from lower order organisms; 2) the aromatic CH absorption band actually may be present in Coals 1-3 but obscurred by the strong OH absorption band typical of low rank coals; 3) if a reasonably high degree of aromaticity is assumed for sub-bituminous C-high volatile A bituminous humic coals (Coals 1-3) then the lack of an absorption band near 3040 cm^{-1} would suggest that the aromatic units within these coals are highly substituted.

The 3040 cm^{-1} absorption band has a slightly broad character although the band appears to be rather symmetrically distributed about the maximum.

2955 cm^{-1} Band

This absorption band is discernible as a shoulder of weak intensity on the more intense 2920 cm^{-1} absorption band in each of the coal samples. The absorption maximum of the shoulder generally is sharp for each coal.

Range 2920 to 2910 cm^{-1} Band

This distinct absorption band occurs with moderate intensity for each coal. A gradual decrease in absorption band intensity apparently occurs with increasing rank from Coal 1 to Coal 7. The absorption maximum occurs at approximately 2920 cm^{-1} for Coals 1-3, shifts to approximately 2915 cm^{-1} for Coal 6, and finally occurs at approximately 2910 cm^{-1} for Coals 4, 5, and 7. This observed frequency shift of the maximum to lower wavenumbers, correlative with increasing rank, may indicate a stronger bonding character for the alkyl CH moieties in higher rank coals.

Very minor broadening of the 2920 cm^{-1} absorption band is obvious for each coal. The band broadening generally is symmetrically distributed about the absorption maximum. It is well established that different bond lengths yield a broadening of the overall absorption band. The observed symmetrical broadening of the 2920 cm^{-1} absorption band may be attributed to a normal (Gaussian) distribution of various

alkyl CH bond lengths presumed to exist in most coals.

The 2910 cm^{-1} absorption band of Coal 7 is poorly resolved and not distinct from the 2850 cm^{-1} absorption band (Figure 3, Coal 7).

2850 cm^{-1} Band

This distinct absorption band has a maximum absorption intensity at approximately 2850 cm^{-1} for each coal. The 2850 cm^{-1} absorption band generally is not as well resolved as the accompanying 2920 cm^{-1} absorption band described above. The 2850 cm^{-1} band distinction is better developed in Coals 1-3 than in the other coal samples. The 2850 cm^{-1} absorption band becomes broader and less clearly resolved from the 2920 cm^{-1} absorption band progressing from Coal 1 to Coal 7 with increasing carbon (daf) values. Generally, absorption band broadening is symmetrically distributed about the absorption maximum.

Coals 1-4 have a broad absorption shoulder at approximately 2820 cm^{-1} superposed on the 2850 cm^{-1} absorption band, whereas for Coals 5-7 the 2820 cm^{-1} absorption band is absent. The appearance of the 2820 cm^{-1} absorption shoulder in Coals 1-4 and not in Coals 5-7 may be attributed to alkoxy ($-OCH_3$) functionalities (Smith, 1979; Alpert et al., 1970; Bellamy, 1958) within the structure of lower rank coals. These alkoxy moieties may represent (1) primary features of organic materials contributing to the formation of coals, (2) a secondary

feature resulting from oxidation during sample preparation, or (3) both. Oxidation of Coals 1-4 is consistent with the observation that more immature organic matter is more susceptible to oxidation effects during preparation than higher rank (Coals 5-7) organic matter (Durand and Nicaise, 1980).

The 2850 cm^{-1} absorption band intensity ranges from medium in Coal 1 to weak in Coal 7 which is roughly inversely correlative with increasing rank.

1700 cm^{-1} Band

The 1700 cm^{-1} absorption band occurs as a shoulder on the 1590 cm^{-1} absorption band for Coals 1-4 and 6. The absorption band maximum occurs at 1700 cm^{-1} for Coals 2 and 4, and shifts to 1690 cm^{-1} for Coals 1, 3 and 6.

The 1700 cm^{-1} absorption intensity is strong for Coals 1-3 while decreasing markedly to a weak absorption intensity in Coals 4 and 6, Figure 3.

1660 cm^{-1} Band

The 1660 cm^{-1} absorption band occurs as a shoulder on the 1590 cm^{-1} absorption band for Coals 2, 3, 5 and 7 only. The absorption shoulder for Coal 2 is poorly resolved from the 1590 cm^{-1} absorption band. The absorption shoulder becomes better resolved as carbon (daf) increases.

1590 cm^{-1} Band

The 1590 cm^{-1} absorption band is for many coals the most prominent spectral feature (Fujii et al., 1970; Durie et al., 1967; and Czuchajowski and Lawson, 1963). This absorption band is present in all seven coal samples. The 1590 cm^{-1} absorption band occurs as a significantly distinct, broad absorption band generally symmetrically distributed about the absorption maximum. The absorption band maximum is centered around 1580 cm^{-1} for Coal 7 whereas all the other coals have an absorption maximum centered at approximately 1590 cm^{-1}. Coals 1-3 have slightly broader bandwidths than Coals 4-7 where the degree of band broadening is such that Coals 1, 2 and 3 are about equal to each other and greater than Coals 4, 5, 6 and 7 which are also equal to each other.

The apparent better resolution of the 1660 cm^{-1} shoulder with increasing rank, described above, may be explained by the progressive loss of carbonyls and carboxyls coupled with a frequency shift to lower wavenumbers so that increasing rank permits enhanced resolution of the

1660 cm^{-1} shoulder, particularly for Coal 7.

1440 cm^{-1} Band

The 1440 cm^{-1} absorption band is present for all seven coal samples. The absorption band character ranges from a shoulder on the 1375 cm^{-1} absorption band for Coal 1 to a well resolved absorption band of medium intensity for Coals 3 to 7. The absorption band maximum occurs at approximately 1440 cm^{-1} for each coal sample. Coal 2 has a better developed absorption shoulder than Coal 1 although not completely resolved.

The increasingly better-resolved 1440 cm^{-1} absorption band appears to be symmetrically distributed about the absorption maximum for Coal 2. The well resolved absorption band is slightly skewed toward the low wavenumber side of the absorption maximum for Coals 3-7 with the degree of skewness following the pattern:

$$4 \approx 5 \approx 6 < 3 \approx 7.$$

1375 cm^{-1} Band

The 1375 cm^{-1} absorption band occurs as a distinct absorption band of medium intensity for each of the coals. The maximum occurs at approximately 1375 cm^{-1} for each of the coals.

The 1375 cm^{-1} absorption band for Coal 1 has a medium intensity absorption and very broad bandwidth, i.e. broad enough to have the 1440 cm^{-1} absorption band appear as a shoulder on the 1375 cm^{-1} absorption. The 1375 cm^{-1} absorption band for Coal 2 has a much narrower bandwidth and is better resolved from the 1440 cm^{-1} absorption band than Coal 1, whereas Coals 3-7 show the 1375 cm^{-1} band as a well resolved and distinct from the 1440 cm^{-1} absorption band.

The 1375 cm^{-1} absorption band for Coal 1 appears to be skewed toward the high wavenumber side of the absorption maximum. Coals 6 and 7 show only a very slight skewness in the same direction as Coal 1. Coals 2 and 5 show the absorption band as being symmetrically broadened about the absorption maximum. Coals 3 and 4 show the 1375 cm^{-1} absorption band to be equally and slightly skewed toward the low wavenumber side of the absorption maximum.

The absorption band intensity is moderately strong and conspicuous for Coals 1-6, whereas for Coal 7 the absorption band intensity is weak.

1265 cm^{-1} Band

The 1265 cm^{-1} absorption region for Coals 1-6 is present as a very broad, poorly resolved shoulder on the more intense 1165 cm^{-1} absorption. The 1265 cm^{-1} absorption region for Coal 7 shows no improved resolution, but unlike the other coals, the band occurs as a

high point of minor absorption within a broad region of greater absorption between 1500 cm^{-1} and 1000 cm^{-1}, as shown in Figure 3. A medium absorption intensity for the 1265 cm^{-1} absorption region prevails for Coals 1-6, whereas a weak absorption intensity occurs in Coal 7.

The position of the absorption maximum shifts from 1275 wavenumber to 1255 wavenumber with increasing rank. The absorption maximum occurs at approximately 1275 cm^{-1} for Coals 1-3, at approximately 1265 for Coal 4, and approximately 1255 cm^{-1} for Coals 5 and 6.

1165 cm^{-1} Band

The 1165 cm^{-1} absorption band occurs as a very broad absorption maximum in all seven coals. The absorption maximum for this band appears at 1170 cm^{-1} for all the coals here studied.

The absorption intensity of the 1165 cm^{-1} absorption band ranges from medium to strong. The 1165 cm^{-1} absorption band is the most intense absorption in the 1500-1000 cm^{-1} region for Coals 2, 3, 5, and 6. The demineralized coal spectra, Figure 5, of those coals with initially high mineral matter contents (Coals 4 and 7) suggest the existence of an intense absorption maximum at approximately 1165 cm^{-1}.

The symmetry of the 1165 cm^{-1} absorption band is difficult to determine adequately since this is the region of the spectrum where mineral matter (primarily phyllosilicates) influences band shape and intensity (Van der Marel and Beutelspacher, 1976; Farmer, 1974). Spectral information from the demineralized coals suggest that the broad 1165 cm^{-1} absorption band for Coals 1 and 5 is slightly skewed toward the high wavenumber side of the absorption maximum. Coals 2, 3, 4 and 6 show the 1165 cm^{-1} absorption band to be moderately skewed toward the high wavenumber side of the absorption maximum, whereas for Coal 7 the absorption band is symmetrically distributed about the absorption maximum. Possible oxidation effects, e.g. ether group (C-O-C) formation, resulting from the coal demineralization technique may influence the character of the prominent 1165 cm^{-1} absorption band. The qualitative aspects of coal modification resulting from the coal demineralization technique are discussed in more detail below.

1100-1000 cm^{-1} Band

This broad absorption region is easily discernible in all the coals. The absorption maxima for coals with high mineral matter content occur at approximately 1090 cm^{-1} and 1035 cm^{-1}, which is correlative with kaolinite mixtures (Van der Marel and Beutelspacher, 1976; and Farmer, 1974). The 1090 cm^{-1} and 1035 cm^{-1} absorption maxima are well resolved, distinct absorption bands showing minor to no band broadening.

940 cm^{-1} Band

The 940 cm^{-1} absorption band occurs for Coals 4 and 7 only. For coal 4, it appears as a distinct, well resolved absorption band symmetrically broadened about the absorption maximum. The 940 cm^{-1} absorption band for Coal 7 occurs as a distinct shoulder on the 1100-1000 cm^{-1} absorption region. Moderately weak absorption intensities characterize the 940 cm^{-1} absorption band for Coals 4 and 7.

915 cm^{-1} Band

The 915 cm^{-1} absorption band occurs as a well resolved, distinct absorption band for Coals 1, 2, 4, and 7 only. Slight band broadening appears symmetrically distributed about the 915 cm^{-1} absorption maximum. The absorption intensity ranges from weak for Coal 1 to moderately weak for Coal 7.

860 cm^{-1} Band

The 860 cm^{-1} absorption band is found in spectra of Coals 4, 5, 6 and 7 only. The 860 cm^{-1} band for Coal 4 is a distinct, well resolved band of moderately weak intensity. Coal 4 shows slight band broadening symmetrically distributed about the 860 cm^{-1} absorption maximum. The absorption band for Coals 5, 6, and 7 occurs as a distinct shoulder of

poor resolution and medium intensity.

820 cm^{-1} Band

The 820 cm^{-1} absorption band exclusively occurs for Coal 7. The 820 cm^{-1} absorption appears as a rather distinct, well resolved absorption band of weak intensity. Generally, the 820 cm^{-1} absorption band broadening is symmetrically distributed about the absorption maximum.

795 cm^{-1} Band

The 795 cm^{-1} absorption band is present for Coals 2-7. The 795 cm^{-1} absorption band for Coal 2 appears as a weak, poorly resolved shoulder with an apparent band broadening which is moderately skewed towards the high wavenumber side of the absorption maximum. The 795 cm^{-1} absorption band for Coal 3 shows slightly better resolution with the weak absorption band more distinct than compared to Coal 2. The absorption band for Coals 4-7 occurs as a well resolved, distinct absorption of medium intensity. Coals 4, 5 and 7 show the 795 cm^{-1} absorption band to be slightly to moderately skewed toward the low wavenumber side of the absorption maximum, whereas for Coal 6 the absorption band is skewed towards the high wavenumber side of the absorption maximum.

740 cm^{-1} Band

The 740 cm^{-1} absorption band occurs for Coals 2-7. The 740 cm^{-1} absorption band for Coal 2 occurs as an almost indistinguishable absorption band of extremely weak absorption intensity. Coal 3 shows the 740 cm^{-1} absorption band as a sharp, very well resolved absorption band of distinctly weak intensity. The 740 cm^{-1} absorption band for Coal 3 is symmetrically distributed about the maximum. Coals 5 and 6 have a distinct, well resolved, broad absorption band of moderately weak intensity. The absorption band for Coals 5 and 6 is skewed slightly towards the low wavenumber side of the absorption maximum. The 740 cm^{-1} absorption band for Coals 4 and 7 occurs as a very well resolved, sharp, distinct band of medium intensity. Coals 4 and 7 generally show the 740 cm^{-1} band to be symmetrically distributed about the absorption maximum.

685 cm^{-1} Band

The 685 cm^{-1} absorption band only occurs for Coals 4-7. Coal 6 shows the 685 cm^{-1} absorption band as a poorly resolved, distinct absorption band with considerable band broadening symmetrically distributed about the maximum. The 685 cm^{-1} absorption band for Coals 4, 5 and 7 occurs as a well resolved, distinct absorption band of medium intensity.

Determination of absorption band symmetry about the absorption maximum is not possible in this region of generally high non-specific background. Also, an instrumental grating change at 665 cm^{-1} further complicates the determination of absorption band symmetry of the 685 cm^{-1} band.

CHEMICALLY DEMINERALIZED WHOLE COALS--QUALITATIVE CONSIDERATIONS

The objective of chemical methods for coal demineralization is to isolate the organic matter by making the mineral species soluble while keeping modifications in the chemical composition of the organic matter to a minimum. Chemical demineralization methods permit good recovery of the organic matter which shows minor modification, except for recent organic matter such as peat and soil (Durand and Nicaise, 1980).

Acid Digestion Effects on Minerals

Hydrochloric acid (HCl) is used to cause the dissolution of carbonates, sulfides, sulfates, oxides and hydroxides, whereas hydrofluoric acid (HF) results in the dissolution of silicates. Principal limitations encountered with this acid digestion method are as follows:

a) dissolution of all the minerals doesn't occur. Mineral species frequently remaining after the acid digestion method are heavy oxides (e.g. rutile and zircon) and iron sulfide such as pyrite and marcasite (Durand and Nicaise, 1980).

b) an organic coating may encase a mineral preventing solution.

Acid Digestion Effects on Organic Matter

Hydrochloric acid (HCl) and hydrofluoric acid (HF) tend to hydrolyze organic matter. Less evolved (immature) organic matter is more strongly hydrolyzed by HCl-HF acids than more mature organic matter. The hydrolytic effect on organic matter is generally low for ancient sediments (Durand and Nicaise, 1980).

Reactions other than hydrolysis may occur with the HCl-HF demineralization method. Oxidation of the organic matter occurs if the temperature exceeds 70°C, especially when the whole coal-acid preparations run dry (Smith, 1961).

Conceivably, chlorine and fluorine fixation could occur by addition and substitution reactions. This halogen fixation also could occur by absorption of HCl and HF in the microporosity of coals. The likelihood that this will occur is a function of the reactivity of the coal which decreases with increasing rank. Chlorine and fluorine fixation parallels the ability of coals to be hydrolyzed. Since our coals range from sub-bituminous B to low volatile bituminous coal the likelihood of chlorine or fluorine fixation or both is low.

QUALITATIVE EFFECTS OF THE CHEMICAL DEMINERALIZATION METHOD ON THE COALS STUDIED

Chemical demineralization techniques were used on the seven coals in order to establish which absorption bands in whole coal spectra have absorptions partially or totally due to mineral species. Only four coals (see Fig. 5) comprising the range of spectral changes are discussed below.

It is well established that absorption bands centered close to 3700, 1100, 1030, 1005 and 915 cm^{-1} almost certainly belong to kaolinite or a mixture containing large amounts of kaolinite (Solomon and Miknis, 1980; Van der Marel and Beutelspacher, 1976; Farmer, 1974; Murchison, 1966). The 1100-1000 cm^{-1} absorption region is the region of the IR spectrum where the OH (stretch) absorption band, attributed to alcohol functions, and $\rangle C-O-C\langle$ (deformation) absorption band, attributed to ether functions, also occur. Therefore chemical demineralization methods for coals permit a more confident and definitive functional group assignment for particular absorption bands.

Figure 5 shows the infrared spectra of four demineralized whole coals (coal samples 2, 4, 5 and 7). The most conspicuous difference between whole coal spectra (Figure 3) and demineralized coal spectra (Figure 5) is the diminished absorption in the 1100-1000 cm^{-1} region. Spectral features of the 1500-1000 cm^{-1} region for demineralized coals

Fig 5

Page 56

show that an absorption maximum of strong intensity occurs at approximately 1160 cm^{-1} for each coal. On the low wavenumber side of the 1160 cm^{-1} band maximum, the absorption decreases at a steep angle (for the recording scale used) toward the 1000 cm^{-1} range in the demineralized coals. The angle of decrease lies between the range of approximately 35° to 60° from the horizontal (abscissa) on the chart scale used for the demineralized coals.

The qualitative spectral changes resulting from the chemical demineralization method for each coal shown in Figure 5 are discussed below. All observations are based on the infrared spectra of the whole coals and the chemically demineralized coals.

Coal 2

The infrared spectrum for demineralized Coal 2 suggests a complete removal of mineral species from the coal. No apparent absorptions are observed in the 3700 cm^{-1} and 1100-1000 cm^{-1} regions of the spectrum which would suggest phyllosilicate mineral species are present. A broad moderately resolved maximum occurs at approximately 1160 cm^{-1} within the broad absorption region between 1500 cm^{-1} and 1000 cm^{-1} (Figure 5).

A significantly large absorption increase in the 1700 cm^{-1} absorption (>C=O) band suggests that the organic matter in Coal 2 was oxidized by this chemical demineralization method. A slight but

noteworthy absorption increase in the 1300-1100 cm^{-1} region (≥C-O-C≤) indicates the coal oxidized or hydrolyzed during demineralization. This increased oxidation of the coal probably reflects the fact that the Coal 2-acid preparation ran dry for a short time.

The 3400 cm^{-1} absorption band shows a slight absorption decrease indicating a slight loss of hydroxyl and NH groups.

If HCl-HF acids have hydrolyzing effects on organic matter, then these hydrolysis effects should appear as an absorption increase in the 3400 cm^{-1} absorption band. A slight absorption decrease for the 3400 cm^{-1} absorption band is noted for each chemically demineralized coal. This information suggests two possible explanations to account for this observed absorption decrease:

1) If we assume that the 3600 cm^{-1} absorption band, characteristic of hydrated and hydroxyl-bearing minerals, is broad enough to influence the 3400 cm^{-1} absorption band, then the dissolution and removal of these hydrated and hydroxyl-bearing minerals could yield no increase or would yield a decrease in the 3400 cm^{-1} band.

2) If we assume negligible OH and NH group contributions to the 3400 cm^{-1} band from mineral species, then any change in absorption as a consequence of chemical demineralization must be the result of hydrolysis or oxidation. This may explain the apparent slight absorption decrease of the 3400 cm^{-1} absorption band for chemically

demineralized coals. This case seems most plausible for all our coals for the following reasons:

a) Absorption contributions to the 1300-1100 cm^{-1} absorption region due to mineral species (e.g. carbonates and silicates) enhance the 1300-1100 cm^{-1} absorption band intensity in whole coals. The chemically demineralized coal spectra show an increased 1300-1100 cm^{-1} absorption band suggesting possible hydrolysis or oxidation or both has occurred.

b) Comparing whole coal spectra with demineralized coal spectra supports the assumption that only minor OH and NH group contributions to the 3400 cm^{-1} absorption band occur from mineral species. This was tested by attempting to correlate ash content and absorption intensity of the 3400 cm^{-1} absorption band. No reasonable correlation was found. Thus the absorption for the 3400 cm^{-1} absorption band is primarily attributed to OH and NH groups with organic affinities. Quantitative data will further confirm this observation later in this paper.

All seven chemically demineralized coals show a slight absorption decrease at the 3400 cm^{-1} band. This slight absorption decrease for demineralized coals in the 3400 cm^{-1} region does not suggest significant hydrolysis of the organic matter has occurred with demineralization but possibly reflects the removal of hydrated or hydroxyl-bearing minerals. This is consistent with the fact that hydrolysis effects on organic matter are generally low for ancient sediments (Durand and Nicaise, 1980).

c) All four demineralized coal spectra show varying degrees of increased absorption intensity for the 1700 cm^{-1} (>C=O) absorption band. This absorption increase in the 1700 cm^{-1} absorption band for demineralized coals indicates varying degrees of oxidation resulted from this chemical demineralization technique. Oxidation effects may be significantly reduced by reaction of the coals with the acids in an inert atmosphere.

The spectral evidence presented above tends to suggest that oxidation effects modify the organic matter of coals more than hydrolysis effects. If hydrolysis of the organic matter does occur in the seven coals, then the effects are of minor extent since no significant spectral change attributable to hydrolysis of organic matter is obvious.

Coal 4

A very weak absorption band at approximately 1030 cm^{-1} is obvious on the steeply inclined background in the 1100-1000 cm^{-1} region of this chemically demineralized coal. A weak absorption band at 940 cm^{-1} is present also. The presence of these two weak absorption bands suggests only partial demineralization of Coal 4 occurred because these bands are known to be correlative with phyllosilicates (kaolinite).

A broad moderately resolved absorption maximum occurs at approximately 1160 cm^{-1} in the broad absorption region between 1500 and 1000 cm^{-1}. The spectrum of Coal 4 shows that slight oxidation and hydrolysis has occurred with chemical demineralization as indicated by the slight increase of the 1300-1100 cm^{-1} absorption band. A slight absorption increase for the 1700 cm^{-1} absorption band is noticable suggesting some oxidation of the organic matter has occurred.

The 3400 cm^{-1} absorption band shows a slight absorption decrease indicating a slight loss of hydroxyl (OH) and NH groups.

Coal 5

The infrared spectrum for Coal 5 suggests a complete removal of mineral species from the coal. No apparent absorptions specifically attributable to mineral species are obvious. A broad, moderately resolved absorption maximum occurs at approximately 1160 cm^{-1} in the broad absorption region between 1500 and 1000 cm^{-1}.

A minor absorption increase in the 1700 cm^{-1} band suggests that slight oxidation of the organic matter occurred with demineralization. A minor absorption increase in the 1300-1100 cm^{-1} region indicates the organic matter oxidized and hydrolysized slightly during demineralization.

Here also, the 3400 cm^{-1} absorption band shows a slight loss of hydroxyl (OH) and NH groups.

Coal 7

A very broad, minor absorption band is superposed on the steeply inclined background absorption in the 1100-1000 cm^{-1} absorption region of chemically demineralized coals. A very weak absorption band at 940 cm^{-1} is discernible. The presence of these two weak absorption bands suggests only partial demineralization of Coal 7 occurred since these two particular absorption bands are correlative with phyllosilicates (kaolinite) mixtures.

Oxidation of the organic matter occurred with the chemical demineralization method since a moderate absorption increase for the 1700 cm^{-1} absorption band is obvious. Coal 7 shows that minor oxidation and hydrolysis occurred with demineralization as indicated by the minor absorption increase of the 1300-1100 cm^{-1} band. A broad, moderately resolved absorption maximum occurs at approximately 1160 cm^{-1} in the broad region between 1500 and 1000 cm^{-1}.

The weak 3400 cm^{-1} absorption band shows a very slight absorption decrease suggesting minor losses of hydroxyl (OH) and NH groups.

ADDITIONAL QUALITATIVE SPECTRAL FEATURES OF CHEMICALLY DEMINERALIZED COAL SPECTRA

The apparent success of the chemical demineralization method appears to be a function of the initial mineral matter (ash) content of the whole (raw) coal. Coals with initially high mineral matter (ash) contents (exceeds 20% ash, moist. free basis), i.e. Coals 4 and 7, show only partial demineralization after the HCl-HF acid attack, whereas coals with initially lower mineral matter (ash) contents (less than 15% ash, moist. free basis), i.e. Coals 1, 2, 3, 5 and 6, show complete demineralization of the coals after the acid attack. These observations are based solely on the spectral information shown on the infrared spectrograms.

There are no spectral features on the chemically demineralized coal spectra suggesting significant chlorine and fluorine fixation did occur with the chemical demineralization method.

Vibrational frequencies for sulfide minerals, e.g. pyrite (FeS_2) and marcasite (FeS_2), generally lie below 400 cm^{-1} (Farmer, 1974). Sulfide mineral absorption contributions to absorption bands in the coal spectra are not encountered since all coal spectra were recorded from 4000 cm^{-1} (2.5μm) to approximately 550 cm^{-1} (≈18.2μm). Moreover, the rather low sulfur values reported in the ultimate analysis for New Mexico coals suggest that if pyrite is present in these coals it is

present in small amounts. The presence of mineral species remaining after the acid digestion method have little quantitative importance during later analysis of coal other than as diluents.

Hydrolysis and oxidation effects on the organic matter of the seven coals generally decrease with increasing carbon (daf) values, i.e. with increasing rank. This is consistent with less evolved (immature) organic matter being more strongly hydrolyzed than more evolved (mature) organic matter.

QUANTITATIVE ANALYSIS OF WHOLE COAL INFRARED SPECTROGRAMS

QUANTITATIVE ANALYSIS OF ABSORPTIVITIES AT A GIVEN FREQUENCY PLOTTED AGAINST PROXIMATE ANALYSIS DATA

Absorptivity at 3400 cm^{-1} versus Fixed Carbon Content

Plotting absorptivity at 3400 cm^{-1} against fixed carbon (FC) values on an ash-free basis, Figure 6, demonstrates that a curvilinear relation is apparent when measured by the 3700-3000 cm^{-1} method (see pp.22-25) or Robin-Rouxhet method for determining the absorbance of the very broad 3400 cm^{-1} band. Both methods of measuring the 3400 cm^{-1} band show similar trends, that is the 3400 cm^{-1} absorptivity for the whole coals studied regularly decreases with increasing fixed carbon (ash-free basis) content, i.e. increasing rank. The major difference between the two measurement methods is the Robin-Rouxhet method exhibits a more rapid decrease in absorptivity with increasing fixed carbon than the 3700-3000 cm^{-1} method. This difference between the two measurement methods decreases with increasing rank. The general trend or relationship between the 3400 cm^{-1} band and fixed carbon (ash-free) content is the most noteworthy feature of Figure 6.

Regression analysis of the data for the 3700-3000 cm^{-1} method fit to an exponential equation has a 0.985 correlation coefficient. The exponential equation best describing this fit is: $\ln a = 0.407 - 0.069$

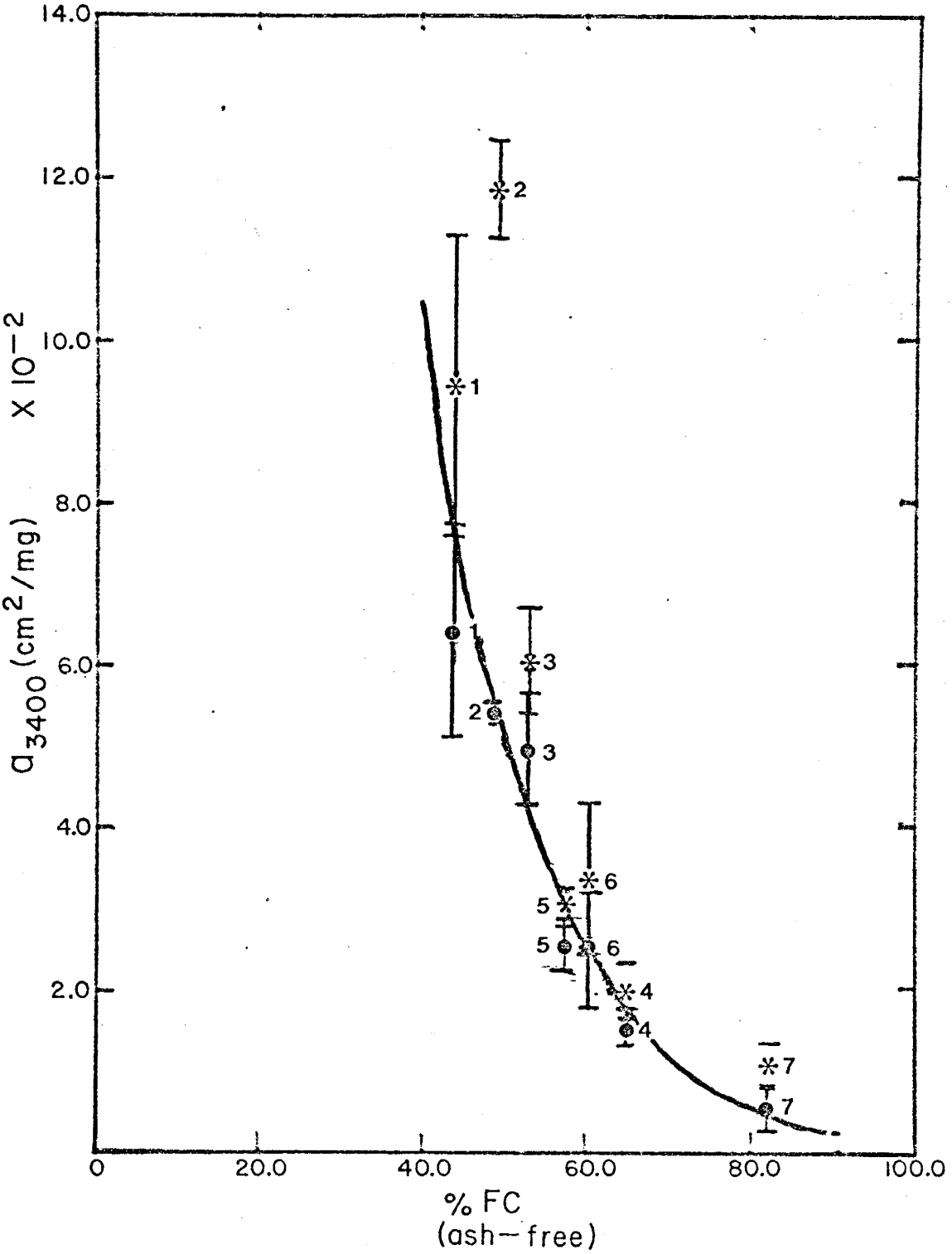

Figure 6. Mean absorptivity values at 3400 cm-1 plotted against fixed carbon on an ash-free basis for Coals 1-7. * indicates the Robin-Rouxhet method of measurement and ● indicate the 3700-3000 cm-1 method of measuring the 3400 cm-1 band. Vertical bars indicate the sample standard deviation.

(%FC, ash-free).

Absorptivity at 3400 cm^{-1} versus Calorific Value

Plotting absorptivity for the 3400 cm^{-1} band versus calorific value (BTU/lb) on an ash-free basis, Figure 7, shows a linear trend exists for both measurement methods. A best-fit correlation line having a correlation coefficient of -0.944 is shown in Figure 7 for the Robin-Rouxhet measurement method. The linear correlation line for the Robin-Rouxhet method is defined by the equation: $a = 0.266 - 1.66X10^{-5}$ (BTU/lb, ash-free). The 3700-3000 cm^{-1} method of measurement shows a similar general linear relation for the values, although the correlation coefficient for the 3700-3000 cm^{-1} method is -0.912.

The data suggest that with decreasing absorptivities there is a correspondingly significant increase in calorific values attending increasing rank. Extrapolation of the best-fit correlation line to the abscissa (i.e. $a = 0.000$ cm^2/mg) for the Robin-Rouxhet method suggests that whole coals with calorific values greater than or equal to 16025 BTU/lb (ash-free) should show no discernible absorption in the 3400 cm^{-1} region.

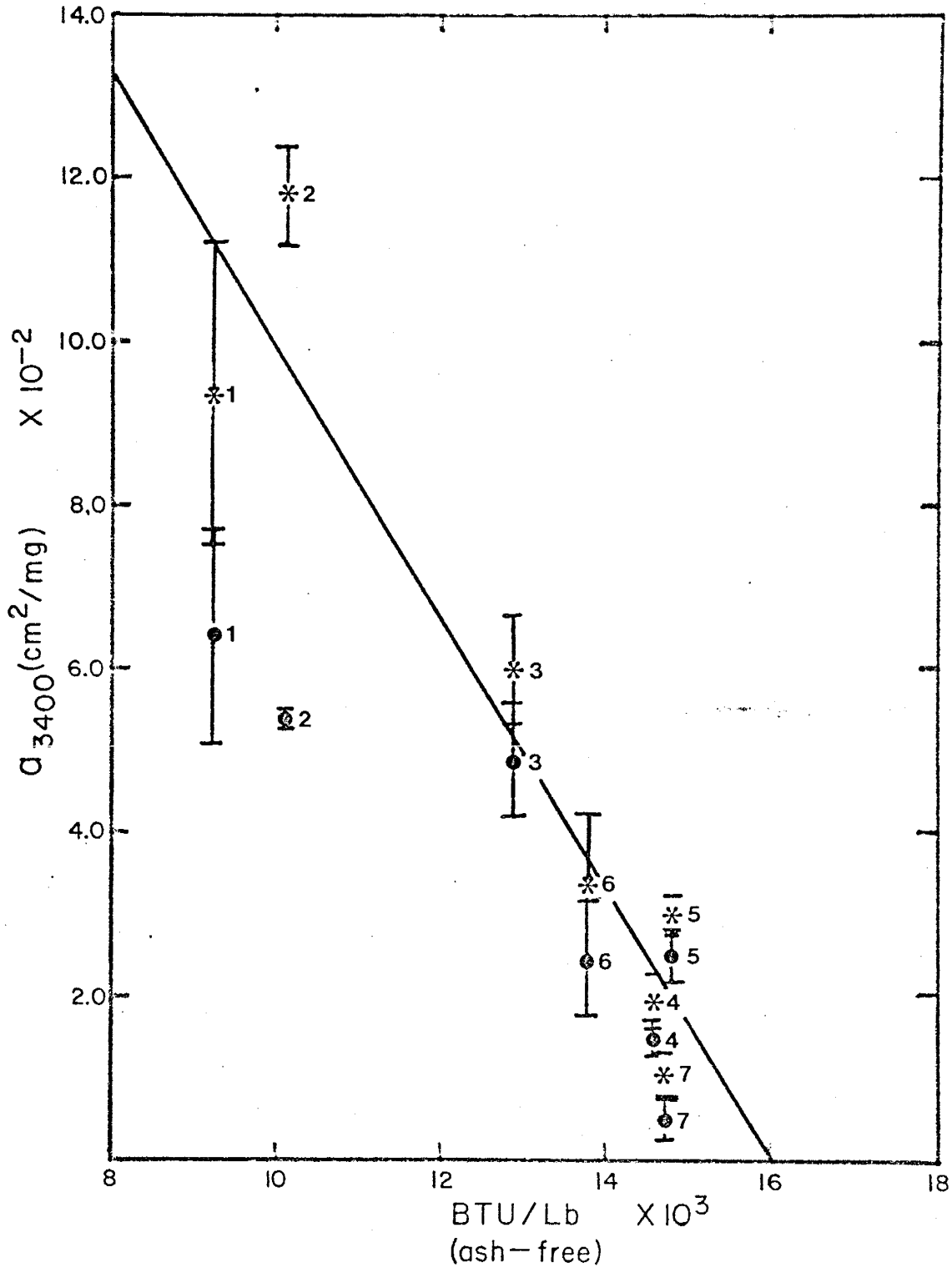

Figure 7. Mean absorptivity values at 3400 cm-1 plotted as a function of calorific value on an ash-free basis for Coals 1-7. * indicates the Robin-Rouxhet method of measurement and ● indicates the 3700-3000 cm-1 method of measuring the 3400 cm-1 band. Vertical bars indicate the sample standard deviation.

Absorptivity at 3400 cm^{-1} versus Volatile Matter Content

Figure 8 demonstrates that a curvilinear relationship exists for both absorption band measurement methods. The data suggest a rather large decrease in absorptivity accompanied by a small decrease in volatile matter (VM, ash-free) content occurs in low-rank whole coals, i.e. Coals 1, 2, 3 and 5, whereas whole coals of higher rank, e.g. Coals 4, 6 and 7, show small decreases in absorptivity with relatively large decreases in volatile matter (ash-free) content. These data suggest that the low-rank whole coals (Coals 1, 2, 3 and 5) studied loose significant quantities of hydroxyl(OH)-containing volatiles during early changes of increasing rank. With higher rank the loss of hydroxyl-containing volatiles decreases significantly.

Applying regression analysis to the data from the 3700 - 3000 cm^{-1} measurement method used here yields an exponential best-fit correlation line, $\ln a = 0.0885$ (%VM, ash-free) - 6.840, with a 0.954 correlation coefficient.

Absorptivity at 3400 cm^{-1} versus Moisture Content

Plotting absorptivity at 3400 cm^{-1} versus moisture content on an ash-free basis illustrates absorptivity decreases with decreasing moisture for both band measurement methods, Figure 9. Moisture within the coal and absorbed by the KBr during preparation enhances the

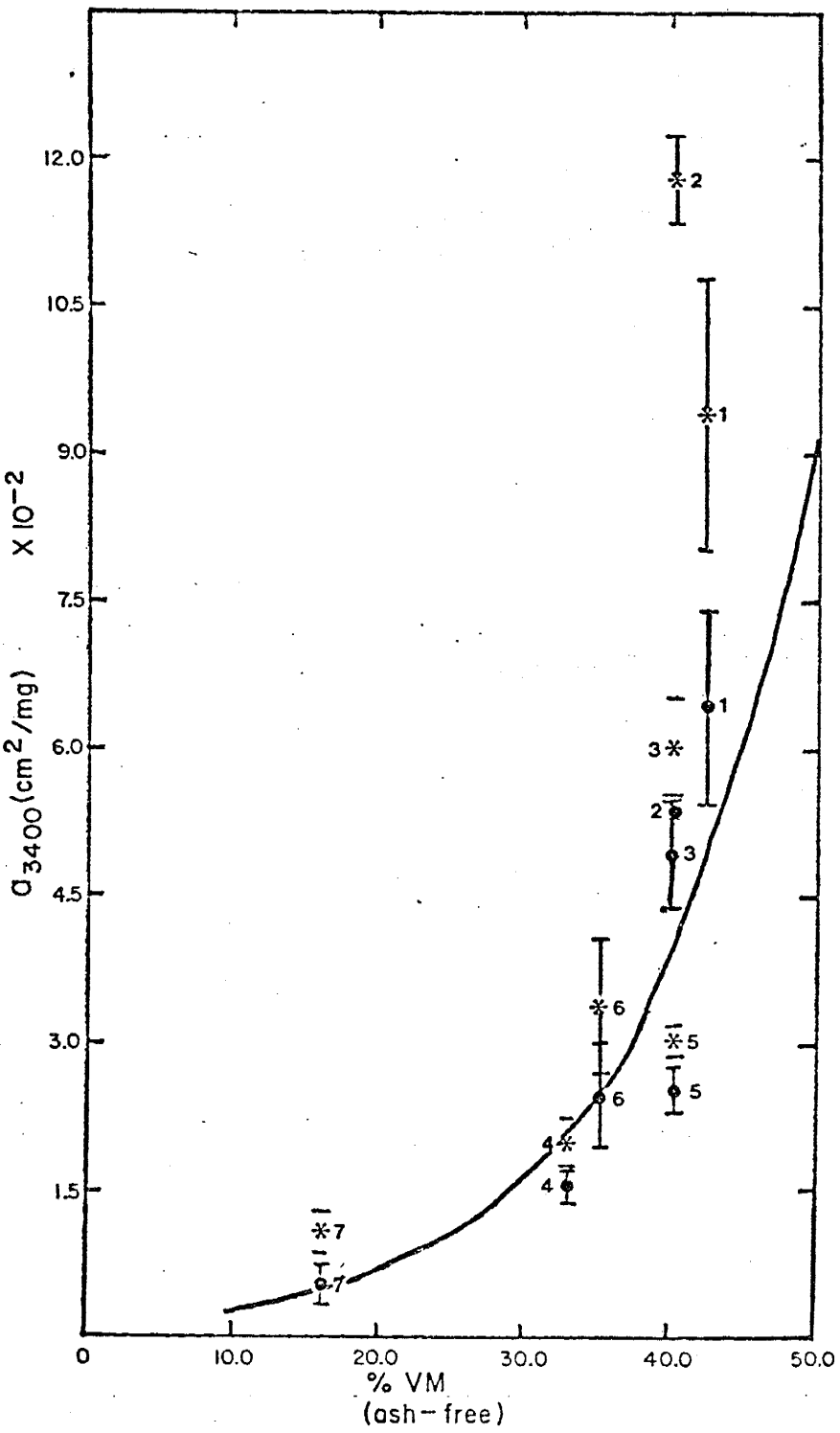

Figure 8. Plot of mean absorptivity values at 3400 cm-1 as a function of volatile matter on an ash-free basis for Coals 1-7. * indicates the Robin-Rouxhet method of measurement and ● indicates the 3700-3000 cm-1 method of measuring the 3400 cm-1 band. Vertical bars indicate the sample standard deviation.

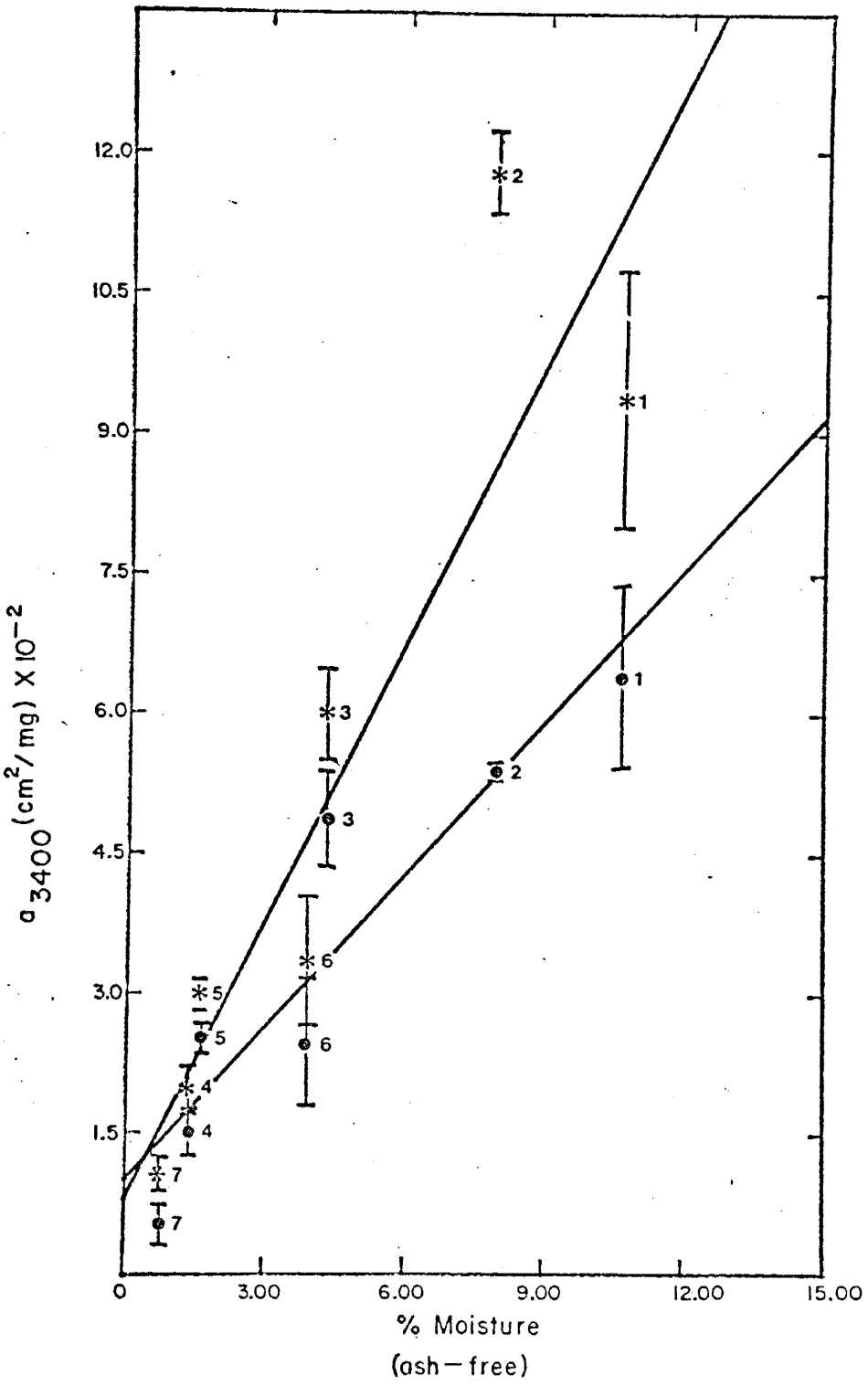

Figure 9. Mean absorptivity values at 3400 cm-1 plotted as a function of moisture on an ash-free basis for Coals 1-7. * indicates the Robin-Rouxhet method of measurement and ● indicates the 3700-3000 cm-1 method of measuring the 3400 cm-1 band. Vertical bars indicate the sample standard deviation.

absorbance of the broad 3400 cm^{-1} band.

Linear regression analysis for the data obtained using the 3700-3000 cm^{-1} band measurement method yields the relation, defined by a = 5.47 X 10^{-3} (% Moist, ash-free) + 0.010, with a 0.923 correlation coefficient. Linear regression analysis on the Robin-Rouxhet band measurement method yields a rectilinear relation having a 0.908 correlation coefficient. Considering the correlation for the 3700-3000 cm^{-1} method it is surmised that moisture significantly contributes to the 3400 cm^{-1} region. Extrapolation of the rectilinear correlation line to the ordinate (i.e. Moist. = 0.00%) yields an absorptivity of 0.010 cm^2/mg which strongly suggests moisture (molecular water) is not the only factor influencing the absorptivity of this band. This observation is consistent with the conclusion of other investigators, for instance Solomon and Carangelo (1982), and Robin and Rouxhet (1976).

Absorptivity at 1700 cm^{-1} versus Fixed Carbon Content

Figure 10, the plot of absorptivity at 1700 cm^{-1} versus fixed carbon content on an ash-free basis, shows absorptivity values decrease with slight increases in fixed carbon content. Low-rank whole coals (Coals 1 and 2) have relatively high absorptivity values while higher rank whole coals (Coals 6 and 4) have low absorptivity values.

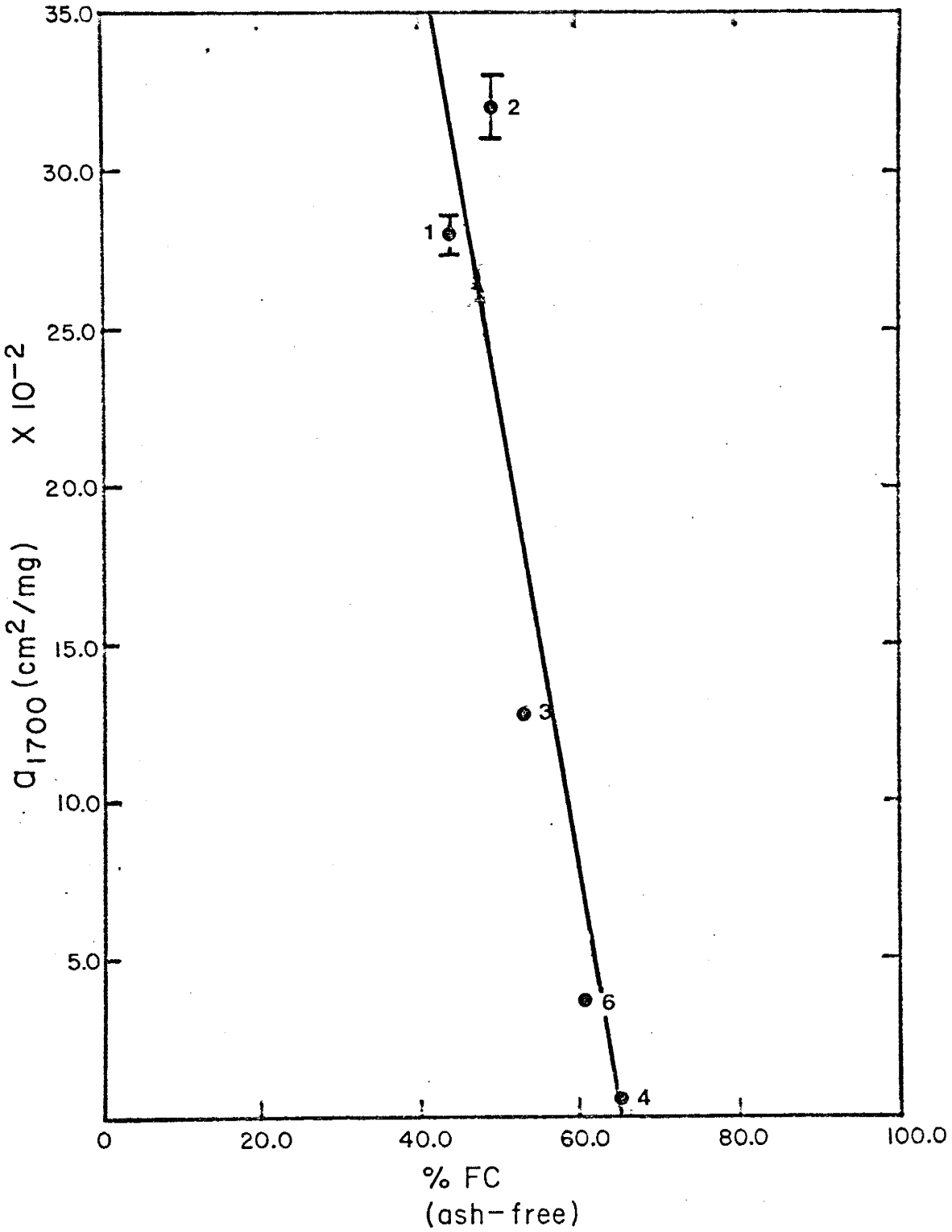

Figure 10. Mean absorptivity values at 1700 cm-1 plotted against fixed carbon on an ash-free basis for Coals 1-4 and 6. Vertical bars indicate the sample standard deviation.

Linear regression analysis for these data demonstrate that both a rectilinear and a curvilinear (exponential) correlation line can be used to describe the trend. The rectilinear correlation line for these data is a = 0.972 - 0.015 (%FC, ash-free) with a correlation coefficient of 0.927. The curvilinear (exponential) correlation line is described by ln a = 7.424 - 0.183 (%FC, ash-free) with a 0.958 correlation coefficient.

The high slope of the correlation line(s) for the whole coals with approximately 40% to 65% FC (ash-free) may indicate the region where carbonyl(>C=O) or carboxyl moiety cleavage (or losses) is at a maximum. Figure 10 illustrates that at approximately 65% FC (ash-free) no absorption should be distinguishable for the 1700 cm^{-1} spectral region suggesting if carbonyl or carboxyl groups are present in high rank whole coals then these functional groups are present in quantities small enough to be undetected by the spectrophotometer, or as rank increases, the carbonyl or carboxyl absorption shifts to lower frequencies (e.g. approx. 1660 cm^{-1}). Further support of this statement follows in the section on pages to . The occurrence of the 1700 cm^{-1} band in whole coals with greater than or equal to 65% FC (ash-free) indicates oxidation of the coal has occurred. Oxidation effects on lower rank whole coals, i.e. whole coals with less than or equal to 65% FC (ash-free), are difficult to assess on the basis of this study.

Absorptivity at 1700 cm^{-1} versus Calorific Value

Plotting absorptivity at 1700 cm^{-1} versus calorific values on an ash-free basis (Fig. 11) shows a linear best-fit relationship, defined by $a = 0.868 - 5.9X10^{-5}$ (BTU/lb, ash-free) with a correlation coefficient of -0.968. The linear best-fit relation demonstrates that as absorptivity decreases the ash-free calorific value shows a correspondingly significant increase. Low-rank whole coals (Coals 1 and 2) have relatively high absorptivities whereas higher rank whole coals (Coals 4 and 6) have low absorptivities. Extrapolation of the rectilinear correlation line to the abscissa (i.e. $a = 0.000$ cm^2/mg) suggests that no absorption should be discernible at 1700 cm^{-1} for whole coals with calorific values greater than 14700 BTU/lb (ash-free). If the 1700 cm^{-1} band is discernible in a whole coal with a rather high calorific value (more than 14700 BTU/lb, ash-free), then the whole coal presumably has oxidized.

Absorptivity at 1700 cm^{-1} versus Volatile Matter Content

Figure 12 shows that a curvilinear relation, defined by $\ln a = 0.335$ (%VM, ash-free) - 15.699 with a 0.945 correlation coefficient, characterizes this evolutionary trend for the whole coals studied. This plot of absorptivity at 1700 cm^{-1} versus volatile matter content on an ash-free basis shows that as volatile matter decreases with increasing rank absorptivity rapidly decreases. In general, low-rank whole coals

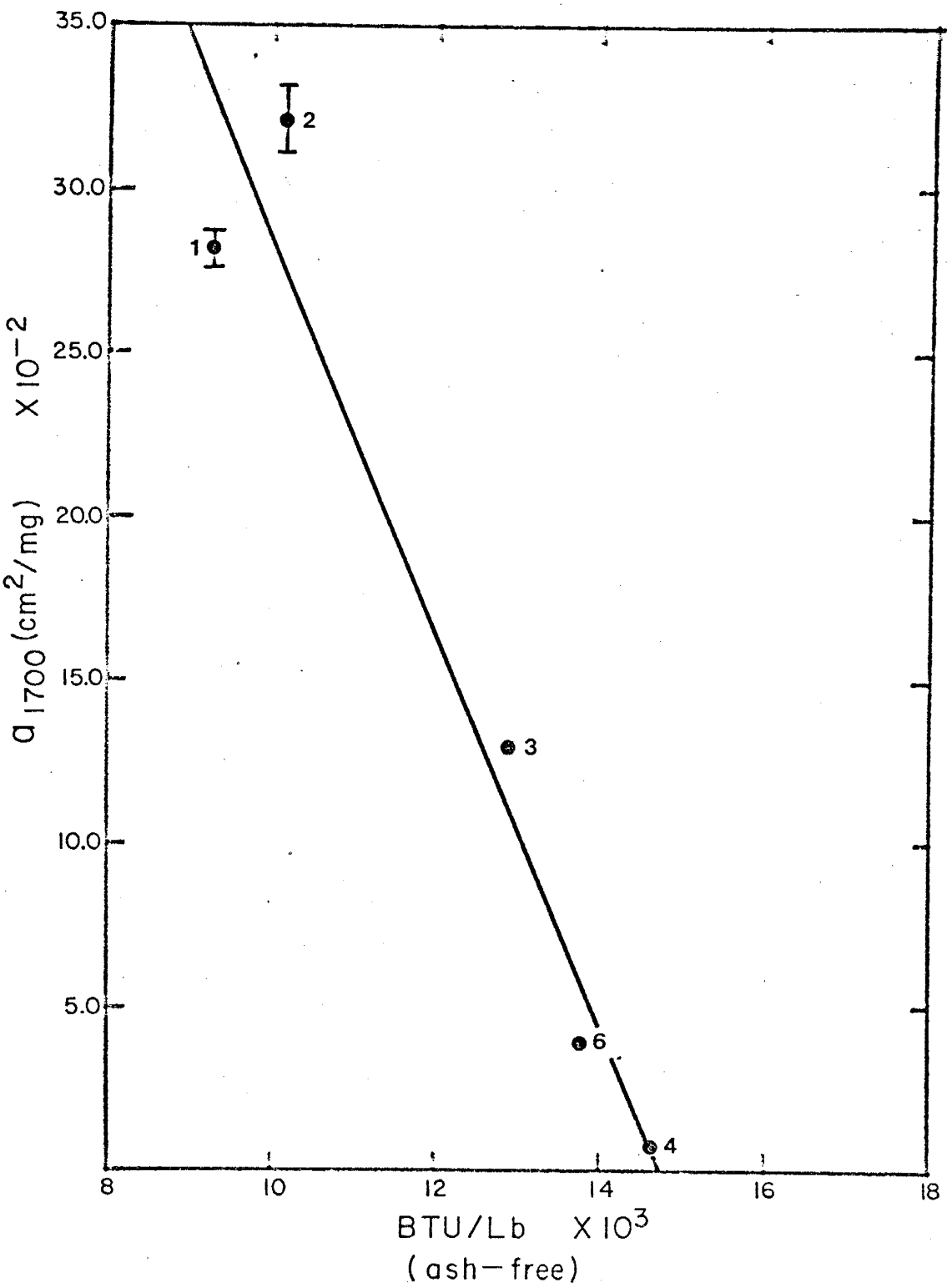

Figure 11. Mean absorptivity values at 1700 cm-1 plotted as a function of calorific value on an ash-free basis for Coals 1-4 and 6. Vertical bars represent the sample standard deviation.

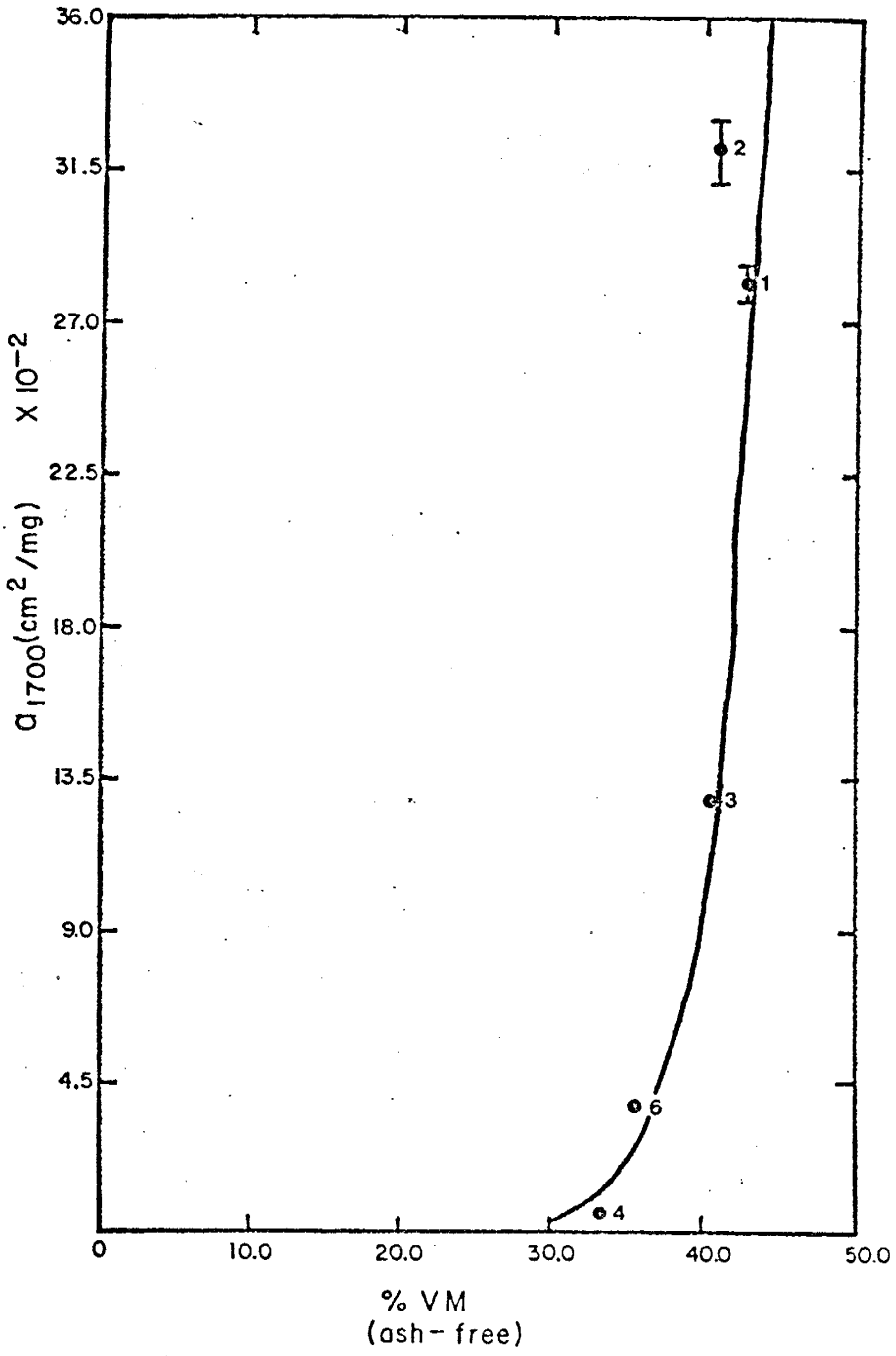

Figure 12. Mean absorptivity values at 1700 cm-1 plotted against volatile matter on an ash-free basis for Coals 1-4 and 6. Vertical bars indicate the sample standard deviation.

have rather high absorptivities while higher rank whole coals have rather low absorptivities. It is noteworthy that Coals 2 and 3 have similar volatile matter content, although the absorptivity for Coal 2 (a = 0.320 cm^2/mg) is approximately 2.5 times larger than the absorptivity for Coal 3 (a = 0.129 cm^2/mg). This disparity in absorptivity values for whole coals of similar volatile matter content in part can be attributed to experimental errors and in part to the natural variability in coal parameters that occur even in whole coals of the same rank. Several other lines of evidence suggest that Coal 3 is slightly more mature than Coal 2 in spite of similar volatile matter contents, Table 2.

Absorptivity at 1660 cm^{-1} versus Moisture Content

Figure 13 illustrates that a rectilinear relation appears when absorptivity at 1660 cm^{-1} is plotted against moisture content on an ash-free basis. The linear best-fit correlation line, defined by a = 0.0421 (%Moist, ash-free) - 0.0049 with a 0.989 correlation coefficient, demonstrates that as moisture content decreases with increasing rank corresponding decreases in absorptivity occur. Low-rank whole coals, e.g. Coals 2 and 3, have high absorptivities whereas higher rank whole coals, Coals 4, 5 and 7, have relatively low absorptivities.

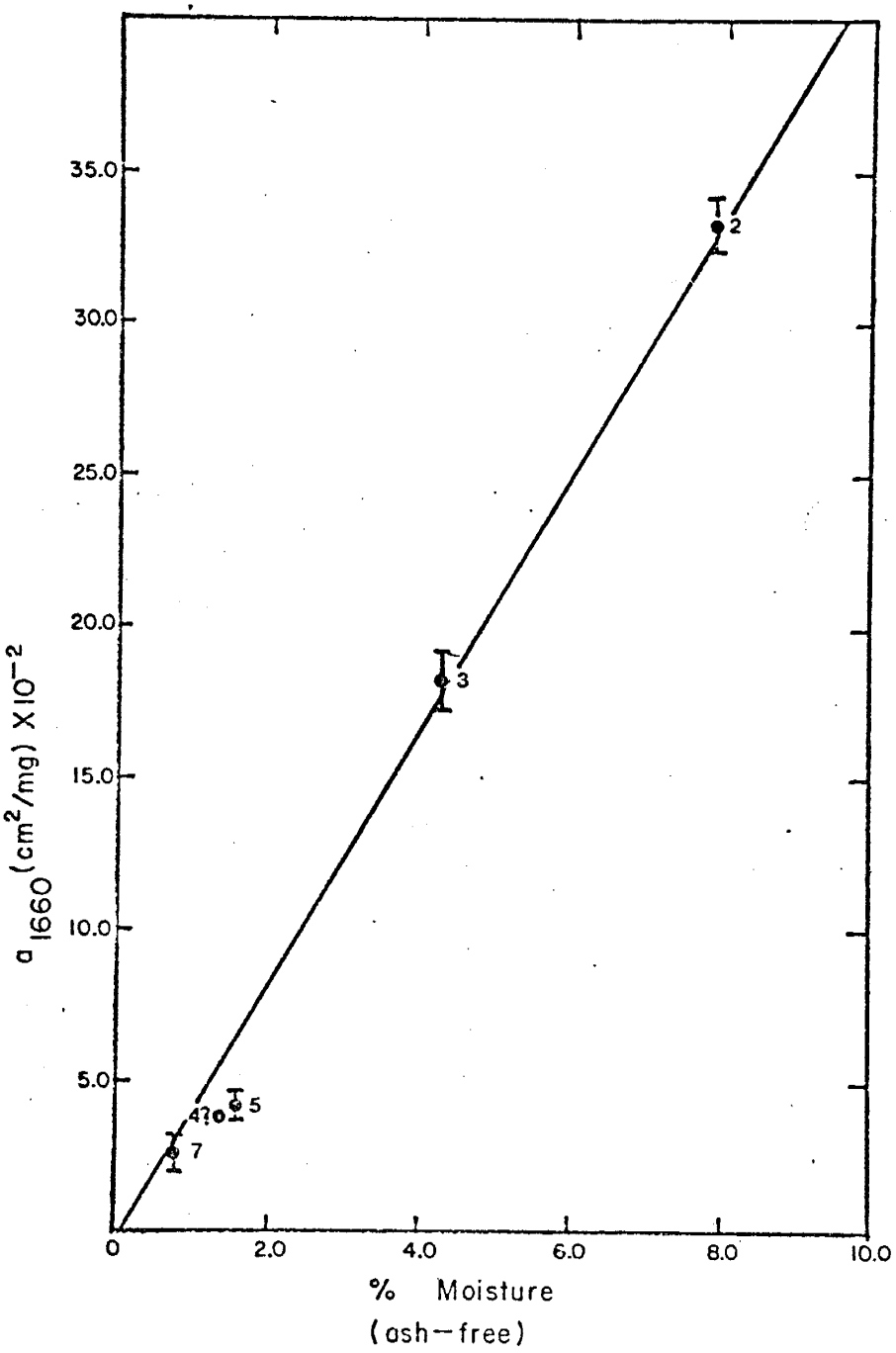

Figure 13. Plot of mean absorptivity values at 1660 cm-1 versus moisture on an ash-free basis for Coals 2-5 and 7. Vertical bars represent the sample standard deviation. ? means not confident of mean absorptivity value due to insufficient data.

The high correlation coefficient for the linear correlation line in Figure 13 suggests that the principal contribution to the 1660 cm^{-1} band results from hydroxyl(OH) functional groups (OH bending mode) of molecular water within the coal and a minor amount adsorbed in the KBr. This inference is consistent with the work of others ¼Rouxhet et al., 1980; Painter and Coleman, 1979; Robin and Rouxhet, 1976; Murray and Evans, 1972, who have assigned the 1660 cm^{-1} band to molecular water (OH bending mode).

Extrapolation of the linear correlation line to the abscissa, i.e. a = 0.000 cm^2/mg, yields a moisture (ash-free) value of approximately 0.116%. Thus whole coals with moisture contents less than or equal to 0.12% should reveal no observable absorbance at 1660 cm^{-1}. A possible explanation for the non-zero intercept of the correlation line with the abscissa may reflect the effect of moisture adsorbed by the KBr in addition to experimental errors.

Absorptivity at 1660 cm^{-1} versus Calorific Value

Plotting absorptivity at 1660 cm^{-1} versus calorific value on an ash-free basis, Figure 14, reveals a linear relation demonstrating that as absorptivity decreases calorific value shows a corresponding increase. The linear correlation line is a = 1.003 - $6.5X10^{-5}$ (BTU/lb, ash-free) with a 0.994 correlation coefficient. No discernible absorption band occurs in the spectra for Coals 1 and 6. Low-rank whole

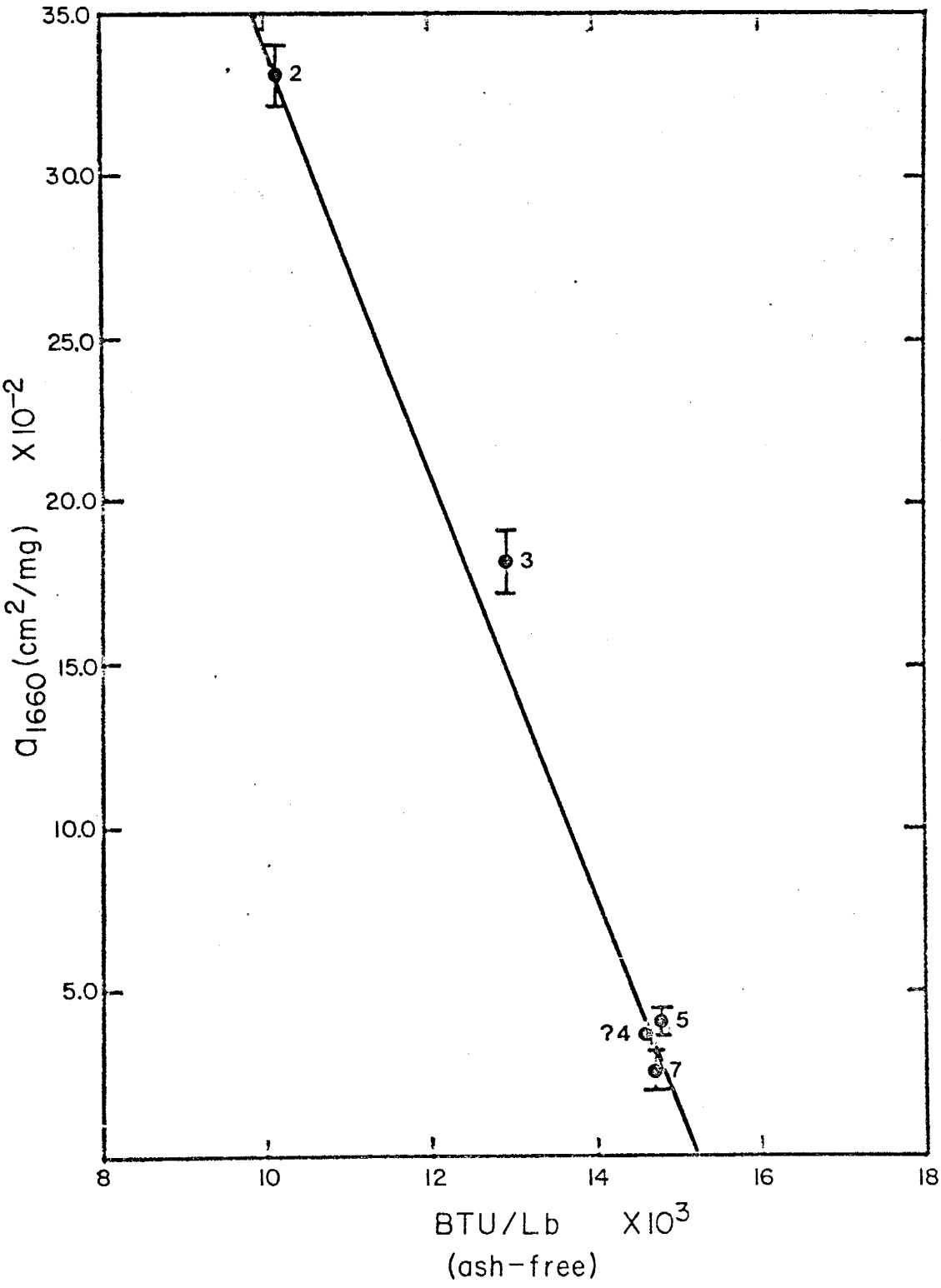

Figure 14. Mean absorptivity values at 1660 cm-1 plotted against calorific value on an ash-free basis for Coals 2-5 and 7. Vertical bars represent the sample standard deviation. ? means not confident of mean absorptivity value due to insufficient data.

coals have high absorptivities while higher rank whole coals have relatively low absorptivities. Extrapolation of the correlation line to the abscissa (a = 0.000 cm^2/mg) yields a calorific value of approximately 15425 BTU/lb (ash-free). Therefore whole coals desiccator-dried at room temperature with calorific values more than 15425 BTU/lb (ash-free) should exhibit no discernible absorption in the 1660 cm^{-1} region.

When absorptivity is plotted against calorific value on an ash-free basis, the significantly high linear correlation coefficient for the 1660 cm^{-1} (r = -0.994) in addition to the high linear correlation coefficients for the 1700 cm^{-1} (r = -0.968) and 3400 cm^{-1} (r = -0.944) regions suggest calorific values of whole coals are an inverse function of oxygen functionalities.

Absorptivity at 1590 cm^{-1} versus Fixed Carbon Content

Figure 15 shows absorptivity at 1590 cm^{-1} plotted against fixed carbon content on an ash-free basis. An exponential relation, defined by ln a = 1.010 - 0.040 (%FC, ash-free) with a 0.963 correlation coefficient, illustrates that as fixed carbon increases with increasing rank absorptivity decreases. Small changes in fixed carbon on an ash-free basis result in significantly large changes in absorptivity for whole coals with 45% to 60% FC (ash-free). Whole coals in this study with more than 60% FC (ash-free) are characterized by small changes in

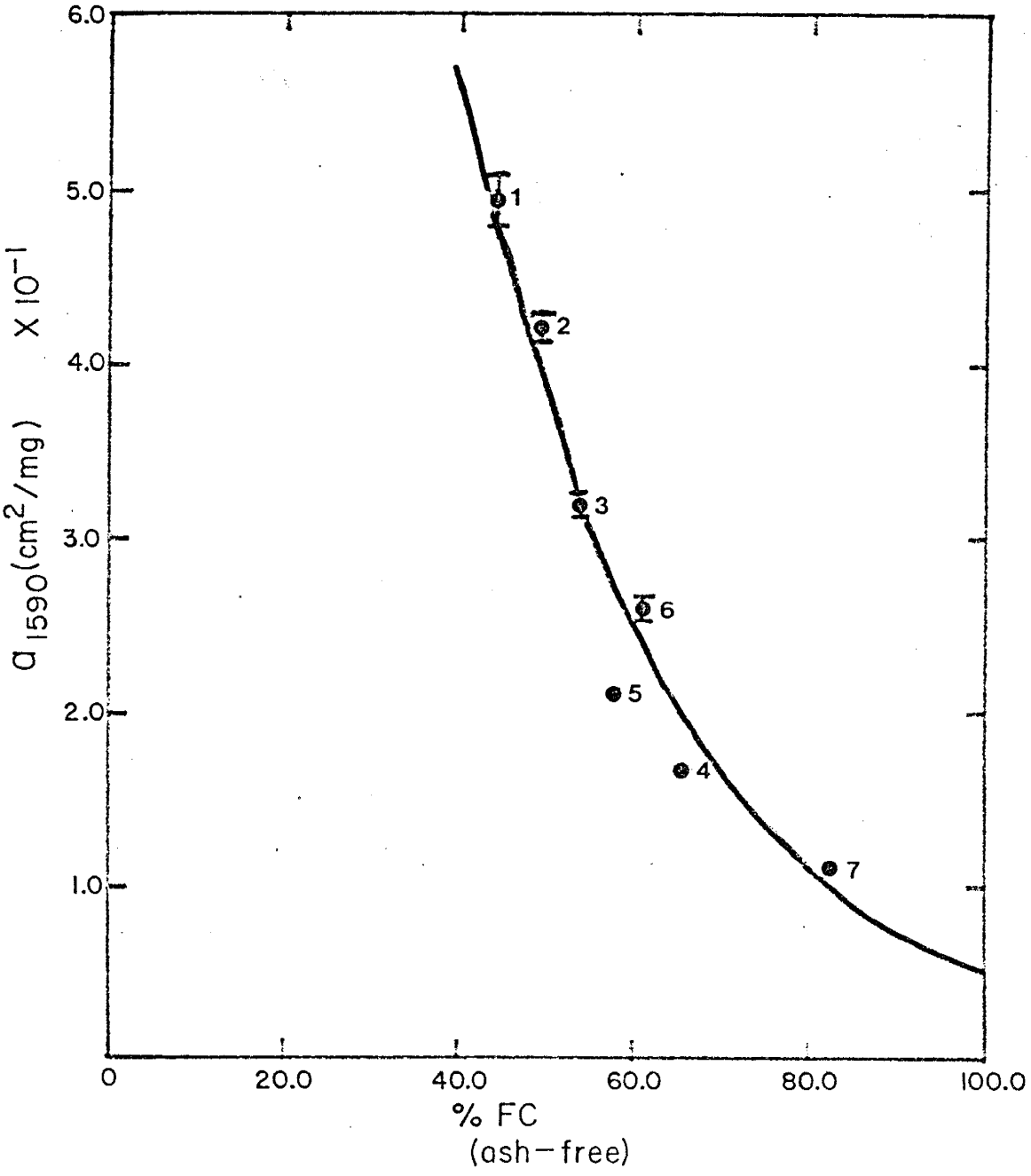

Figure 15. Plot of mean absorptivity values at 1590 cm-1 versus fixed carbon on an ash-free basis for Coals 1-7. Vertical bars represent the sample standard deviation.

absorptivity which directly correspond to small changes in fixed carbon. Low-rank whole coals have high absorptivities whereas higher-rank whole coals have relatively low absorptivities. Extrapolation of the curvilinear correlation line to 100% FC (ash-free) yields an absorptivity of 0.0487 cm^2/mg. This is a rational estimated absorptivity value for the following reason. The functional groups contributing to the band near 1590 cm^{-1} are summarized in Table 4. Brown (1955), Brown and Hirsch (1955), and others demonstrated that the aromaticity of high rank, humic, whole coals (i.e. more than or equal to 87% fixed carbon, dry ash-free basis) significantly increases with increasing rank while corresponding decreases in aliphaticity and alicyclicity attend increasing rank. The 1590 cm^{-1} band typical of most coals and kerogens in part arises from ring vibrations (>C=C< stretch) characteristic of single- and condensed-ring aromatic compounds. The 1590 cm^{-1} band intensity generally is weak in condensed polyaromatic hydrocarbons containing more than three rings and alkyl-substituted benzenes (Bellamy, 1958; Conley, 1972). Brown (1955, p. 751) states, "a very pronounced absorption band near 1600 cm^{-1} is present in the spectra of all the coals (coals ranged from 74% to 94% carbon, moist. ash-free), except in the anthracites, where the high background absorption obliterates the spectra in this region." Thus considering the statement by Brown coupled with evidence for increasing aromaticity accompanying increasing rank suggest that a weak 1590 cm^{-1} band hypothetically should persist in whole coals with extremely high carbon (ash-free) contents, e.g. anthracite and meta-anthracite. Magnitude of

the estimated absorptivity value (a = 0.0487 cm^2/mg) should be evaluated by Fourier Transform Infrared (FTIR) spectroscopy techniques on a large number of anthracites and meta-anthracites in order to substantiate the accuracy of this calculated absorptivity.

A rectilinear best-fit correlation line defined by a = 0.372 $1.0X10^{-2}$ (%FC, ash-free) with a -0.914 correlation coefficient, also characterizes the apparent inverse relationship between absorptivity at 1590 cm^{-1} and fixed carbon (ash-free). Extrapolation of the rectilinear correlation line to the abscissa yields a fixed carbon value of approximately 87.2% FC (ash-free). This case does not seem plausible and so is not given any further attention.

Absorptivity at 1590 cm^{-1} versus Volatile Matter Content

Considerable dispersion of the points about a curvilinear best-fit correlation line occurs when plotting absorptivity at 1590 cm^{-1} against volatile matter, Figure 16. In general, absorptivity decreases correspond to decreases in volatile matter content accompanying increasing rank for the seven whole coals studied. Coals 2 and 5 have similar volatile matter content, Table 2, although Coal 2 (a = 0.421 cm^2/mg) has an absorptivity twice as large as the absorptivity of Coal 5 (a = 0.213 cm^2/mg). This relationship strongly suggests that all the data are not independent particularly for the 1590 cm^{-1} band.

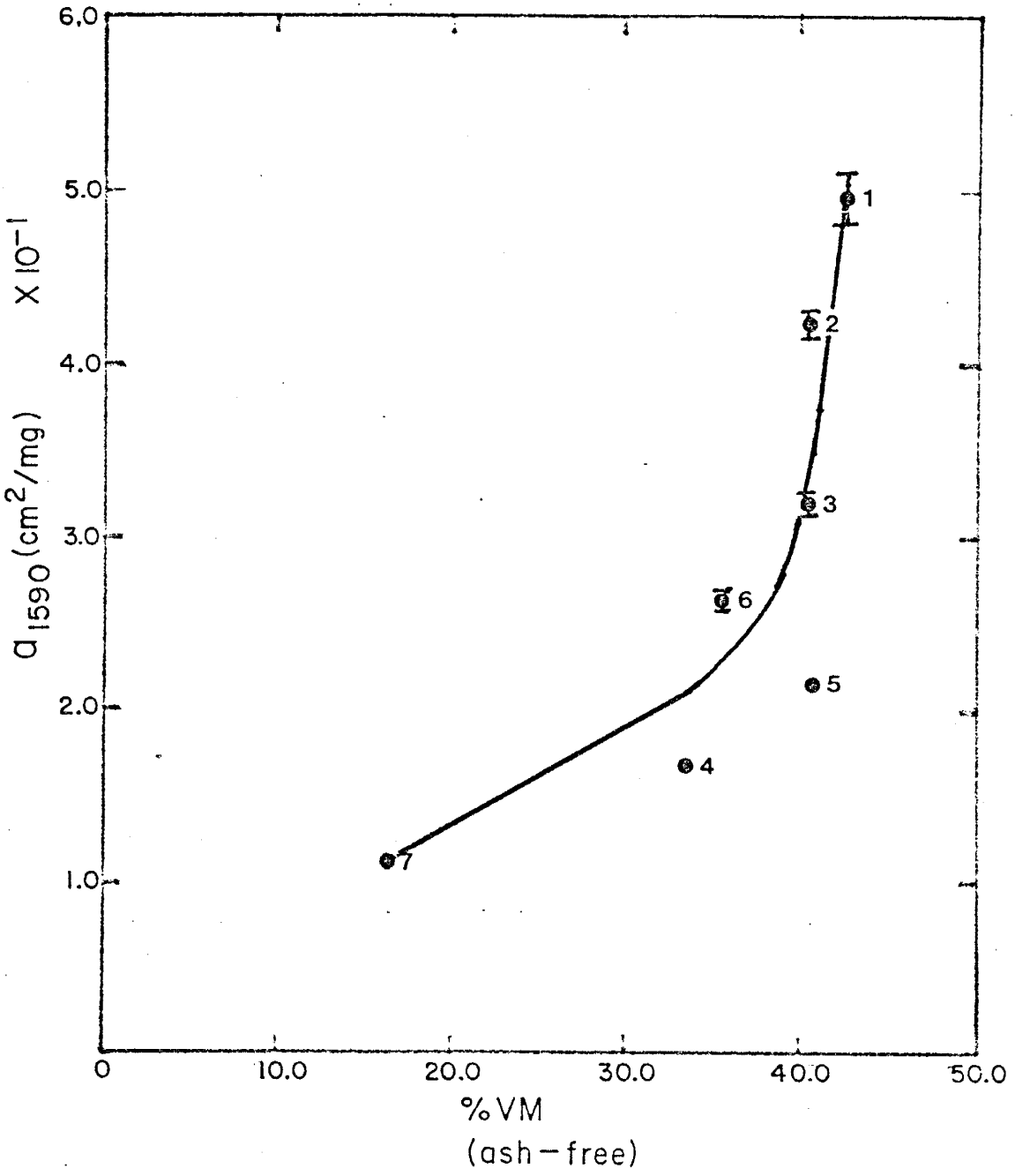

Figure 16. Mean absorptivity values at 1590 cm-1 plotted against volatile matter on an ash-free basis for Coals 1-7. Vertical bars indicate the sample standard deviation.

Absorptivity at 1590 cm^{-1} versus Moisture Content

Plotting absorptivity at 1590 cm^{-1} against moisture content on an ash-free basis, Figure 17, reveals a linear relation, defined by $a = 3.66X10^{-2}$ (%Moist, ash-free) + 0.124 with a 0.980 correlation coefficient, which demonstrates that as moisture content decreases absorptivity decreases. Low-rank whole coals have high absorptivities whereas higher rank whole coals have relatively low absorptivities. Extrapolation of the rectilinear correlation line to the ordinate, i.e. %moist = 0.00%, shows an absorptivity of 0.124 cm^2/mg which is attributable to deformational modes of functional groups other than hydroxyl (OH) groups of molecular water. These data and the resultant interpretation of the 1590 cm^{-1} band support the assertion offered above to explain the presence of this band in whole coals of every rank.

Absorptivity at 1590 cm^{-1} versus Calorific Value

A curvilinear relation having good correlation appears when plotting absorptivity at 1590 cm^{-1} against calorific value on an ash-free basis, Figure 18. In general, absorptivity decreases with increasing calorific value and rank. Figure 18 shows small changes in calorific value (ash-free) result in relatively large changes in absorptivity for the 9000 to 13800 BTU/lb region while small changes in calorific value result in relatively large changes in absorptivity for the more than 13800 BTU/lb (ash-free) whole coals. Low-rank whole coals

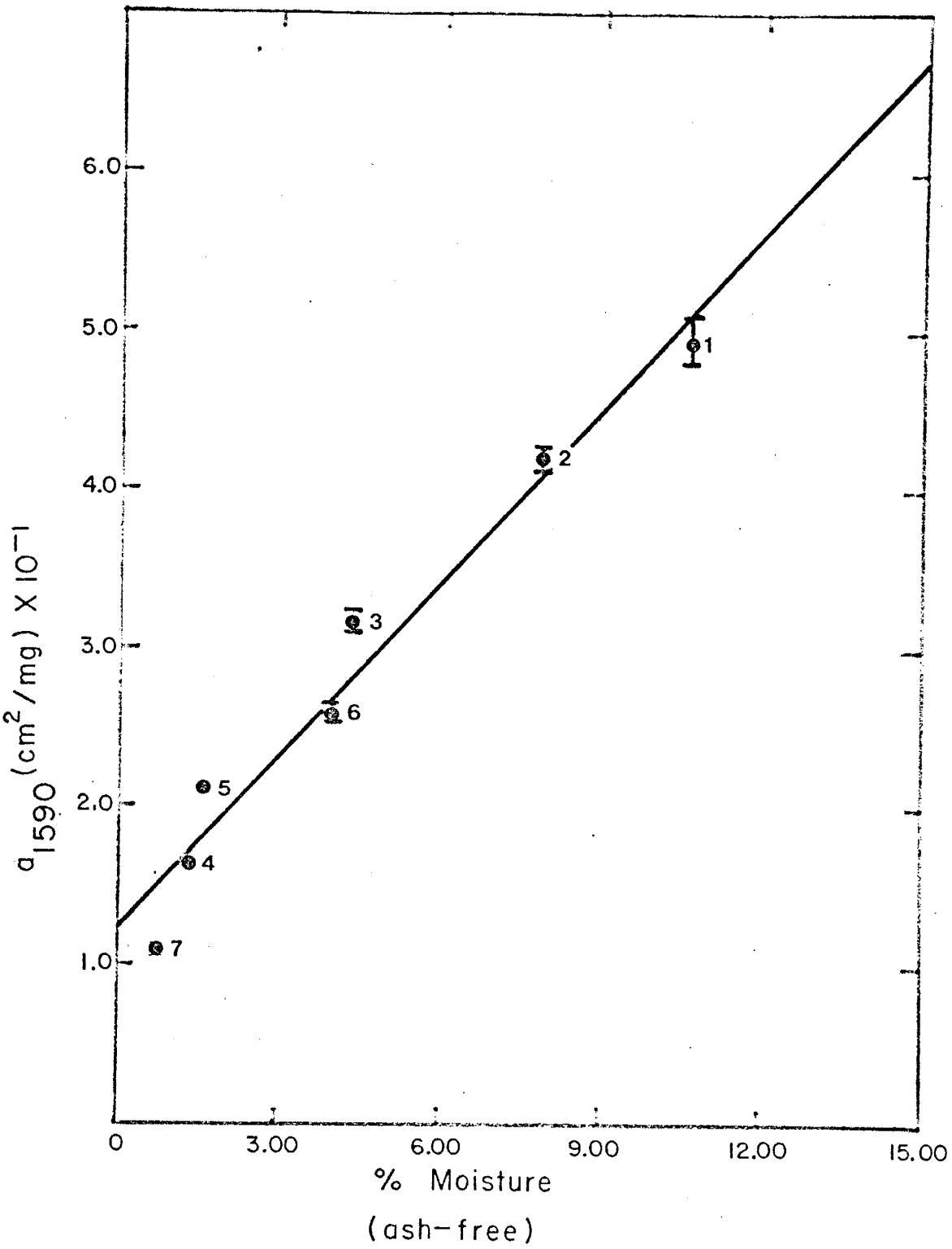

Figure 17. Mean absorptivity values at 1590 cm-1 plotted as a function of moisture on an ash-free basis for Coals 1-7. Vertical bars represent the sample standard deviation.

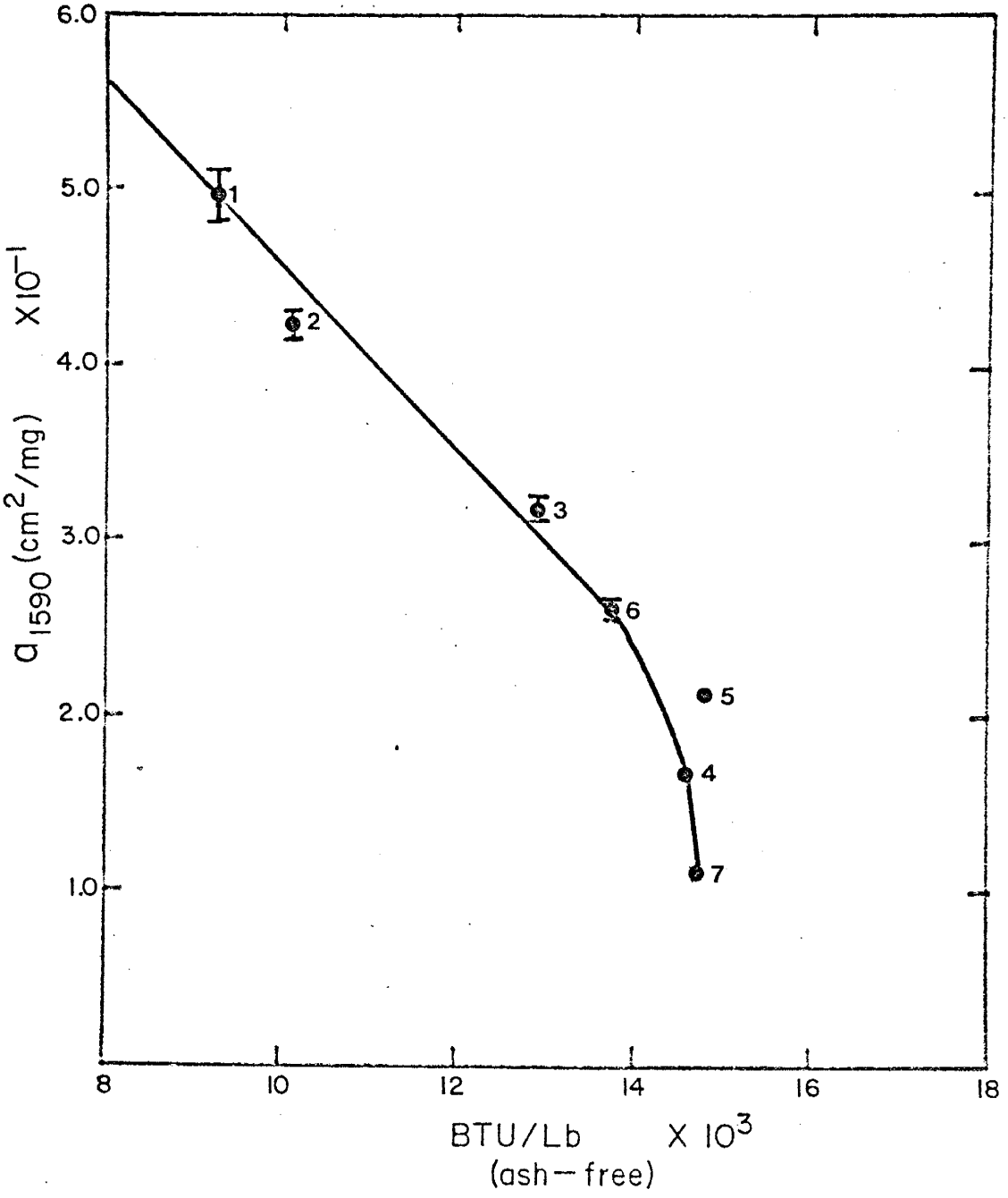

Figure 18. Plot of mean absorptivity values at 1590 cm-1 against calorific value on an ash-free basis for Coals 1-7. Vertical bars indicate the sample standard deviation.

have high absorptivities corresponding to low calorific values (ash-free) whereas high-rank whole coals have low absorptivities attending high calorific values (ash-free).

Linear regression analysis on the data reveals that a rectilinear relation, defined by $a = 1.025 - 5.8X10^{-5}$ (BTU/lb, ash-free) with a -0.961 correlation coefficient, can be used to describe the inverse relationship between absorptivity at 1590 cm^{-1} and calorific value. Extrapolating this rectilinear correlation line to the abscissa, i.e. $a = 0.000$ cm^2/mg, has no practical utility since as previously noted the 1590 cm^{-1} band is present in the spectra of all coals. This rectilinear relationship between absorptivity at 1590 cm^{-1} and calorific value (BTU/lb) on an ash-free basis shows absorptivity decreases with increasing calorific values or with increasing rank.

Absorptivity at 1440 cm^{-1} versus Fixed Carbon Content

Figure 19 shows absorptivity at 1440 cm^{-1} plotted against fixed carbon on an ash-free basis. A linear relation, defined by $a = 0.530 - 5.87X10^{-3}$ (%FC, ash-free) with a 0.984 correlation coefficient, demonstrates that as fixed carbon increases absorptivity decreases correspondingly. Low-rank whole coals characteristically have high absorptivities while high-rank whole coals have relatively low absorptivities. Extrapolation of the rectilinear correlation line to the abscissa ($a = 0.000$ cm^2/mg) yields a fixed carbon value of 90.3%

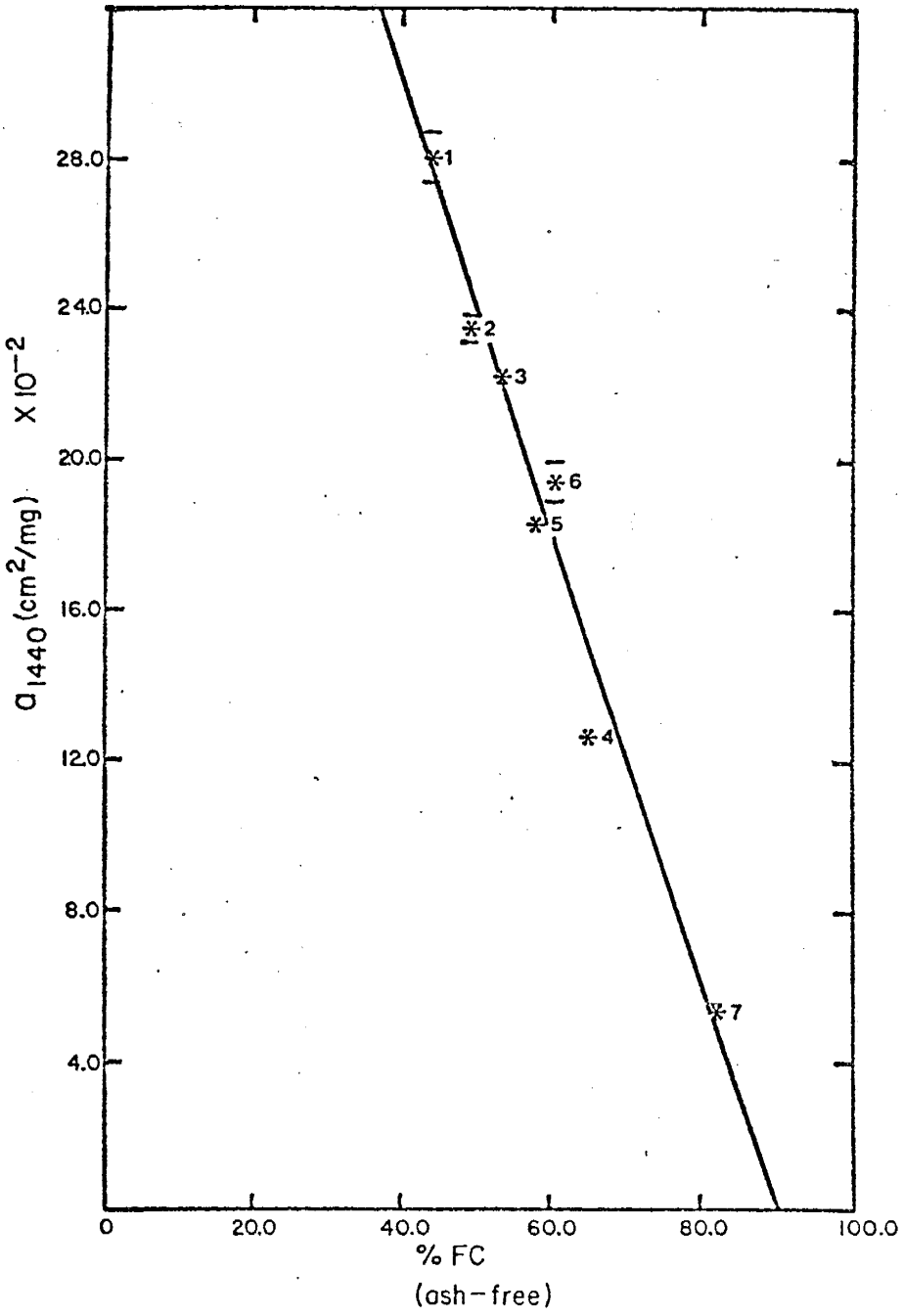

Figure 19. Mean absorptivity values at 1440 cm-1 plotted as a function of fixed carbon on an ash-free basis for Coals 1-7. Vertical bars represent the sample standard deviation.

suggesting that no absorbance should be discernible in whole coals with more than or equal to 90% FC (ash-free). The strong, ubiquitous electronic absorption characterizing high-rank whole coals (anthracite), here masks the zero absorbance (Brown, 1955) corresponding to more than or equal to 90% FC (ash-free). These data support the contention that whole coals with high carbon contents, such as anthracite, have the carbon atoms arranged dominantly in polyaromatic clusters and stacks with alkyl (C-H) groups representing quantitatively minor constituents in the structure.

Absorptivity at 1440 cm^{-1} versus Volatile Matter Content

Figure 20, the plot of absorptivity at 1440 cm^{-1} versus volatile matter on an ash-free basis, shows absorptivity decreases with decreasing volatile matter. High-rank whole coals such as Coals 4 and 7 have relatively low volatile matter contents and thus low absorptivities, whereas low-rank whole coals such as Coals 1, 2 and 3 have relatively high volatile matter contents and thus high absorptivities.

An exponential correlation line, defined by $\ln a = 0.0581$ (%VM, ash-free) - 3.898 with a 0.977 correlation coefficient, shows that small changes in volatile matter content for whole coals with approximately more than 35% volatile matter result in significantly large changes in absorptivities. The loss of volatile components contributing to the

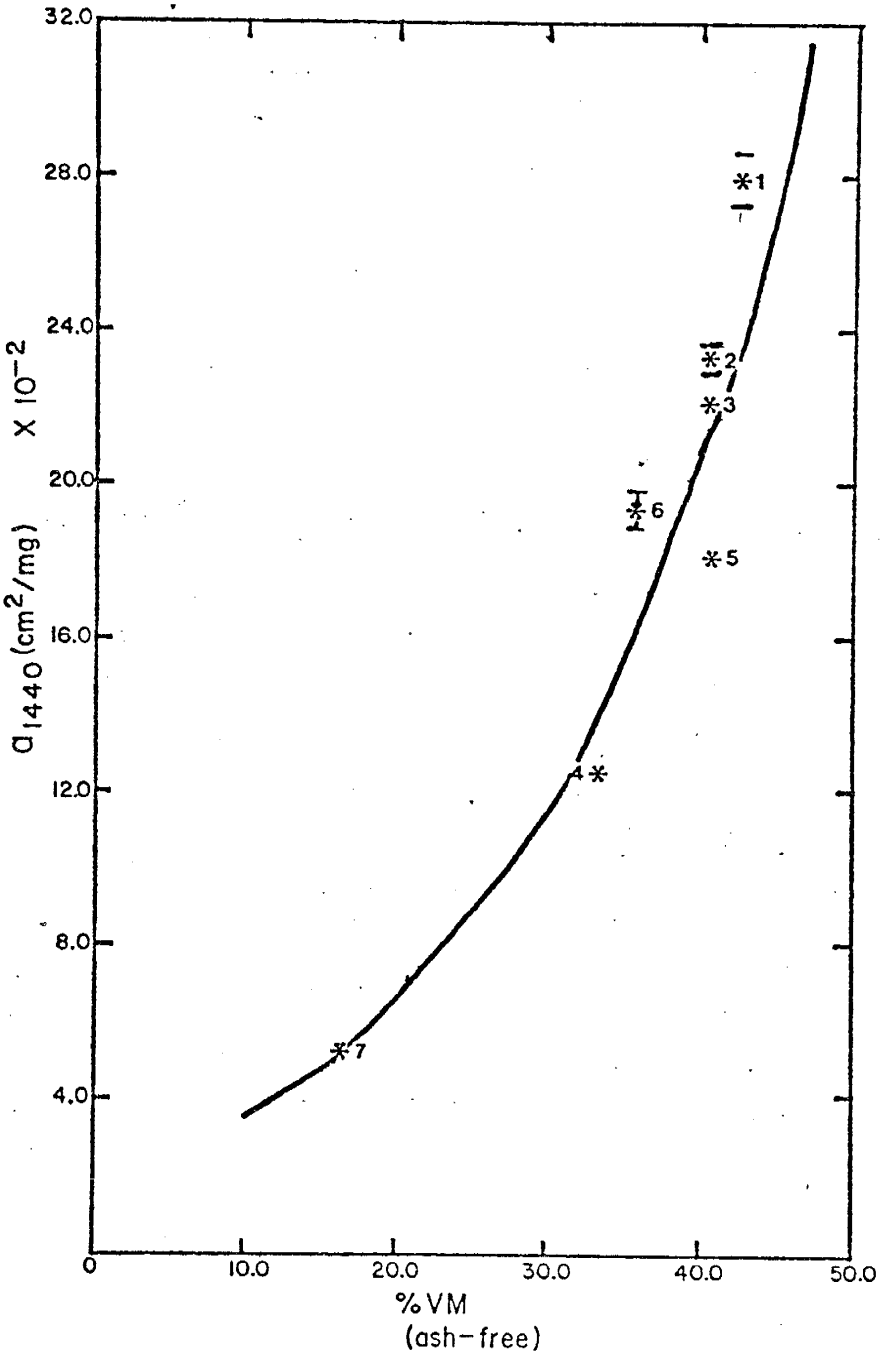

Figure 20. Mean absorptivity values at 1440 cm-1 plotted against volatile matter on an ash-free basis for Coals 1-7. Vertical bars indicate the sample standard deviation.

1440 cm^{-1} band absorption for whole coals with less than 35% volatile matter apparently occucs more gradually than for whole coals with relatively greater volatile matter contents.

Extrapolation of the exponential correlation line to the ordinate, i.e. VM = 0.00%, yields an absorptivity of 0.020 cm^2/mg suggesting that as volatile matter (ash-free) content of whole coals approaches zero a weak but detectable absorbance should persist. This absorptivity value seems unreasonably high when considering the highly aromatic nature of whole coals containing virtually no volatile matter (ash-free) such as meta-anthracite, since the 1440 cm^{-1} band is generally assigned to alkyl C-H (CH_2 - CH_3 asymmetrical bending) deformational modes.

Linear regression analysis on the data defines a line: a = $7.59X10^{-3}$ (%VM, ash-free) - 0.086 with a 0.913 correlation coefficient. This also may be used to describe the relationship between absorptivity at 1440 cm^{-1} and volatile matter content and shows absorptivity decreases with decreasing volatile matter. Extrapolation of the rectilinear best-fit correlation line to the abscissa (a = 0.000 cm^2/mg) yields a volatile matter value of 11.3% which corresponds to semi-anthracite coal suggesting no absorbance should be detectable in whole coals with approximately less than or equal to 11% volatile matter (ash-free). The intense electronic absorption in high-rank whole coals (Brown, 1955) does not permit a direct determination of the less than or equal to 11% volatile matter value. This relationship between

absorptivity at 1440 cm^{-1} and volatile matter suggests that the absorptivity at 1440 cm^{-1} is strongly related to alkyl moieties within the whole coal.

Absorptivity at 1375 cm^{-1} versus Fixed Carbon Content

Figure 21 shows absorptivity at 1375 cm^{-1} plotted against fixed carbon content on an ash-free basis. An exponential curvilinear relation, defined by $\ln a = 1.068 - 0.052$ (%FC, ash-free) with a 0.980 correlation coefficient, demonstrates that as fixed carbon increases absorptivity decreases. Rapid decreases in absorptivity attend relatively small increases in fixed carbon (ash-free) for fixed carbon contents ranging from approximately 42% to approximately 81%. Extrapolation of the exponential correlation line to 100% FC (ash-free) yields an 0.0165 cm^2/mg absorptivity. This absorptivity value is unreasonable for a system consisting of 100% carbon.

Alternatively a linear best-fit correlation line, defined by $a = 0.546 - 6.55X10^{-3}$ (%FC, ash-free) with a -0.930 correlation coefficient, describes the inverse relationship between absorptivity at 1375 cm^{-1} and fixed carbon. Extrapolation of the linear best-fit correlation line to the abscissa ($a = 0.000$ cm^2/mg) yields an 83.4% FC value, which suggests that whole coals with more than 83% FC (ash-free) should exhibit no discernible absorbance at 1375 cm^{-1}. The strong electronic absorption here in high-rank whole coals (Brown, 1955) obliterates the zero

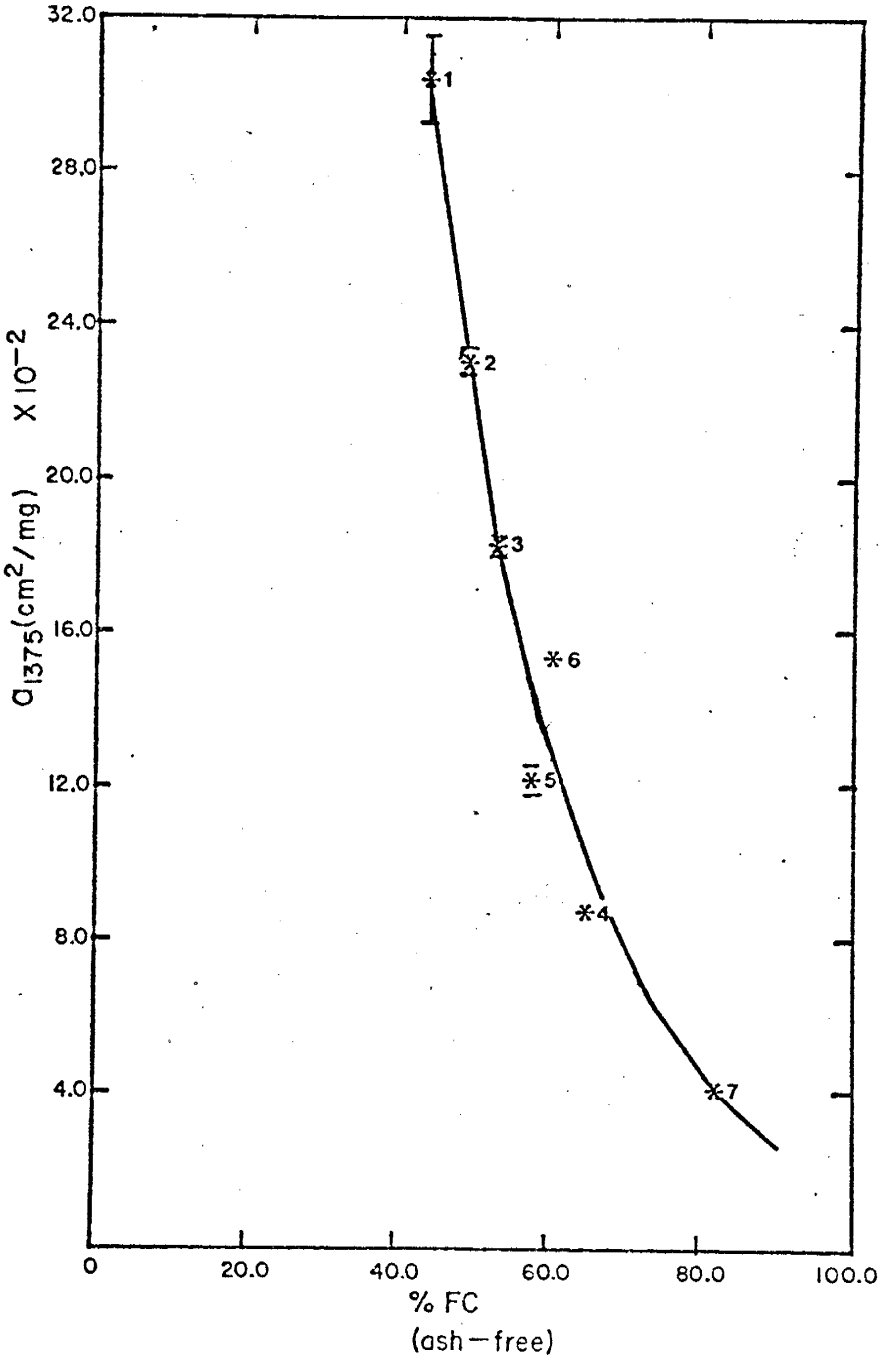

Figure 21. Plot of mean absorptivity values at 1375 cm-1 versus fixed carbon on an ash-free basis for Coals 1-7. Vertical bars indicate the sample standard deviation.

absorbance corresponding to more than 83% FC (ash-free). In light of the present knowledge of coal structure, the 83% FC (ash-free) value, which corresponds to no discernible absorbance at 1375 cm^{-1}, is a creditable estimate for this relationship.

Absorptivity at 1375 cm^{-1} versus Volatile Matter Content

Plotting absorptivity at 1375 cm^{-1} against volatile matter content on an ash-free basis, Figure 22, shows absorptivity decreases with decreasing volatile matter. An exponential curvilinear correlation line, defined by ln a = 0.065 (%VM, ash-free) - 4.343 with a 0.927 correlation coefficient is not shown in Figure 22. Extrapolation of the exponential correlation line to the ordinate, i.e. VM = 0.00%, yields an 0.013 cm^2/mg absorptivity. Here again considering the high degree of aromaticity characteristic of high rank whole coals with virtually no volatile matter (ash-free) such as meta-anthracite, the 0.013 cm^2/mg absorptivity does not appear to be a creditable estimate of the absorptivity for high-rank whole coals (whole coals with less than approximately 15% volatile matter), or coals with a rank equal to or higher than low volatile bituminous coal. ½NOTE: extrapolation of the exponential best-fit curvilinear correlation line (shown in Figure 22) to the abscissa (a = 0.000 cm^2/mg) yields approximately 1.5% volatile matter (ash-free) suggesting that the 1375 cm^{-1} band persists as a discernible absorption band up to the meta-anthracite rank. The intense electronic absorption here in high-rank whole coals (anthracites) does

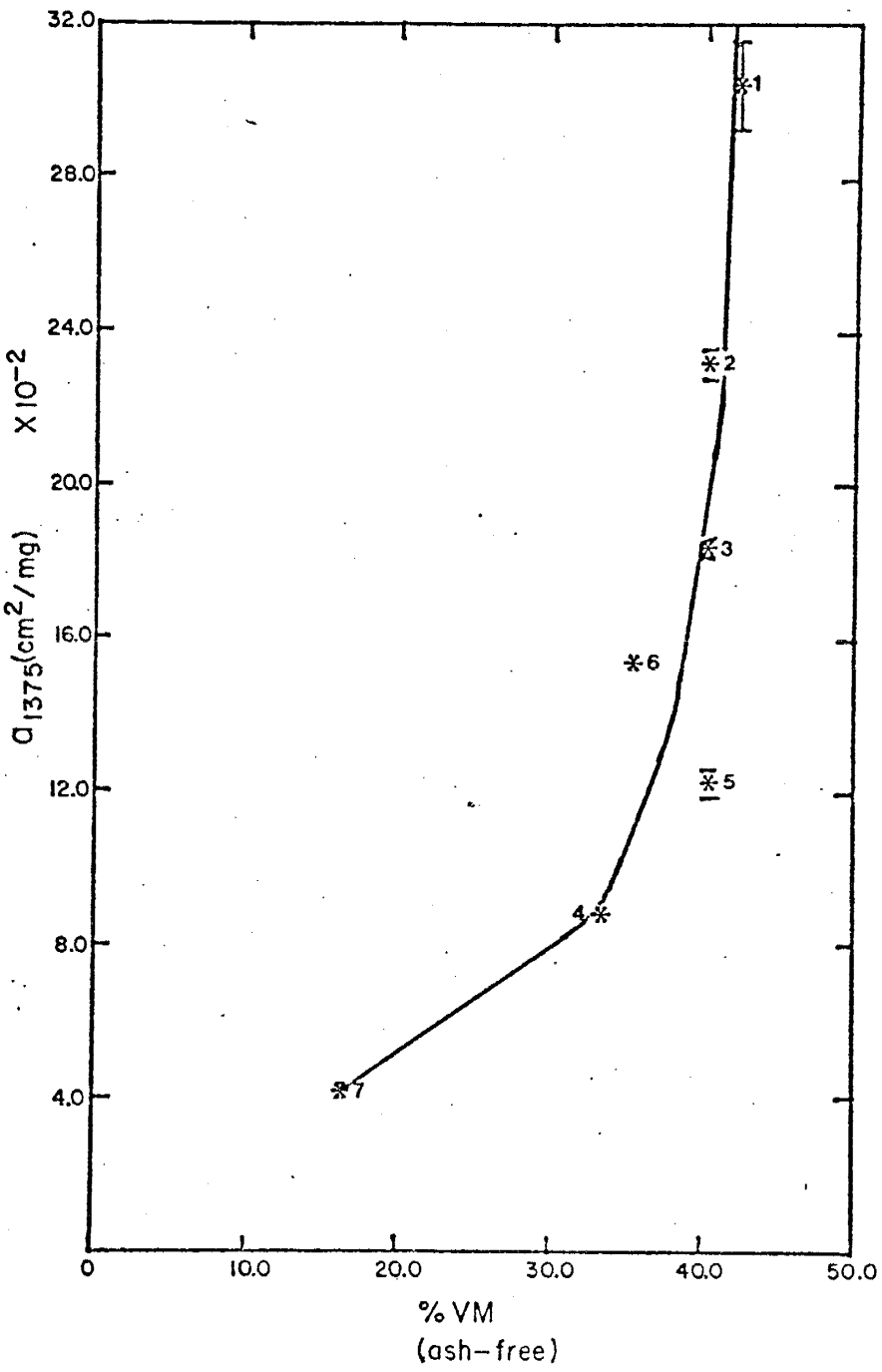

Figure 22. Mean absorptivity values at 1375 cm-1 plotted as a function of volatile matter on an ash-free basis for Coals 1-7. Vertical bars indicate the sample standard deviation.

not permit a direct determination of the approximately 1.5% volatile matter value. This case seems to yield a more plausible value than the previous case although work by Rouxhet et al. (1980) shows that the absorbance of aliphatic functional groups becomes immeasurably small in anthracite (volatile matter range for anthracite is more than 2% but less than 8%).

The relationship between absorptivity at 1375 cm^{-1} and volatile matter (ash-free) may be more apparent than real since as noted by Bent et al. (1964, p. 9), "the intensity of the 1375 cm^{-1} band depends to some extent on the nature of the attached molecule. . . ., the intensity of the methyl group adsorption remains fairly constant provided that it is attached to a system of saturated carbon atoms, but tends to be less intense when the methyl group is attached to an aromatic carbon atom system." According to Rouxhet et al. (1980) the 1375 cm^{-1} band is mainly due to symmetrical bending of methyl ($-CH_3$) groups with only negligible contributions from methylene ($>CH_2$) groups. The contribution of methylene groups to the 1375 cm^{-1} band becomes more significant when methylene groups are close to an oxygenated function (Francis, 1951, pp 944-945). The loss of many oxygenated functionalities is rather rapid for low-rank whole coals, i.e. whole coals with rank less than high volatile A bituminous (Rouxhet et al., 1980; and Rouxhet et al., 1979). In other words, many oxygenated functionalities inherent to organic matter in low-rank whole coals are lost early in the maturation of coal. This fact to some extent may explain the rapid decrease in absorptivity

at 1375 cm^{-1} for whole coals with more than approximately 38% VM (ash-free), i.e. rank less than high volatile B bituminous coal. The exponential relationship between absorptivity at 1375 cm^{-1} and volatile matter on an ash-free basis perhaps reflects concomitant losses of oxygenated functionalities and hydrocarbons in whole coals covering a wide range of rank. The range of rank covered in this study is from sub-bituminous to low volatile bituminous.

Absorptivity at 1250 cm^{-1} versus Fixed Carbon Content

Plotting absorptivity at 1250 cm^{-1} against fixed carbon content on an ash-free basis, Figure 23, demonstrates that absorptivity decreases correspond to increasing fixed carbon content. A linear relation, defined by $a = 0.490 - 5.86X10^{-3}$ (%FC, ash-free) with a -0.952 correlation coefficient, illustrates that the low-rank whole coals studied have high absorptivities and conversely high-rank whole coals have low absorptivities. Extrapolation of this inverse linear correlation line to the abscissa ($a = 0.000$ cm^2/mg) yields 83.6% FC (ash-free) which suggests whole coals with approximately 83% FC (ash-free) should exhibit no discernible absorbance at 1250 cm^{-1}. The intense electronic absorption here in high-rank whole coals (Brown, 1955) obliterates the zero absorbance corresponding to more than 83% FC (ash-free).

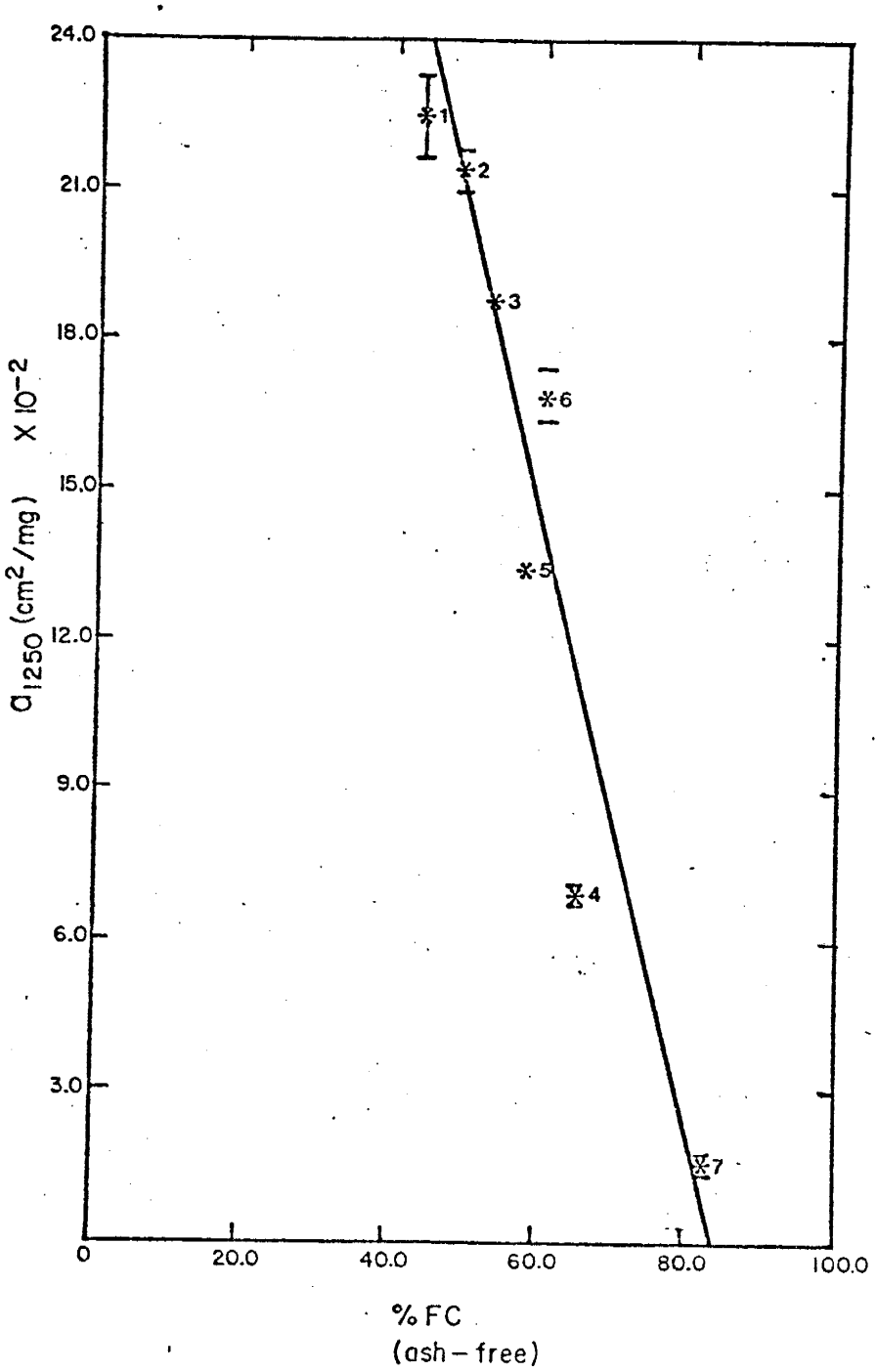

Figure 23. Plot of mean absorptivity values at 1250 cm-1 against fixed carbon on an ash-free basis for Coals 1-7. Vertical bars represent the sample standard deviation.

Absorptivity at 1250 cm^{-1} versus Volatile Matter Content

Figure 24 shows the plot of absorptivity at 1250 cm^{-1} versus volatile matter content on an ash-free basis. An exponential curvilinear relation, defined by ln a =0.098 (%VM, ash-free) - 5.745 with a 0.966 correlation coefficient, illustrates that relatively gradual decreases in absorptivity attend decreases in volatile matter content for the range between approximately 35% VM and 17% VM (ash-free) while absorptivities rapidly decrease with small decreases in volatile matter content for the greater than 35% VM (ash-free) region of Figure 24. Extrapolation of the exponential best-fit curvilinear correlation line to the ordinate, i.e. VM = 0.00%, yields a = 0.0032 cm^2/mg. The low absorptivity value approaches the lower limit of detection for the instrumental conditions employed and thus probably represents experimental errors rather than the absorptivity expected for whole coals with virtually no volatile matter. It can be rationally inferred from the data that absorptivity at 1250 cm^{-1} may approach zero as volatile matter content approaches zero in whole coals.

Absorptivity at 795 cm^{-1} versus Fixed Carbon Content

Figure 25 shows the plot of absorptivity at 795 cm^{-1} versus fixed carbon content on an ash-free basis. A curvilinear best-fit correlation line in Figure 25 shows absorptivity increases with increasing fixed carbon content. Coal 2 with approximately 49% FC has an absorptivity (a

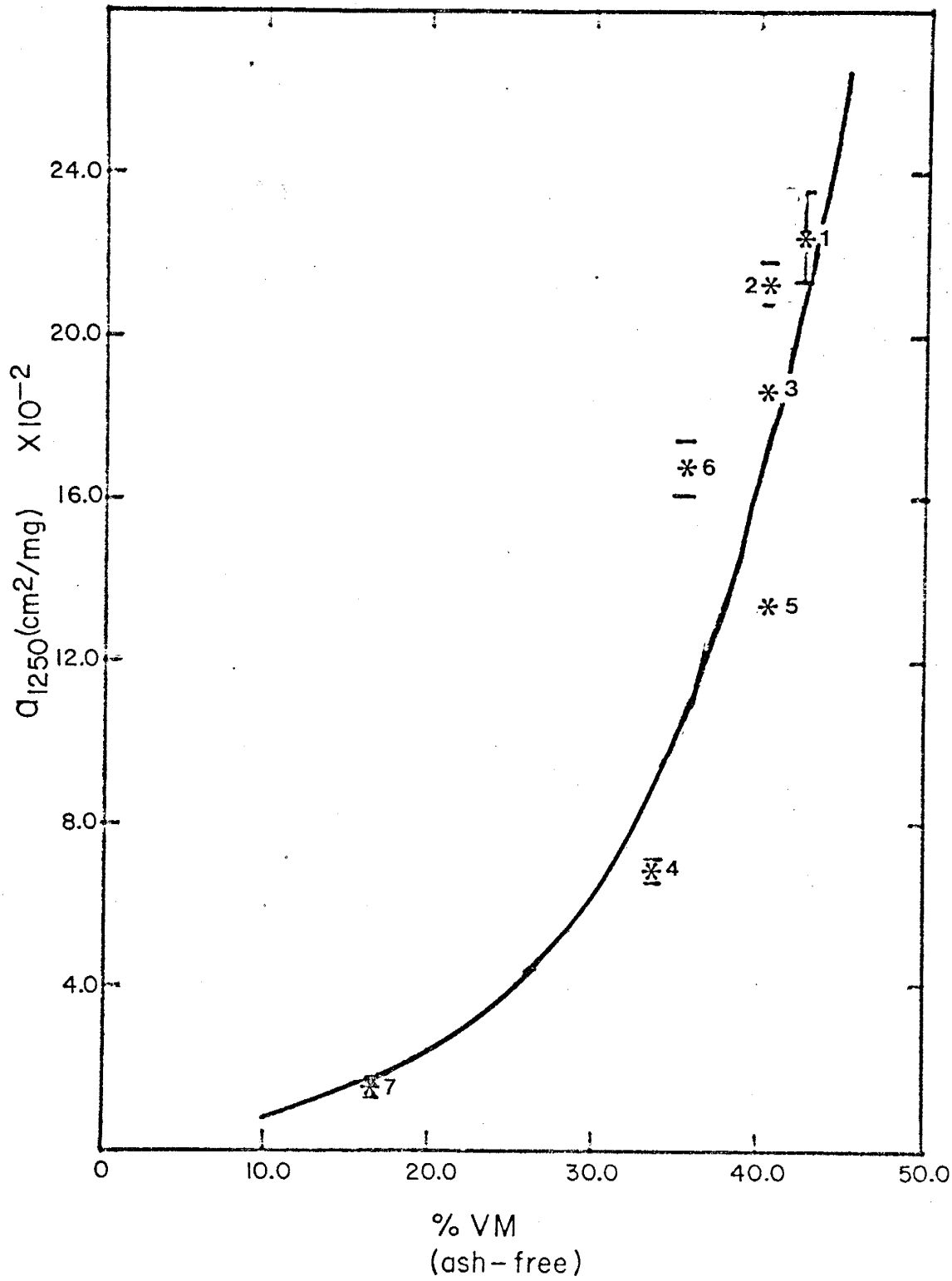

Figure 24. Mean absorptivity values at 1250 cm-1 plotted against volatile matter on an ash-free basis for Coals 1-7. Vertical bars indicate the sample standard deviation.

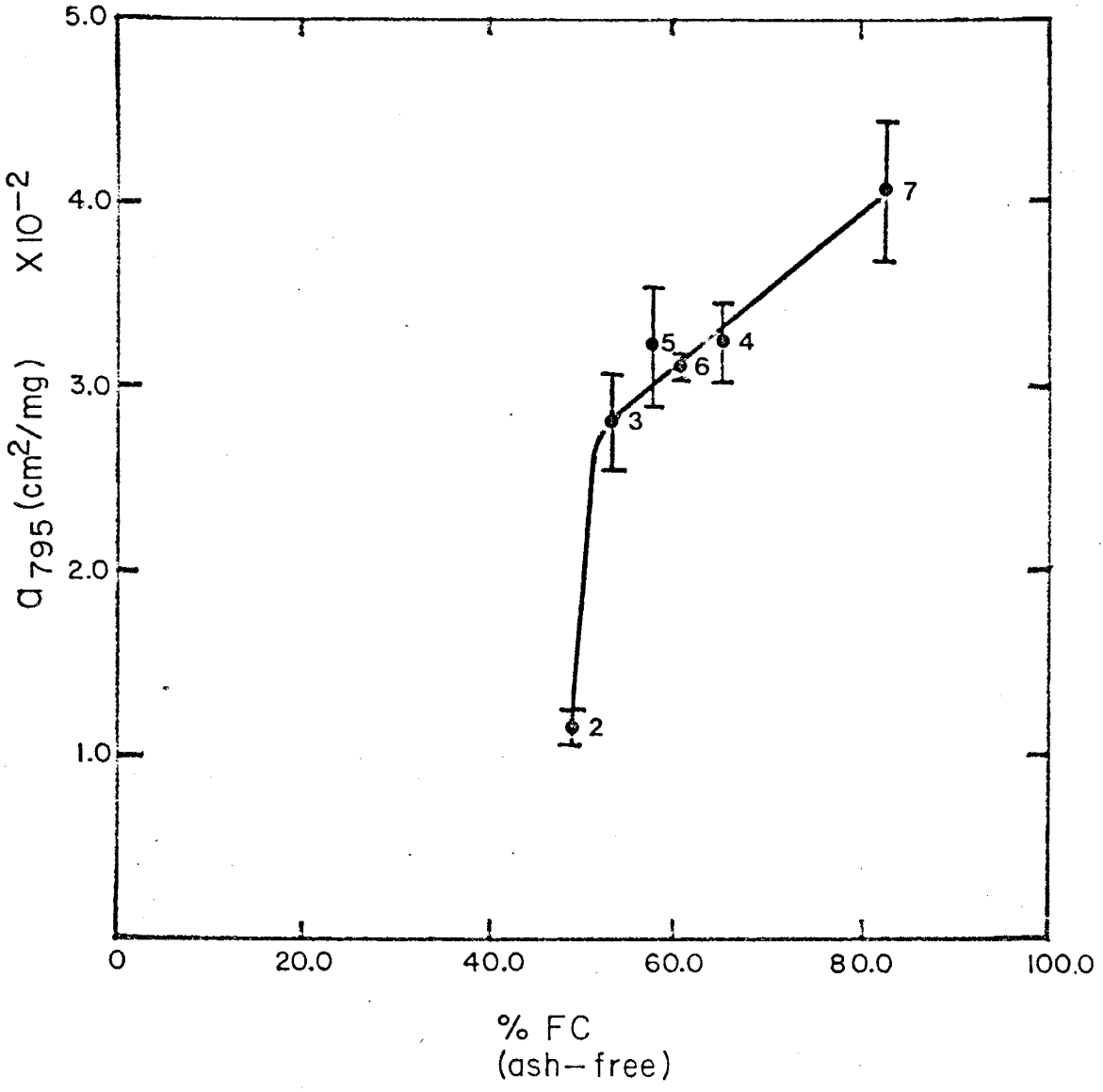

Figure 25. Mean absorptivity values at 795 cm-1 plotted as a function of fixed carbon on an ash-free basis for Coals 2-7. Vertical bars indicate the sample standard deviation.

= 0.0115 cm^2/mg) approximately 2.5 times less than that of Coal 3 (a = 0.0281 cm^2/mg) with approximately 53% FC (ash-free). For the whole coals containing more than approximately 53% FC (ash-free) but less than approximately 83% FC (ash-free) absorptivity increases are correspondingly small for moderate increases in fixed carbon (ash-free) content. High-rank whole coals such as Coal 7 have relatively high absorptivities, whereas low-rank whole coals such as Coal 2 have very low absorptivities to no distinguishable absorptivity at all---such is the case for Coal 1. Extrapolation of the curvilinear best-fit correlation line to the abscissa (a = 0.000 cm^2/mg) yields approximately 47% FC (ash-free) suggesting that whole coals with less than or equal to 47% FC (ash-free) should exhibit no detectable absorbance at 795 cm^{-1}.

Absorptivity at 740 cm^{-1} versus Fixed Carbon Content

The plot of absorptivity at 740 cm^{-1} versus fixed carbon content on an ash-free basis is shown in Figure 26. A rectilinear best-fit correlation line, defined by $a = 1.27X10^{-3}$ (%FC, ash-free) - 0.052 with a correlation coefficient approximately equal to 0.90, illustrates that a positive relationship between absorptivity increases and increasing fixed carbon (ash-free) content occurs here for the whole coals studied. Extrapolation of the rectilinear best-fit correlation line to the abscissa (a = 0.000 cm^2/mg) yields 41.2% FC (ash-free) suggesting that whole coals with less than or equal to 41% FC (ash-free) should exhibit no distinguishable absorbance at 740 cm^{-1}. Coal 6 has a relatively low

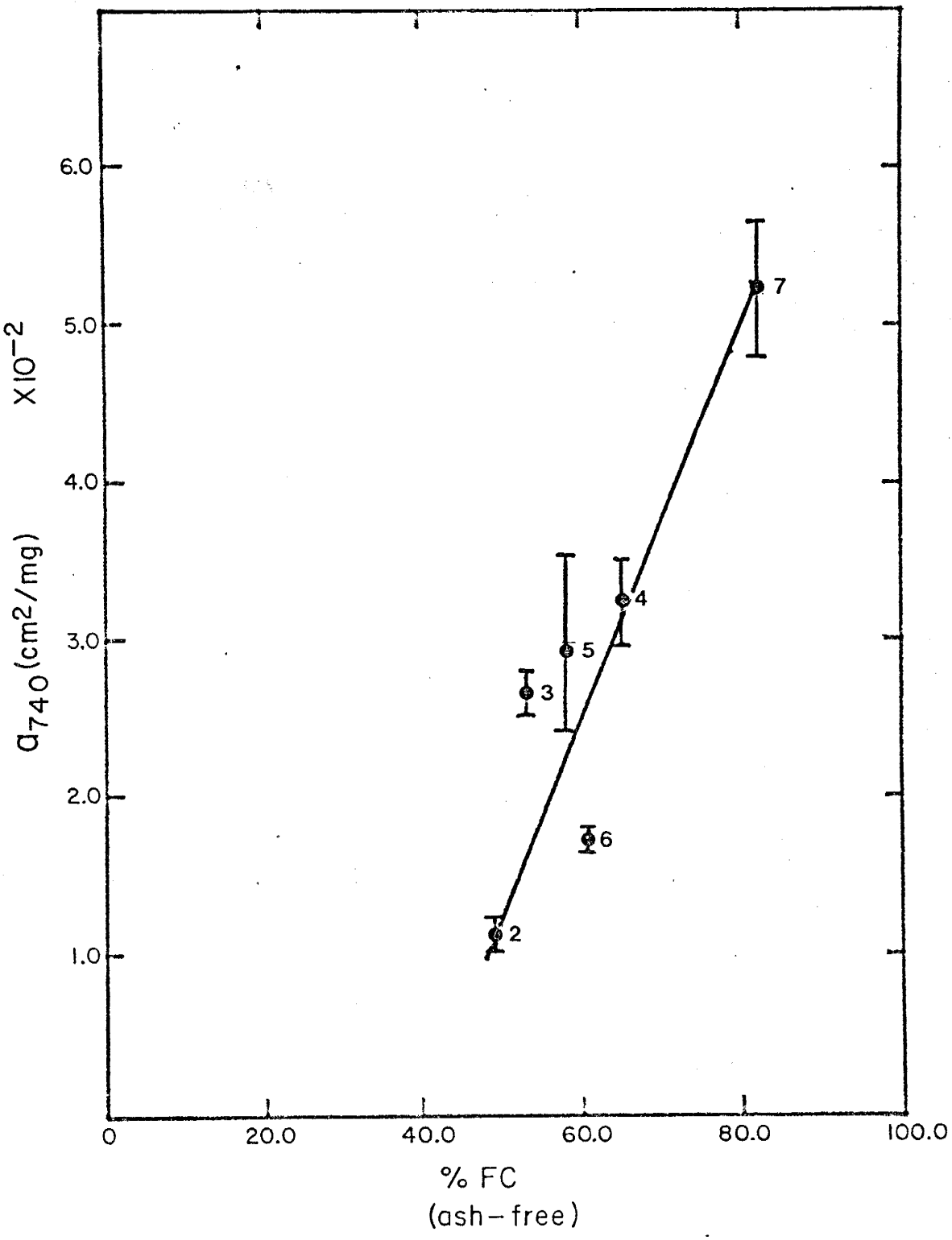

Figure 26. Plot of mean absorptivity values at 740 cm-1 against fixed carbon on an ash-free basis for Coals 2-7. Vertical bars represent the sample standard deviation.

absorptivity in relation to its fixed carbon content (approx. 60.7% FC, ash-free) which suggests Coal 6 has fewer substituted aromatic rings with four adjacent hydrogen atoms than the other whole coals of similar fixed carbon (ash-free) content, such as Coals 4 and 5 in Figure 26.

QUANTITATIVE ANALYSIS OF ABSORPTIVITIES AT A GIVEN FREQUENCY PLOTTED AGAINST ULTIMATE ANALYSIS DATA

Absorptivity at 3400 cm^{-1} versus Carbon Content

Figure 27 shows the plot of absorptivity at 3400 cm^{-1}, measured according to the 3700-3000 cm^{-1} band measurement method, as a function of elemental carbon on a dry, ash-free (daf) basis. The linear correlation line in Figure 27, defined by $a = 0.275 - 3.06X10^{-3}$ (%C, daf) with a -0.957 correlation coefficient, demonstrates rapid absorptivity decreases correspond to small increases in elemental carbon and rank. The linear correlation line (not shown in Figure 27) describing the inverse relationship between absorptivity at 3400 cm^{-1} and elemental carbon (daf), measured according to the Robin-Rouxhet method, is $a = 0.497 - 5.66X10^{-3}$ (%C, daf) with a -0.960 correlation coefficient. Independent of the measurement method employed regression analysis illustrates that an inverse relationship with strong correlation exists between absorptivity at 3400 cm^{-1} and elemental carbon (daf). Extrapolation of the linear correlation line to the abscissa, $a = 0.000$ cm^2/mg, for the 3700-3000 cm^{-1} method yields approximately 89%C (daf) while the Robin-Rouxhet method yields approximately 88%C (daf). These data suggest that whole coals with more than or equal to 88%C (daf) will have no detectable absorbance. Cannon (1953), Friedel and Queiser (1956), and Elofson (1957) showed the 3400 cm^{-1} absorbance is extremely weak for whole coals with more than or

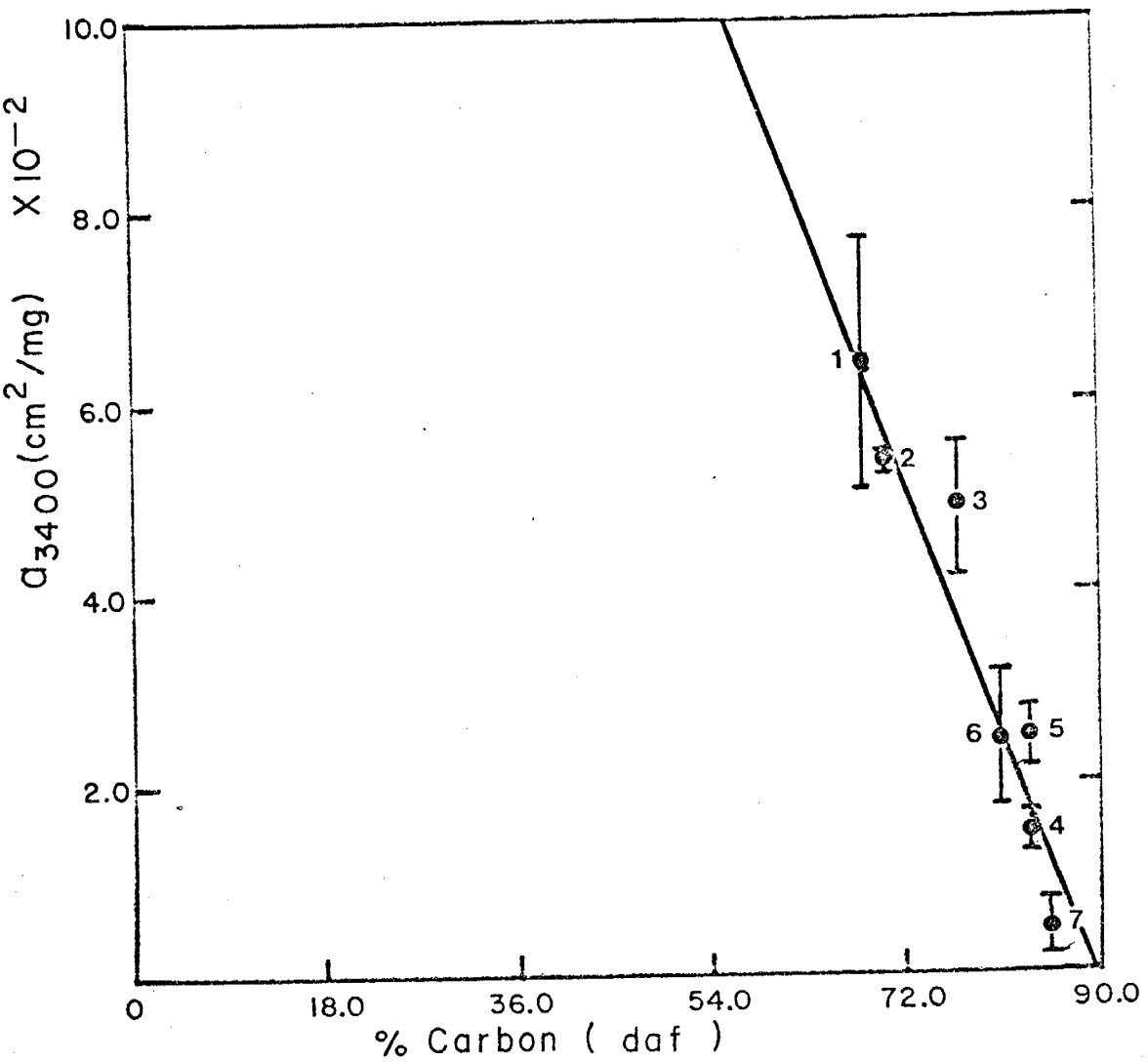

Figure 27. Plot of mean absorptivity values at 3400 cm-1 measured according to the 3700-3000 cm-1 measurement method against carbon concentration for Coals 1-7. Vertical bars indicate the sample standard deviation.

equal to 89%C (daf).

Absorptivity at 3400 cm^{-1} versus Hydrogen Content

Plotting absorptivity at 3400 cm^{-1}, measured according to the 3700-3000 cm^{-1} method, against elemental hydrogen on a dry, ash-free basis, Figure 28, reveals a parabolic relationship. The parabolic relationship illustrates that low-rank whole coals (Coals 1 and 2) with relatively low elemental H (daf) have comparatively high absorptivities while slightly higher rank whole coals (Coals 3-6) with moderate (approx. 5.4% to 5.8% H) but similar elemental H (daf) have decreasing absorptivities corresponding to increasing rank. The highest rank whole coal studied (Coal 7) has an elemental hydrogen (daf) value similar to that of low-rank whole coals (e.g. Coals 1 and 2), although the high-rank whole coal has a very low absorptivity ($a = 0.005$ cm^2/mg) relative to high absorptivities (Coal 1 has $a = 0.064$ cm^2/mg and Coal 2 has $a = 0.054$ cm^2/mg) characterizing the low-rank whole coals. In other words, whole coals of vastly different rank but similar elemental H (daf) contents show high absorptivities corresponding to low-rank whole coals and low absorptivities attending high-rank whole coals.

Absorptivities plotted in Figure 28 were determined by using the 3700-3000 cm^{-1} band measurement method. A parabolic trend very similar to the parabolic trend for the 3700-3000 cm^{-1} method appears when plotting absorptivity at 3400 cm^{-1} measured according to the

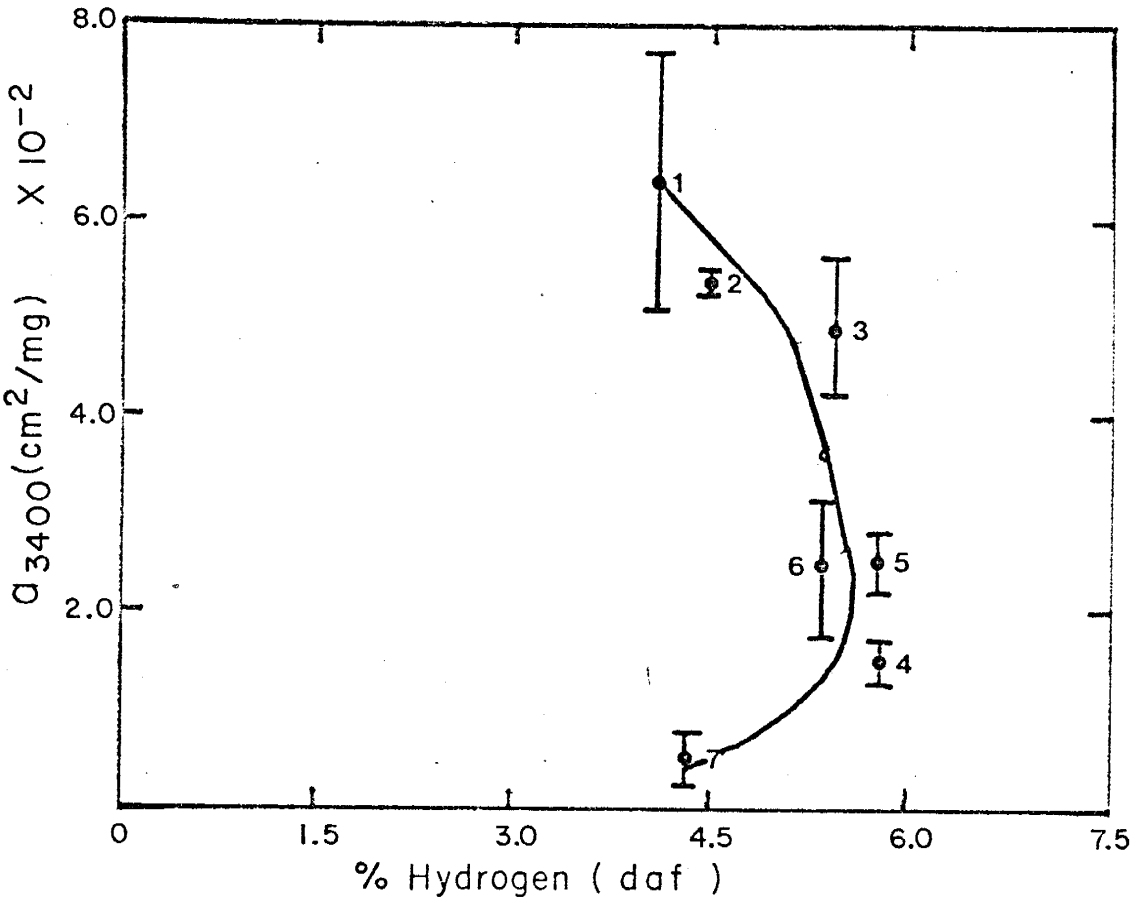

Figure 28. Mean absorptivity values at 3400 cm-1 measured according to the 3700-3000 cm-1 measurement method plotted against hydrogen concentration for Coals 1-7. Vertical bars represent the sample standard deviation.

Robin-Rouxhet method as a function of elemental hydrogen (daf).

Absorptivity at 3400 cm^{-1} versus Oxygen Content

Plotting absorptivity at 3400 cm^{-1}, measured according to the 3700-3000 cm^{-1} method, as a function of elemental oxygen on a dry, ash-free basis, Figure 29, demonstrates that absorptivity decreases generally correspond to decreasing oxygen content. A linear correlation line, defined by $a = 2.68X10^{-3}$ (%O, daf) - $2.9X10^{-3}$ with a 0.926 correlation coefficient, describes the relationship between absorptivity at 3400 cm^{-1} and elemental oxygen content. The low-rank whole coals studied such as Coals 1 and 2 have high elemental oxygen contents (approximately 22-25% O, daf) and thus high absorptivities, whereas the higher rank whole coals, such as Coals 4 and 7, have much lower oxygen contents (approximately 8% O, daf) and hence low absorptivities.

Extrapolation of the linear correlation line to the abscissa, a = 0.000 cm^2/mg, yields an elemental oxygen (daf) value of 1.1% O, suggesting that high-rank whole coals with less than or equal to 1.1% O (daf) will not show a detectable absorbance in the 3400 cm^{-1} region. The linear trend describing the relationship between absorptivity at 3400 cm^{-1} and elemental oxygen, Figure 29, is compatible with the linear trend reported by Osawa and Shih (1971) and Solomon and Carangelo (1982), Figure 30. The absence of a detectable absorbance at 3400 cm^{-1} for whole coals with less than or equal to 1.1% O (daf) suggests that if

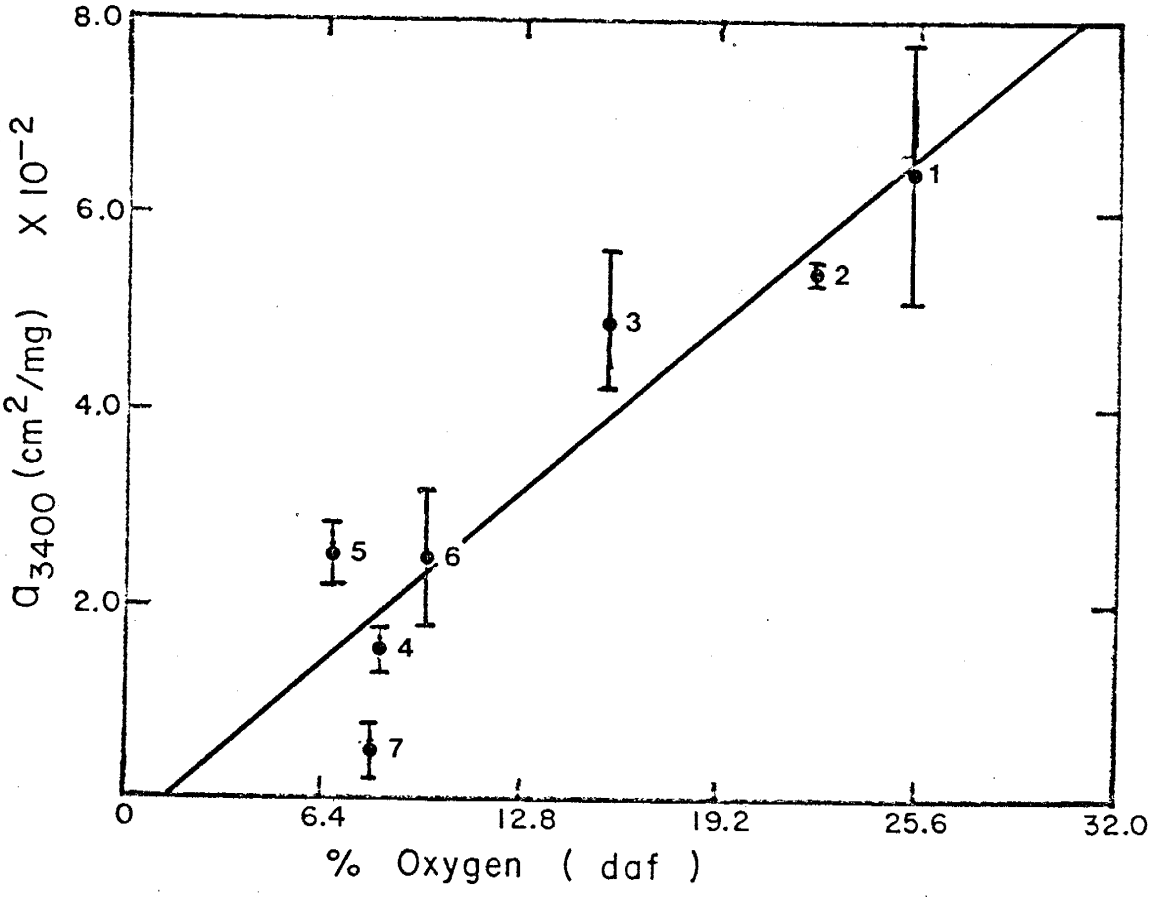

Figure 29. Mean absorptivity values at 3400 cm-1 measured according to the 3700-3000 cm-1 measurement method plotted as a function of oxygen concentration for Coals 1-7. Vertical bars indicate the sample standard deviation.

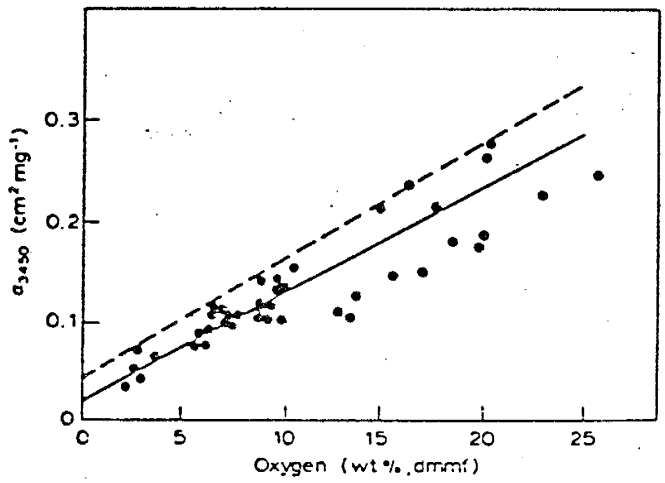

Figure 30. Absorptivity for a number of coals at 3450 cm-1 as a function of oxygen concentration in the coal. ————, Solomon and Carangelo (1982); — — — , Osawa and Shih (1971). (From: Solomon and Carangelo, 1982)

this 1.1% O value does not entirely represent experimental error, then strongly bonded oxygen functionalities (linkages) other than hydroxy groups persist in very high-rank whole coals. The apparent high elemental oxygen values for Coals 4 and 7, i.e. whole coals with more than 20% ash (moist. free), perhaps could be attributed to loosely bound (weakly bonded) oxygen groups associated with the mineral matter (e.g. phyllosilicates (-OH), carbonates ($-CO_3$), sulfates ($-SO_4$), etc.) within the whole coals, thus influencing (increasing) the elemental oxygen values reported for the ultimate analysis data.

Absorptivity at 2955 cm^{-1} versus Hydrogen Content

Figure 31, the plot of absorptivity at 2955 cm^{-1} versus elemental hydrogen on a dry, ash-free basis, shows absorptivity generally increases with increasing elemental hydrogen content. The relationship between increasing absorptivities at 2955 cm^{-1} and elemental hydrogen (daf) for the whole coals studied is described by a linear correlation line, defined by $a = 1.35X10^{-2}$ (%H, daf) - 0.046 with an 0.882 correlation coefficient, shown in Figure 31. Extrapolation of the linear correlation line to the abscissa yields approximately 3.4% H (daf) which suggests whole coals with less than 3.4% H (daf), independent of rank, should show no detectable absorbance at 2955 cm^{-1}. An infrared study of pyrolysis products of lignite (Rouxhet et al., 1979) revealed no detectable absorbance in the 2930-2860 cm^{-1} region occurs in lignite after pyrolysis up to 655°C. Zero absorbance in the

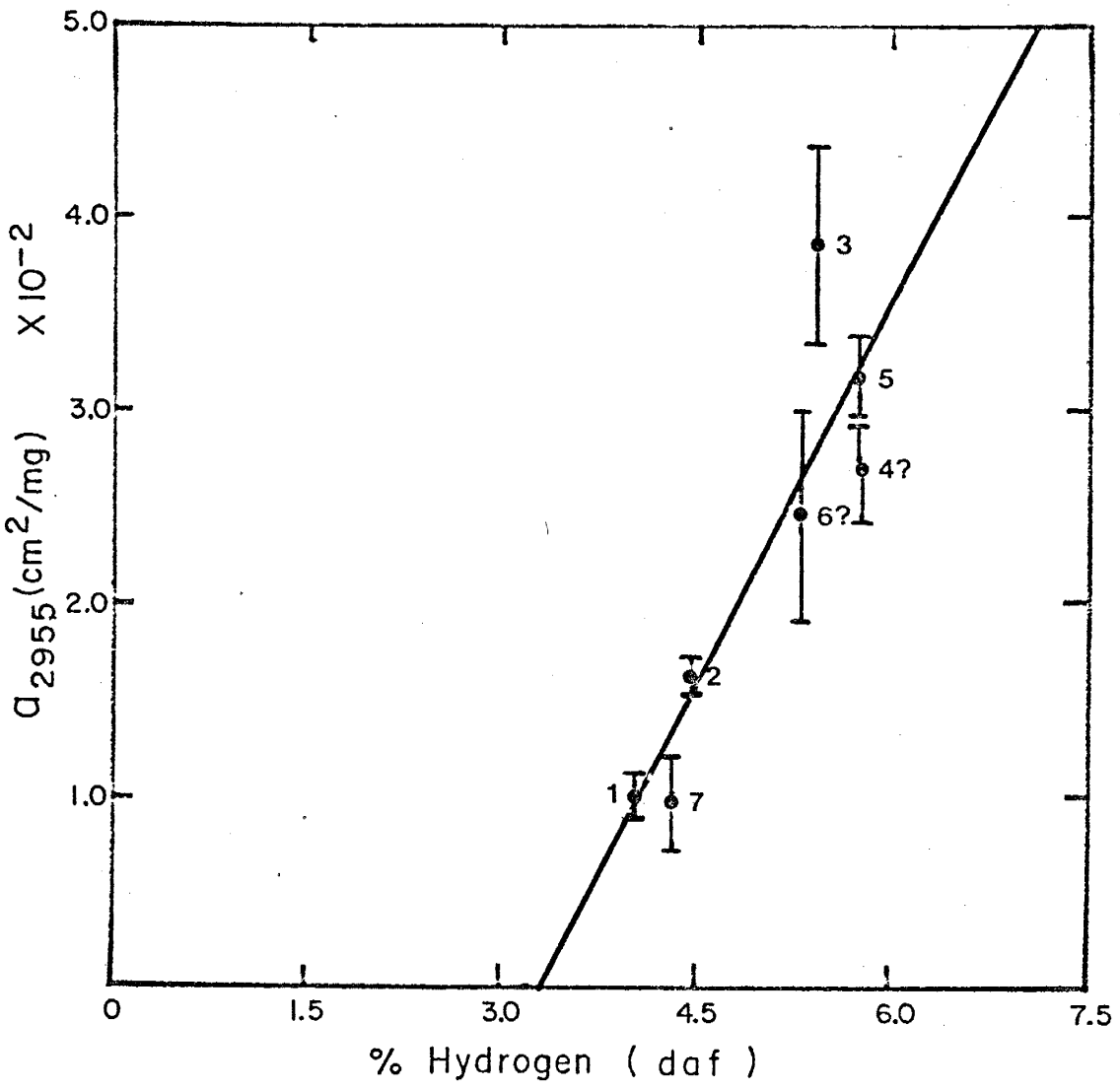

Figure 31. Mean absorptivity values at 2955 cm-1 plotted against hydrogen concentration on a dry, ash-free basis for Coals 1-7. Vertical bars represent the sample standard deviation. ? means not confident of mean absorptivity value due to insufficient data.

2930-2860 cm^{-1} region corresponds to 3.47% H (daf) in the pyrolysis product of the lignite (Rouxhet et al., 1979). Figure 32 shows the relationship between the absorption coefficient (Kal) for the 2930-2860 cm^{-1} region and elemental hydrogen content. These data are compatible with the results reported here.

Several remarkable features of Figure 31 deserve mention here. First, Coal 3 has 5.46% H (daf) while Coal 6 has 5.38% H (daf) and are of similar rank, although the absorptivity at 2955 cm^{-1} for Coal 3 (a = 0.0384 cm^2/mg) is approximately 1.6 times greater than the 2955 cm^{-1} absorptivity for Coal 6 (a = 0.0244 cm^2/mg). Coals 2 and 7 have 4.51% (daf) and 4.35% (daf) hydrogen respectively, but are of vastly different rank--Coal 2 is sub-bituminous A or high volatile C bituminous and Coal 7 is low volatile bituminous--suggesting that whole coals with similar hydrogen contents and similar or different rank may yield highly variable absorptivities for the weak 2955 cm^{-1} band. Therefore absorptivity at 2955 cm^{-1} is a function of the hydrogen content (daf) of whole coals and apparently does not have a strong correlation with certain rank parameters such as elemental carbon (daf) or volatile matter (ash-free) contents.

Methyl ($-CH_3$) groups in high volatile bituminous rank whole coals constitute approximately 0.037 (3.7%) weight fraction (daf) of the whole coal (Solomon, 1981, p. 64). The 2955 cm^{-1} band is only detected as a shoulder on the more prominent 2915-2850 cm^{-1} band, illustrated in

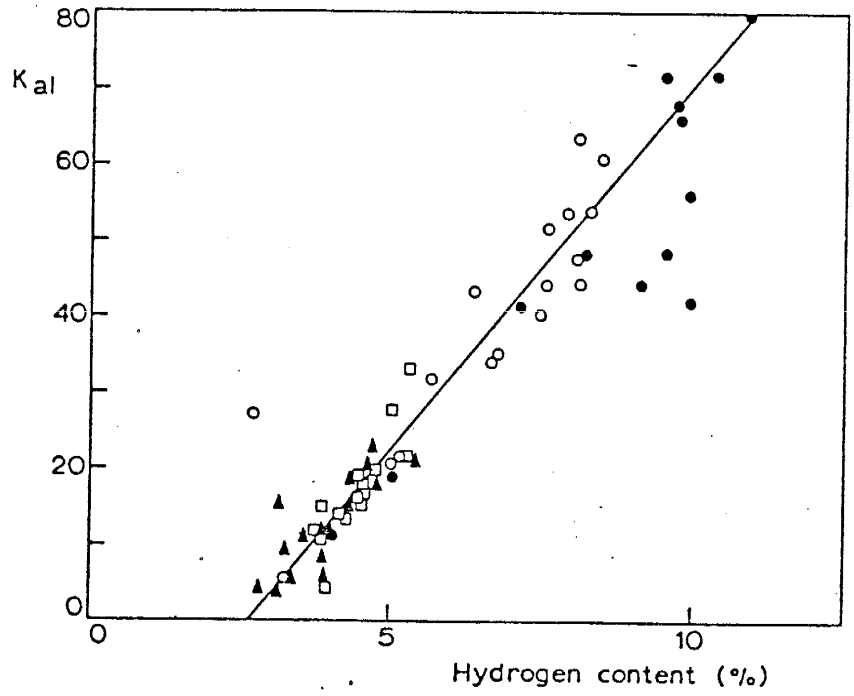

Fig. 32.— Correlation between K_{al} and the hydrogen content (weight %):

●: kerogens of series I. ○: kerogens of series II. ▲: kerogens of series III. □: coals.

(From: Rouxhet et al., 1980.)

Figure 3, suggesting that the methyl content is small in the whole coals studied. This interpretation is compatible with the general conclusion of Oth and Tschamler (1963), Bent et al. (1964) and Mazumdar (1972).

Absorptivity at 2915 cm^{-1} versus Hydrogen Content

Figure 33 shows absorptivity at 2915 cm^{-1} plotted as a function of elemental hydrogen on a dry, ash-free basis. A rectilinear best-fit correlation line, Figure 33, is shown in general to illustrate the weak correlation between increasing absorptivity at 2915 cm^{-1} and increasing elemental hydrogen. Coal 2 (sub-bituminous A or high volatile C bituminous) has an elemental hydrogen content very similar to Coal 7 (low volatile bituminous), although the absorptivity for Coal 7 (a = 0.0135 cm^2/mg) is approximately 2.8 times less than that for Coal 2 (a = 0.0509 cm^2/mg). Coals 2, 4 and 6 have similar absorptivities but significantly different elemental hydrogen contents suggesting that the 2915 cm^{-1} absorptivities apparently are not a function of rank and elemental hydrogen content. The rather high absorptivity for Coal 3 indicates that much of the hydrogen is associated with aliphatic (alkyl) moieties (Solomon, 1981).

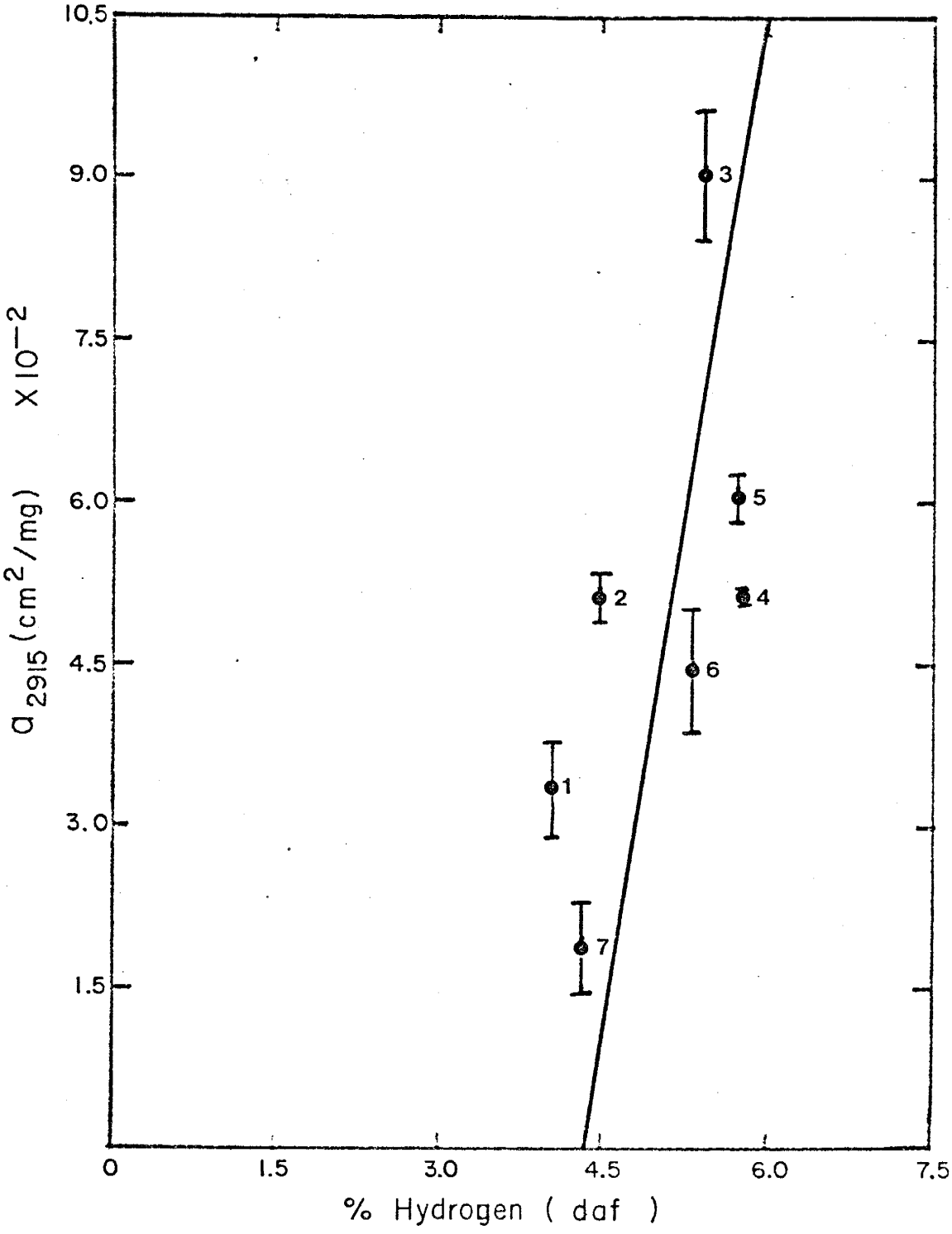

Figure 33. Mean absorptivity values at 2915 cm-1 plotted against hydrogen concentration on a dry, ash-free basis for Coals 1-7. Vertical bars indicate the sample standard deviation.

Absorptivity at 2850 cm^{-1} versus Hydrogen Content

The plot of absorptivity at 2850 cm^{-1} versus elemental hydrogen on a dry, ash-free basis, Figure 34, demonstrates that absorptivity increases generally attend elemental hydrogen increases. Clearly, Figure 34 demonstrates that absorptivities at 2850 cm^{-1} are not a direct function of rank, since Coals 1 (sub-bituminous B) and 7 (low volatile bituminous) have comparable elemental hydrogen contents and absorptivities but have radically different elemental carbon contents --a measure of rank. Variations in absorptivity at 2850 cm^{-1} among whole coals with similar elemental hydrogen contents, such as Coals 1, 2 and 7, and dissimilar elemental carbon contents apparently are a function of whether most of the hydrogen is associated principally with aliphatic or aromatic functionalities. Recalling that the 2850 cm^{-1} band mainly results from asymmetric and symmetric stretching of aliphatic (alkyl) CH_2 groups, Coal 7 has a significantly lower absorptivity than Coals 1 and 2, even though Coals 1, 2 and 7 have comparable elemental hydrogen contents, which presumably indicates that much of the elemental hydrogen in Coal 7 is associated with aromatic (aryl) moieties (polyaromatic structures) rather than aliphatic (alkyl) CH moieties characteristic of Coals 1 and 2. The weak, poorly resolved 3040 cm^{-1} band characteristic of aromatic C-H stretching modes does not permit confirmation of this statement although data for the 3400 cm^{-1} band, Figure 28, and the absorption region between 900-700 cm^{-1}, Figures 56, 58 and 59, characteristic of aromatic C-H out-of-plane deformational

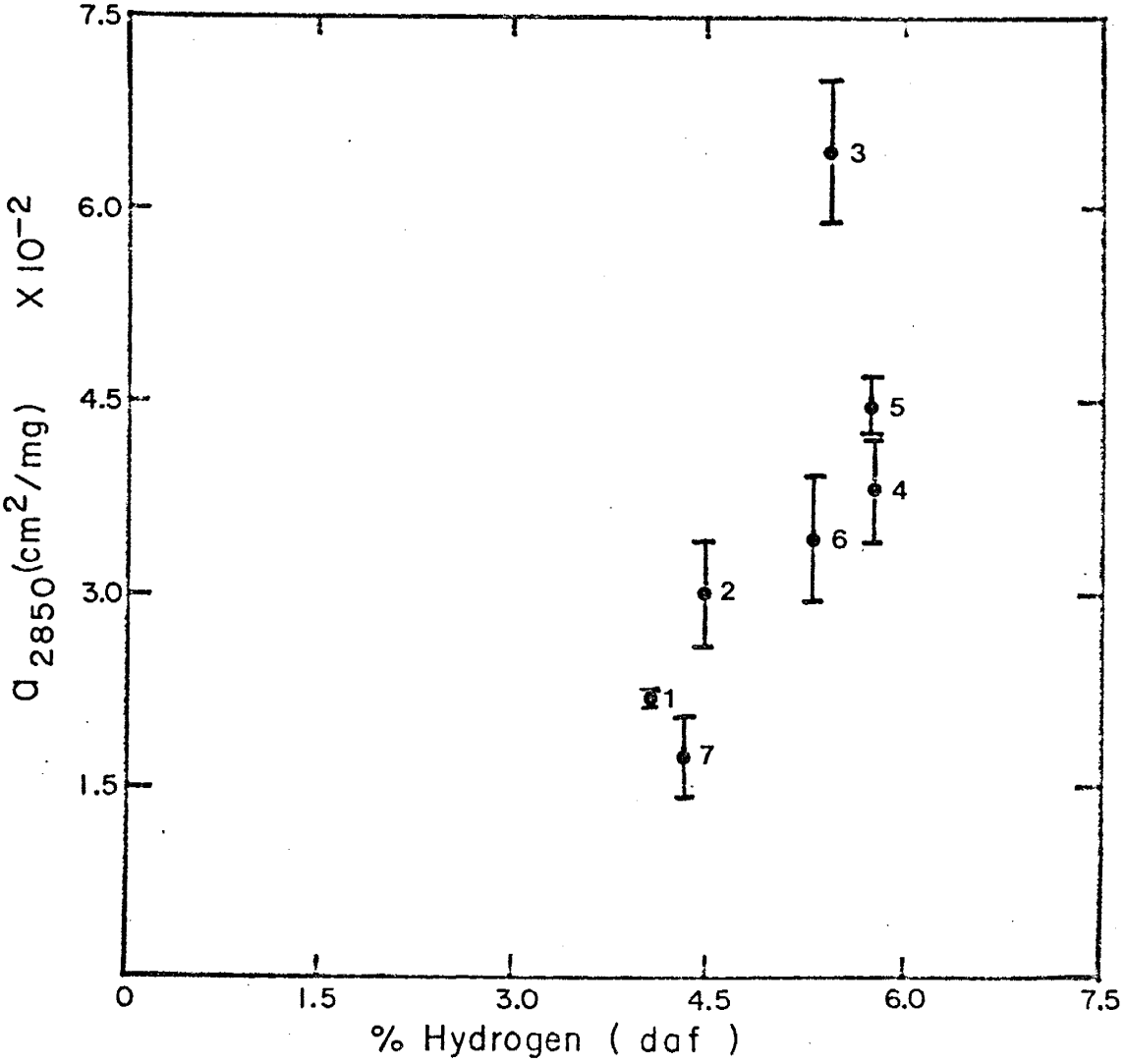

Figure 34. Mean absorptivity values at 2850 cm-1 plotted as a function of hydrogen concentration on a dry, ash-free basis for Coals 1-7. Vertical bars represent the sample standard deviation.

modes, support this statement.

Absorptivity at 1700 cm^{-1} versus Carbon Content

Plotting absorptivity at 1700 cm^{-1} against elemental carbon content on a dry, ash-free basis, Figure 35, reveals a linear relation demonstrating that absorptivity rapidly decreases with slight increases in elemental carbon attending increasing rank. The linear correlation line is a = 1.746 - 0.021 (%C, daf) with a -0.972 correlation coefficient. Extrapolation of the linear correlation line to the abscissa yields 83.6% C (daf) suggesting that whole coals with more than or equal to 84% C (daf) should reveal no distinguishable absorbance at 1700 cm^{-1} unless these whole coals have oxidized. This value for zero absorbance is consistent with results of pyrolysis experiments on lignite reported by Rouxhet et al. (1979).

Absorptivity at 1700 cm^{-1} versus Oxygen Content

Figure 36 shows absorptivity at 1700 cm^{-1} plotted against elemental oxygen content on a dry, ash-free basis. A linear relation, defined by a = 0.018 (%O, daf) - 0.140 with a 0.969 correlation coefficient, illustrates that absorptivity correspondingly decreases as oxygen content decreases with increasing rank. Extrapolation of the linear correlation line to the abscissa yields 7.8% O (daf) suggesting that

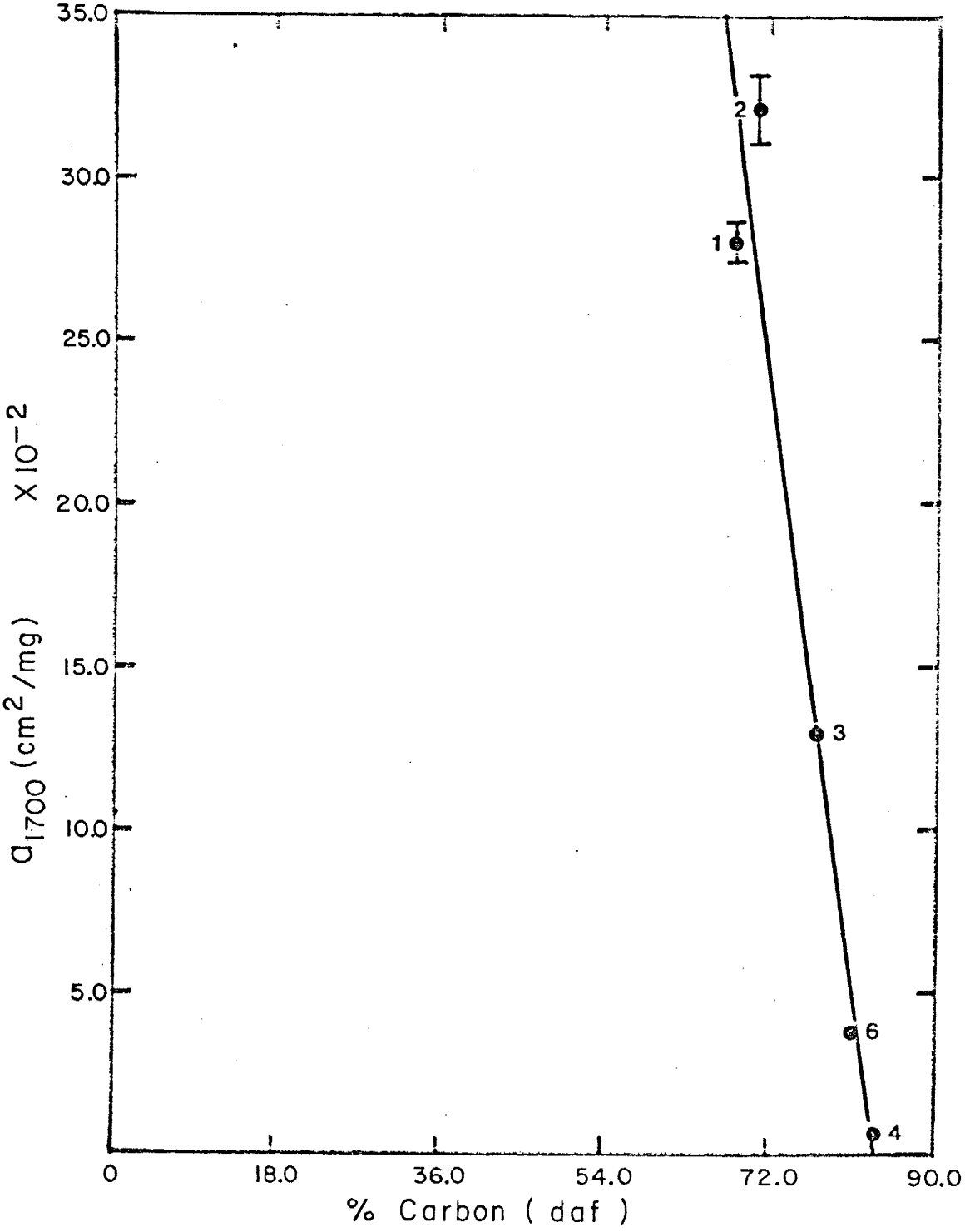

Figure 35. Plot of mean absorptivity values at 1700 cm-1 against carbon concentration on a dry, ash-free basis for Coals 1-4 and 6. Vertical bars represent the sample standard deviation.

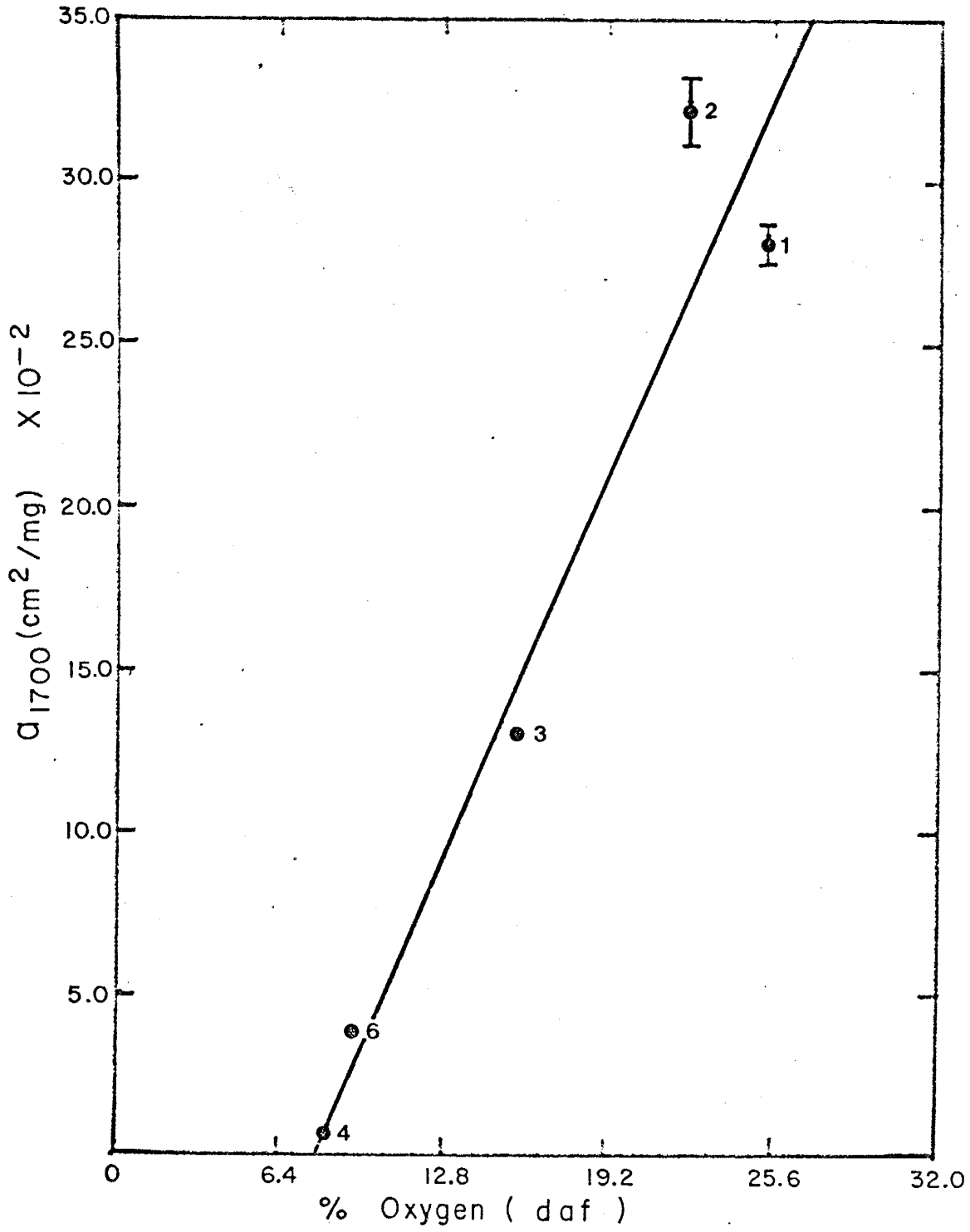

Figure 36. Mean absorptivity values at 1700 cm-1 plotted as a function of oxygen concentration on a dry, ash-free basis for Coals 1-4 and 6. Vertical bars indicate the sample standard deviation.

whole coals with approximately less than or equal to 7.8% O (daf) should show no discernible absorbance at 1700 cm^{-1} unless oxidation has occurred. Figures 37 and 38 show the chemical modifications (evolutionary path) occurring during catagenesis and pyrolysis of various types of organic matter, i.e. kerogens. Series III and IIIa in Figure 37 represent kerogens derived mainly from higher plants deposited in a coastal marine environment (Rouxhet and Robin, 1978). The results obtained in this study support the results reported by Robin and Rouxhet (1978) and Rouxhet et al. (1979).

Absorptivity at 1660 cm^{-1} versus Carbon Content

The plot of absorptivity at 1660 cm^{-1} as a function of elemental carbon on a dry, ash-free basis, Figure 39, demonstrates that increasing carbon content attending increasing rank results in correspondingly rapid absorptivity decreases at 1660 cm^{-1}. The inverse linear correlation line in Figure 39, defined by a = 1.812 - 0.021 (%C, daf) with a -0.995 correlation coefficient, describes the relationship between absorptivity at 1660 cm^{-1} and elemental carbon (daf) content. Extrapolation of the linear correlation line to the abscissa yields 86% C (daf), suggesting that whole coals with more than or equal to 86% C (daf) should reveal no discernible absorbance at 1660 cm^{-1}.

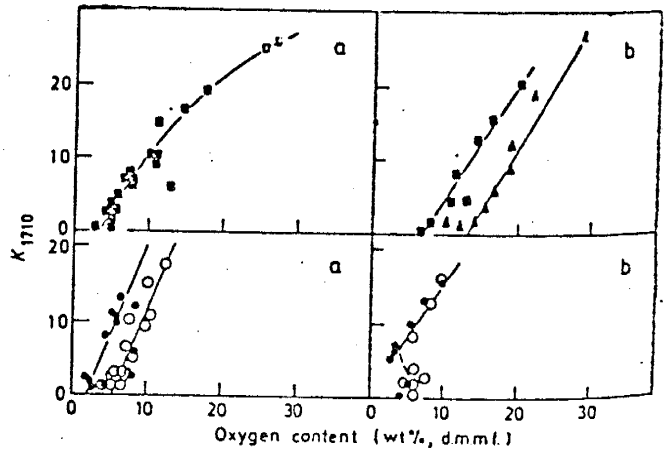

Figure 37. Correlation between K_{1710} and the oxygen content (wt %, dmmf). (a) natural samples; (b) pyrolysed samples; ● Series I and I', ○ Series II and II'; ■ Series III and III'$_a$, ▲ Series III'$_b$

(From: Rouxhet and Robin, 1978.)

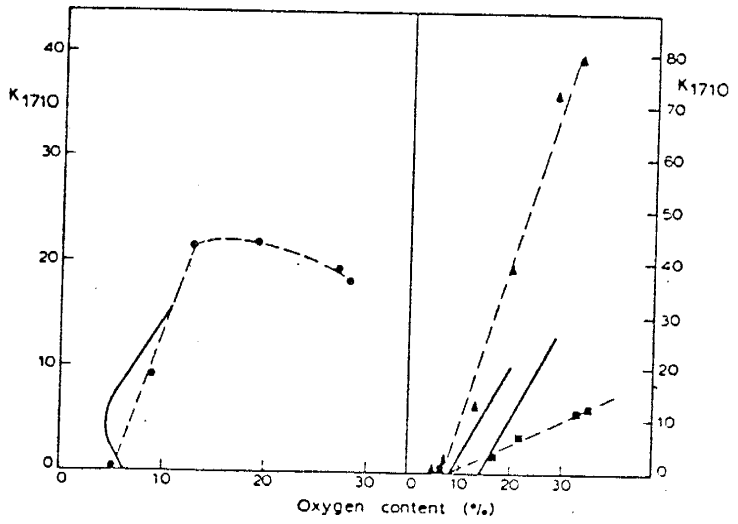

Fig. 38. Plot of K_{1710} ($mg^{-1} \times cm$) as a function of the oxygen content (weight %) for the starting samples and the products obtained by pyrolysis (dashed lines): (●) raw sporopollenin, (▲) oxidized sporopollenin and (■) lignite in thick bed. The full lines relate to pyrolysis of kerogens with an important contribution of spores and algae (left) and kerogens originating from higher plants (right) (ROUXHET and ROBIN, 1978).

(From; Rouxhet et al., 1979.)

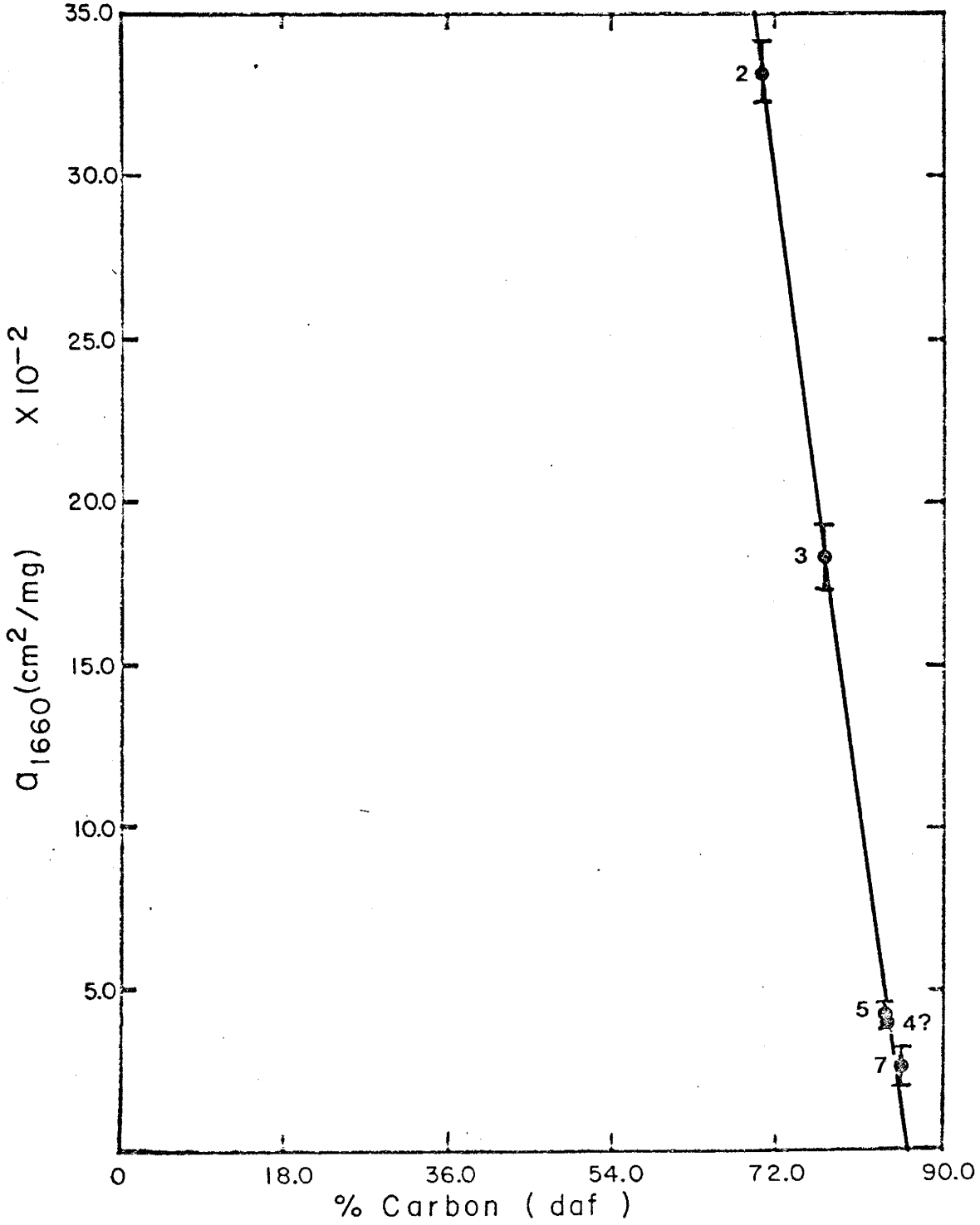

Figure 39. Mean absorptivity values at 1660 cm-1 plotted against carbon concentration on a dry, ash-free basis for Coals 2-5 and 7. Vertical bars indicate the sample standard deviation. ? means not confident of mean absorptivity value due to insufficient data.

Absorptivity at 1660 cm^{-1} versus Hydrogen Content

Figure 40, the plot of absorptivity at 1660 cm^{-1} versus elemental hydrogen content on a dry, ash-free basis, shows the relationship between absorptivity at 1660 cm^{-1} and elemental hydrogen. A linear correlation line excluding Coal 7, defined by a = 1.340 - 0.221 (%H, daf) with a -0.972 correlation coefficient, illustrates that as elemental hydrogen content increases absorptivity rapidly decreases. Coal 7 has a relatively low elemental hydrogen content and absorptivity which does not conform to the apparent trend established by Coals 2, 3, 4(?) and 5. Subsequent graphs, e.g. Figures 56, 58 and 59, show Coal 7 to be more aromatic than the other whole coals studied. Thus whole coals with similar elemental hydrogen contents and widely different absorptivities, i.e. Coals 2 and 7, suggest that Coal 2 with a high absorptivity has a greater abundance of this oxygen-containing (highly conjugated C=O) functional group, presumably associated dominantly with aliphatic moieties, than Coal 7 which has a low absorptivity and presumably these oxygen-containing functional groups are associated dominantly with aromatic moieties (e.g. Ar-$\overset{O}{\overset{\|}{C}}$-Ar). Poor resolution of the 1700-1600 cm^{-1} band using conventional (non-Fourier transform) IR spectroscopy does not permit an unequivocal interpretation of this band in the whole coals studied. Moreover, extrapolation of the linear correlation line to the abscissa yields 6.1% H (daf) suggesting that the absorptivity becomes undetectable in whole coals with more than or equal to 6.1% H (daf). This appears to be inconsistent with the concept of

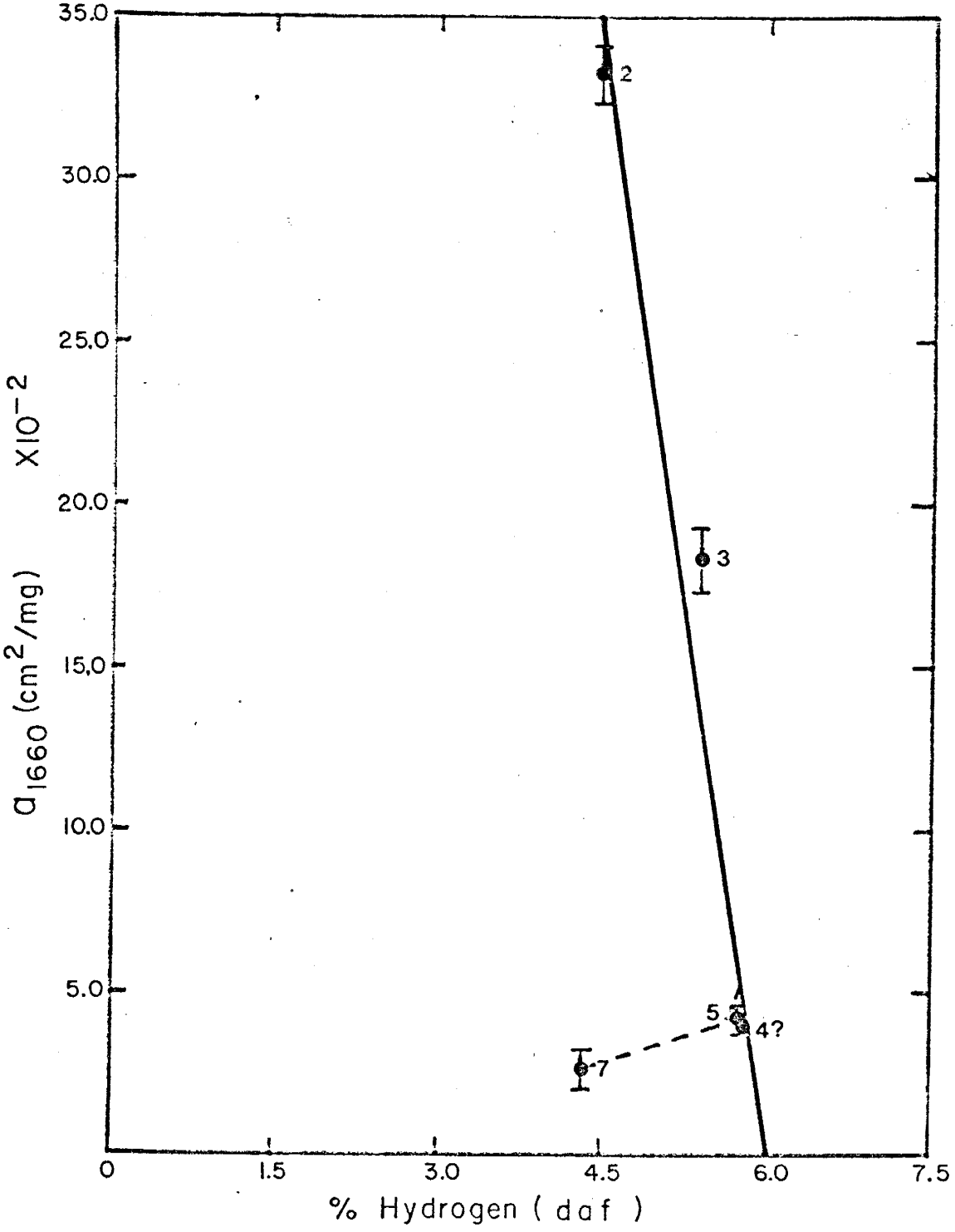

Figure 40. Plot of mean absorptivity values at 1660 cm-1 as a function of hydrogen concentration on a dry, ash-free basis for Coals 2-5 and 7. Vertical bars indicate the sample standard deviation. ? means not confident of mean absorptivity value due to insufficient data.

slightly decreasing hydrogen contents (or decreasing atomic H/C ratio) attending increasing rank in bituminous and anthracite coals, i.e. whole coals with more than or equal to 84% C (daf), Figure 41. Therefore a curvilinear relation, shown by the dashed line in Figure 40, more precisely characterizes the relationship between absorptivity at 1660 cm^{-1} and elemental hydrogen than the rectilinear correlation line. Also the curvilinear correlation line is more compatible with the concept of decreasing elemental hydrogen (daf) content of high-rank whole coals as coalification proceeds, Figure 41.

Absorptivity at 1660 cm^{-1} versus Oxygen Content

Plotting absorptivity at 1660 cm^{-1} as a function of elemental oxygen on a dry, ash-free basis, Figure 42, demonstrates decreasing oxygen content corresponding to increasing rank results in rapidly decreasing absorptivities. A linear correlation line, defined by a = 0.020 (%O, daf) - 0.116 with a 0.992 correlation coefficient, describes the relationship between absorptivity at 1660 cm^{-1} and elemental oxygen. Extrapolation of the linear correlation line to the abscissa yields 5.9% O (daf) suggesting that absorbance at 1660 cm^{-1} becomes indistinguishable in whole coals with less than or equal to 5.9% O (daf).

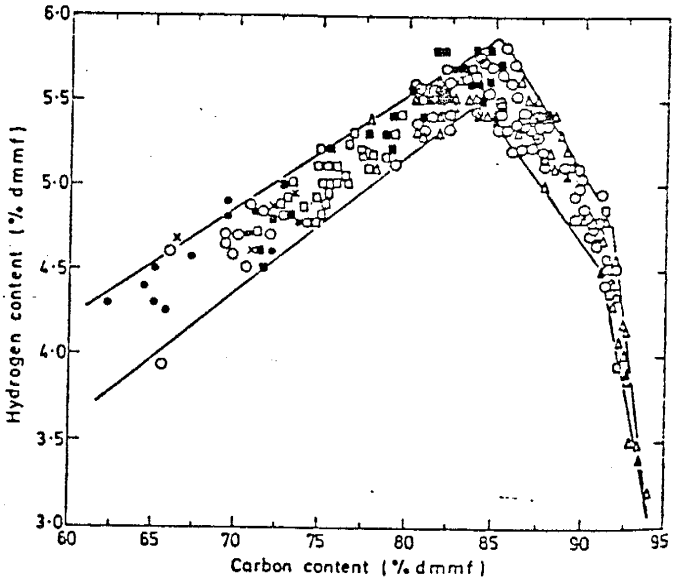

Figure 41. Variation of the hydrogen content of coal with increasing rank in the normal path of coalification
● Australian brown coals, ○ Indian coals, ■ American coals, □ coals of Alberta, ▲ from van Krevelen[3], △ British coals[24], x German brown coals (From: Mazumdar, 1972.)

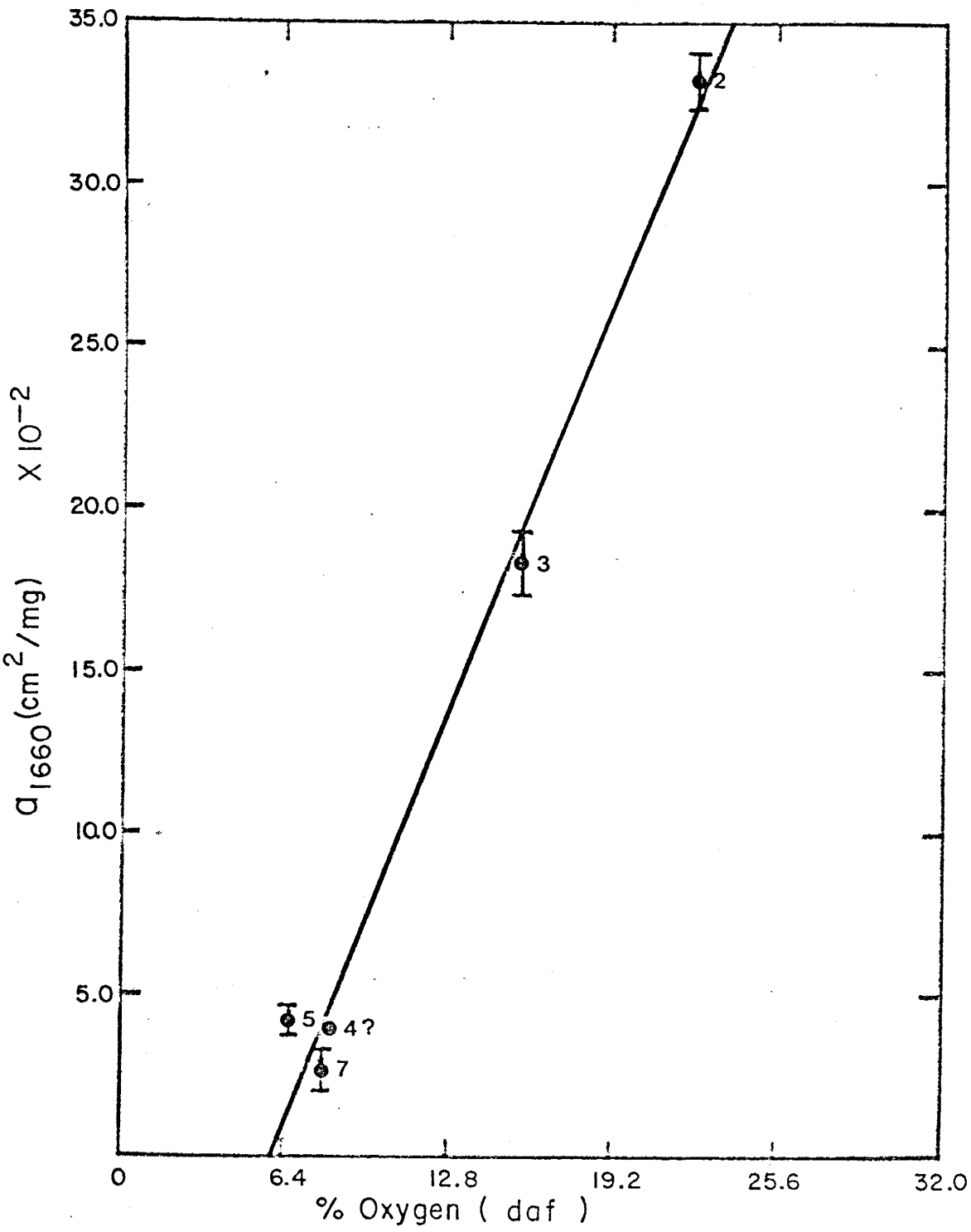

Figure 42. Mean absorptivity values at 1660 cm-1 plotted as a function of oxygen concentration on a dry, ash-free basis for Coals 2-5 and 7. Vertical bars indicate the sample standard deviation. ? means not confident of mean absorptivity value due to insufficient data.

Absorptivity at 1590 cm^{-1} versus Carbon Content

Figure 43 shows the plot of absorptivity at 1590 cm^{-1} versus elemental carbon on a dry, ash-free basis. An inverse rectilinear relationship, defined by a = 1.845 - 0.020 (%C, daf) with a -0.986 correlation coefficient, demonstrates that absorptivity decreases correspond to elemental carbon increases attending increasing rank. Extrapolation of the linear correlation line to the abscissa, a = 0.000 cm^2/mg, yields 92.8% C (daf) suggesting that whole coals with more than or equal to 93% C (daf) should yield no discernible absorbance at 1590 cm^{-1}. This interpretation appears inconsistent with the published data of Brown (1955) and others as previously noted in the discussion for the plot of absorptivity at 1590 cm^{-1} versus fixed carbon content, Figure 15, pages 82 to 85. The absorption band near 1600 cm^{-1} is present in the spectra of all whole coals, except in highly aromatic whole coals such as anthracites, where an intense background attributed to electronic absorption in highly conjugated materials obliterates the spectra in the 1600 cm^{-1} region. The apparent rapid decrease in absorptivity at 1590 cm^{-1} attending coalification presumably represents losses of highly conjugated hydrogen-bonded >C=O (carboxyls) in addition to increasing average ring size (Oberlin et al., 1980).

Absorptivity at 1590 cm^{-1} versus Hydrogen Content

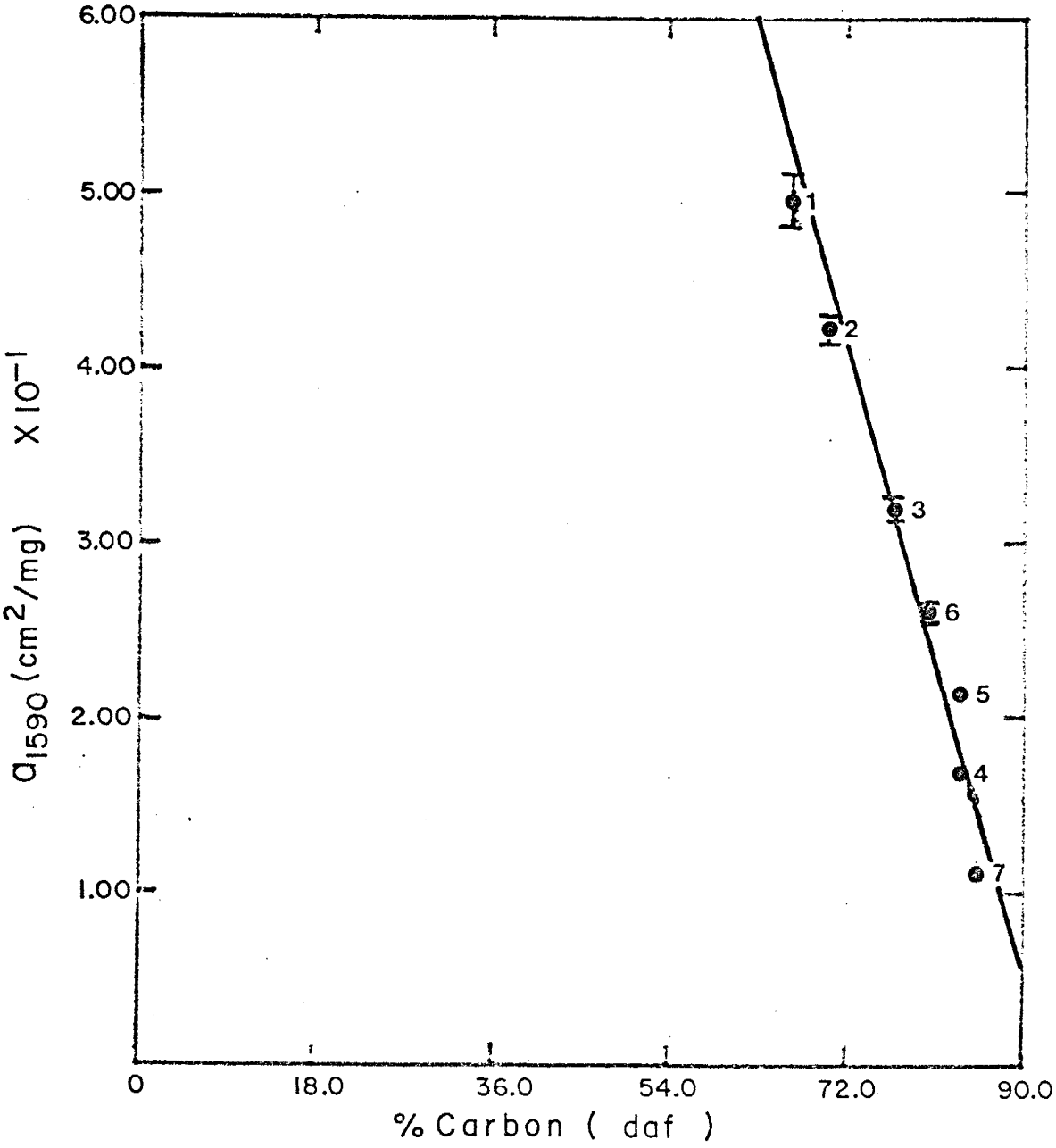

Figure 43. Mean absorptivity values at 1590 cm-1 plotted against carbon concentration on a dry, ash-free basis for Coals 1-7. Vertical bars represent the sample standard deviation.

Figure 44 shows the plot of absorptivity at 1590 cm^{-1} versus elemental hydrogen on a dry, ash-free basis. A curvilinear trend, in general, illustrates that absorptivity rapidly decreases as elemental hydrogen content increases. High-rank whole coals, such as Coal 7, with a relatively high aromaticity may have elemental hydrogen contents similar to lower rank whole coals such as Coal 2, with a significantly lower degree of aromaticity. Absorptivity character of the 1590 cm^{-1} band permits a distinction to be made between high-rank and low-rank whole coals containing similar elemental hydrogen contents. Figure 44 demonstrates that absorptivities are relatively low for high-rank whole coals (Coal 7) whereas low-rank whole coals (Coal 2) have relatively high absorptivities.

Absorptivity at 1590 cm^{-1} versus Oxygen Content

Figure 45, the plot of absorptivity at 1590 cm^{-1} as a function of elemental oxygen on a dry, ash-free basis, illustrates absorptivity decreases generally correspond to decreasing elemental oxygen. A linear best-fit correlation line in Figure 45, defined by a = 0.017 (%O, daf) + 0.046 with a 0.951 correlation coefficient, describes the positive relationship between absorptivity at 1590 cm^{-1} and elemental oxygen. Fujii et al. (1970) reported absorptivity at 1600 cm^{-1} plotted against elemental oxygen (daf) in Japanese coals yields a linear trend very similar to the linear trend shown in Figure 45. Extrapolation of the linear best-fit correlation line to the ordinate, %O (daf) = 0.00%,

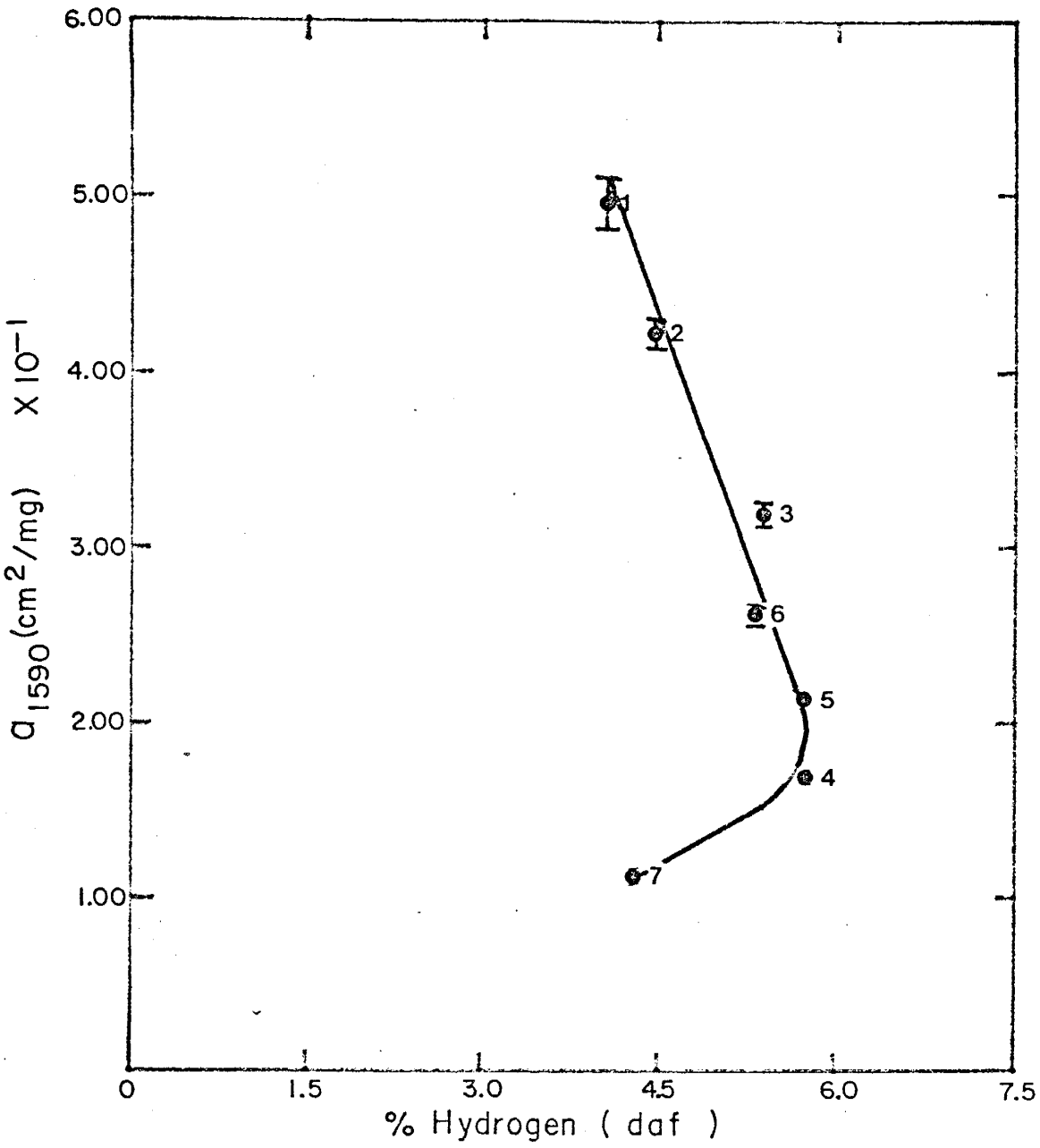

Figure 44. Plot of mean absorptivity values at 1590 cm-1 versus hydrogen concentration on a dry, ash-free basis for Coals 1-7. Vertical bars indicate the sample standard deviation.

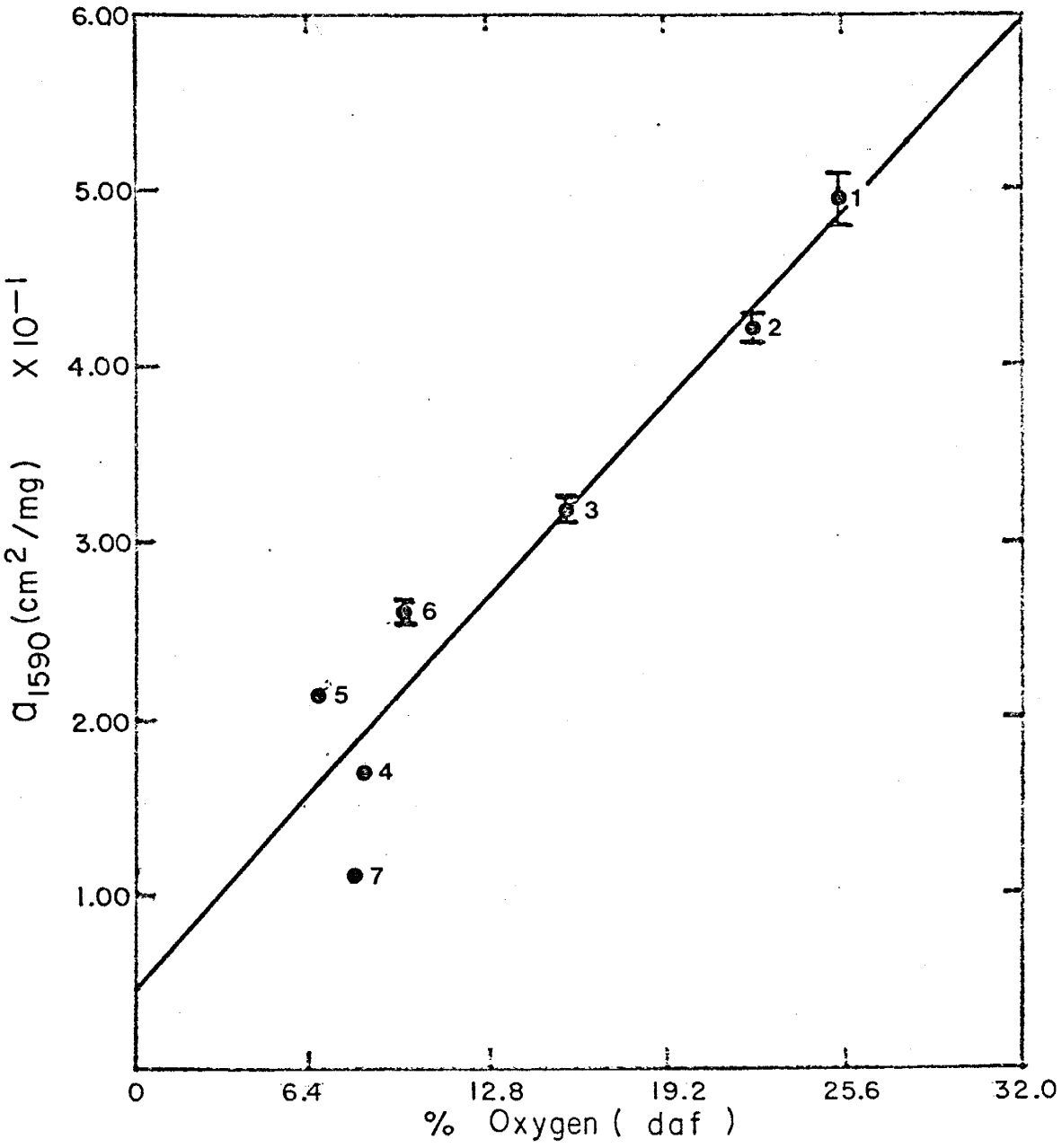

Figure 45. Mean absorptivity values at 1590 cm-1 plotted as a function of oxygen concentration on a dry, ash-free basis for Coals 1-7. Vertical bars represent the sample standard deviation.

yields a = 0.046 cm^2/mg, suggesting that whole coals containing virtually no oxygen exhibit a pronounced absorbance at 1590 cm^{-1}. This persistent and pronounced absorbance in the 1590 cm^{-1} region, characteristic of IR spectra of all whole coals, is ascribed to absorptions of functional groups containing no oxygen, possibly the >C=C< vibration of aromatic structures.

Absorptivity at 1440 cm^{-1} versus Carbon Content

Figure 46 is the plot of absorptivity at 1440 cm^{-1} as a function of elemental carbon on a dry, ash-free basis. The linear best-fit correlation line in Figure 46, defined by a = 0.933 - $9.52X10^{-3}$ (%C, daf) with a -0.866 correlation coefficient, describes the inverse relationship between absorptivity at 1440 cm^{-1} and elemental carbon (daf). This linear best-fit correlation line illustrates that absorptivity at 1440 cm^{-1} significantly decreases with small increases in elemental carbon (daf) and increasing rank. Extrapolation of the best-fit correlation line to the abscissa, a = 0.000 cm^2/mg, yields 97.9% C (daf) suggesting that whole coals with more than or equal to 98% C (daf) should show no distinct absorbance at 1440 cm^{-1}. Figure 47 shows vitrinites containing 98% C (daf) have approximately 0.6% H (daf), or atomic H/C approximately equal to 0.07, suggesting a paucity of aliphatic (alkyl) hydrocarbons. Whole coals with appoximately 98% C (daf) have a highly aromatic (graphitic) nature (Elliott, 1981; Oberlin et al., 1980) and possess relatively few aliphatic (alkyl) hydrocarbons,

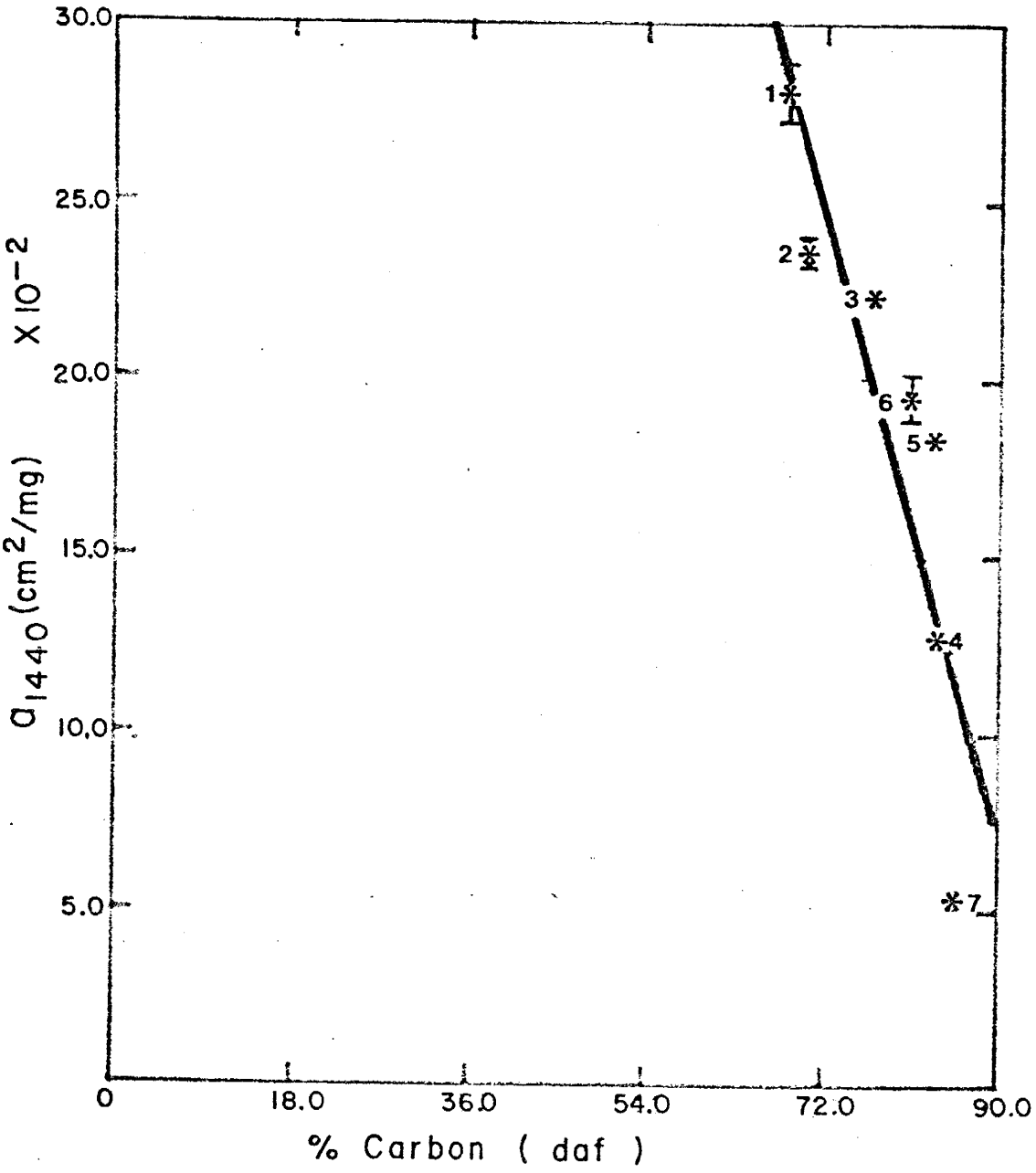

Figure 46. Plot of mean absorptivity values at 1440 cm-1 against carbon concentration on a dry, ash-free basis for Coals 1-7. Vertical bars indicate the sample standard deviation.

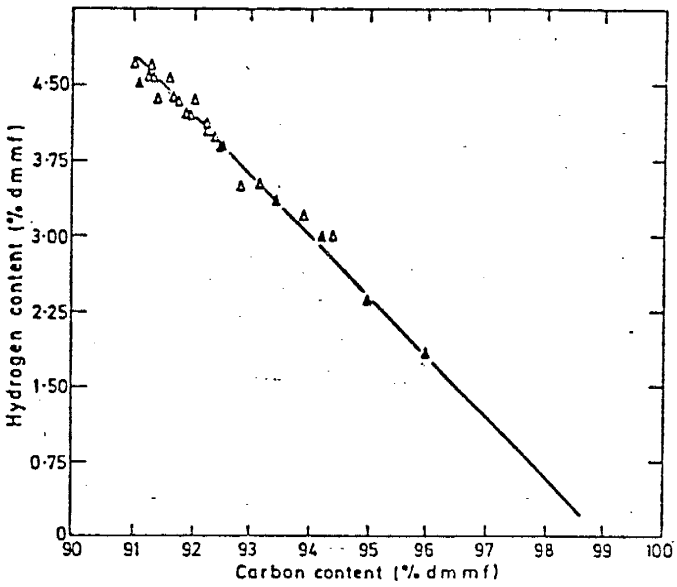

Figure47. Variation of hydrogen content of coal with increasing rank (an extension of *Figure41* in the anthracitic region)

(From: Mazumdar, 1972.)

possibly present as cross-links and bridges in the coal structure (Solomon, 1981; Whitehurst, 1978; Larsen and Kovac, 1978). Thus the conclusion that whole coals with more than or equal to 98% C (daf) show no distinct absorbance at 1440 cm^{-1} appears consistent with available data. Anthracites are considered to be an exception to this generalization since an intense background absorption occurs in this region for anthracites which is a key feature of highly conjugated substances.

Absorptivity at 1440 cm^{-1} versus Hydrogen Content

Figure 48 is the plot of absorptivity at 1440 cm^{-1} as a function of elemental hydrogen on a dry, ash-free basis. A curvilinear (crudely parabolic) relation with considerable scatter, Figure 48, illustrates that, in general, absorptivity correspondingly decreases with increasing elemental hydrogen (daf). This apparent absorptivity decrease with increasing elemental hydrogen content may in part reflect decreases in total oxygen content attending coalification resulting in relatively slight increases in elemental hydrogen and carbon contents, and in part reflects the natural variability of coal parameters that occur even in coals of the same rank. Furthermore, the thermocatalytic degradation of the reactive aliphatic (alkyl) constituents of whole coals attending coalification results in decreasing the number of aliphatic C-H deformations contributing to the absorbance at 1440 cm^{-1}. Figure 41 shows that vitrain-rich whole coals of widely different rank can have

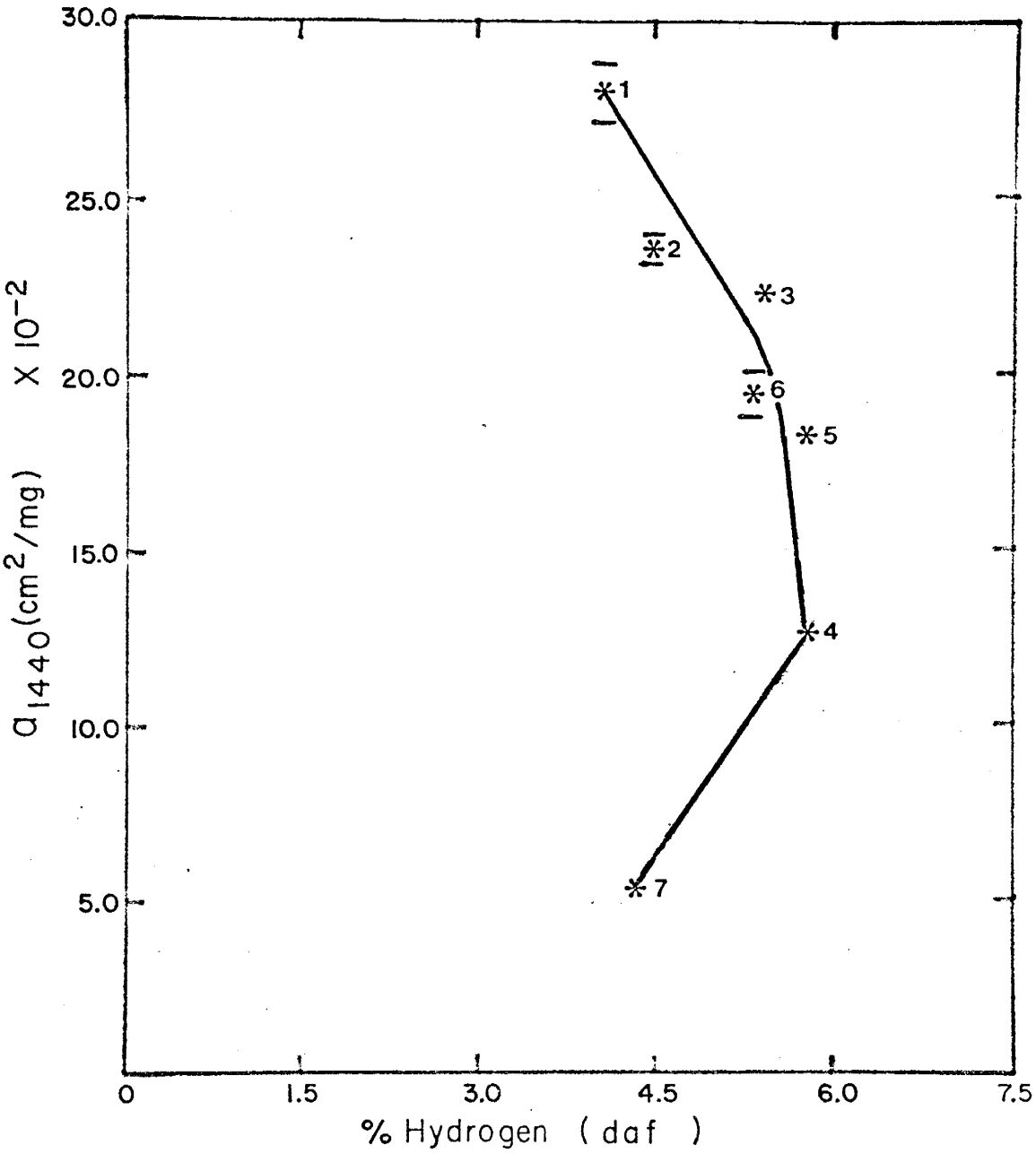

Figure 48. Mean absorptivity values at 1440 cm-1 plotted against hydrogen concentration on a dry, ash-free basis for Coals 1-7. Vertical bars represent the sample standard deviation.

similar elemental hydrogen (daf) contents, e.g. approximately 4.25% H (daf) for high volatile bituminous (approximately 65% C, daf) and anthracite (approximately 92% C, daf). This absorptivity change as a function of elemental hydrogen and rank is compatible with the trend shown in Figure 41. Therefore, high-rank whole coals (Coals 4 and 7) have relatively low absorptivities whereas low-rank whole coals (Coals 1 and 2) are characterized by high absorptivities, Figure 48. Given negligible elemental hydrogen losses occur, i.e. as measured by the near-constancy of the atomic H/C ratio at 0.80 ± 0.03, for whole coals with 62% to 84% C (daf) (Mazumdar, 1972), then the observed decrease in absorptivity at 1440 cm^{-1} for Coals 1, 2, 3, 4, 5 and 6 reflects decreasing numbers of aliphatic C-H bending vibrations per weight percent hydrogen (daf), implying that the hydrogen becomes more strongly associated (bonded) with polycyclic aliphatic/aromatic rings. Support of this implication is gained from data on aromatic functionalities in whole coals, e.g. Figure 59, the plot of absorptivity at 740 cm^{-1} (out-of-plane bending mode of 1,2 substituted aromatic groups) versus elemental hydrogen (daf) content.

Absorptivity at 1375 cm^{-1} versus Carbon Content

Plotting absorptivity at 1375 cm^{-1} versus elemental carbon on a dry, ash-free basis, Figure 49, reveals a linear relation demonstrating that as elemental carbon increases with coalification absorptivity shows a corresponding rapid decrease. The linear correlation line is a =

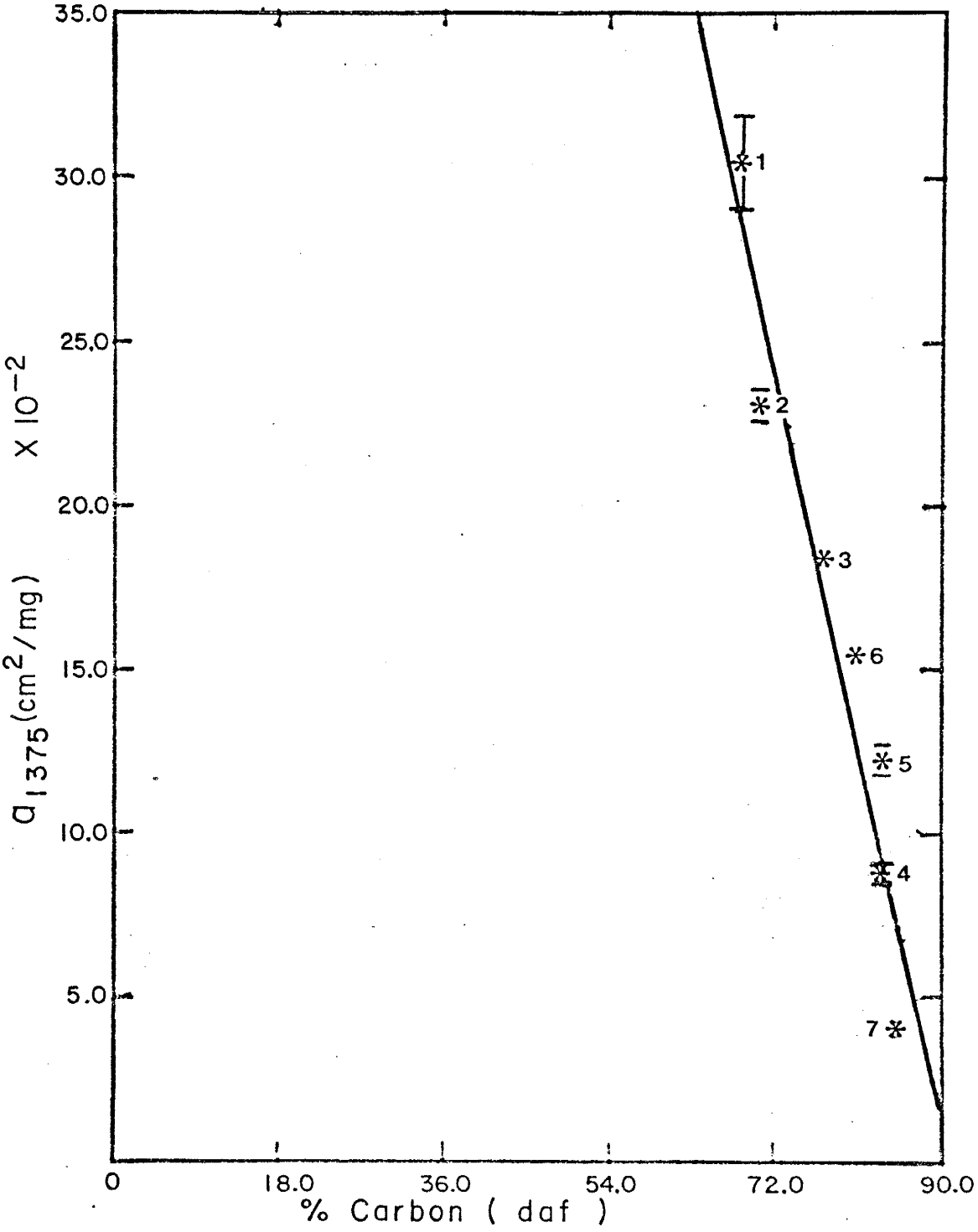

Figure 49. Mean absorptivity values at 1375 cm-1 plotted as a function of carbon concentration on a dry, ash-free basis for Coals 1-7. Vertical bars indicate the sample standard deviation.

1.145 - 0.0125 (%C, daf) with a -0.965 correlation coefficient. Extrapolation of the linear correlation line to the abscissa, a = 0.000 cm^2/mg, yields 91.4% C (daf) suggesting that whole coals with more than or equal to 91.4% C (daf) should show no distinguishable absorbance at 1375 cm^{-1}. The intense background absorption characteristic of anthracites in this region of the spectrum obliterates the 1375 cm^{-1} band yielding unreliable absorbance values. For this reason, an accurate determination of the elemental carbon range where the 1375 cm^{-1} absorbance approaches zero, i.e. the virtual absence of methyl functional groups, appears most difficult for whole coals.

These data in Figure 49 are not consistent with the experimental assessment of the methyl content of coal reported by Mazumdar (1972), Figure 50. Mazumdar (1972) contends that "the methyl content of coal appears to remain virtually constant up to 84% carbon; although incipient demethylation appears to set in from this stage, its extent, at least between 84 and 89-90% carbon, remains small (from 4.8 down to 4% of the total carbon)." I submit that the data in Figure 49 represent the enhancement of the absorbance at 1375 cm^{-1} by oxygen-containing functional groups (Francis, 1951) ubiquitous in low-rank whole coals, whereas demethylation of high-rank whole coals significantly contributes to rapid absorptivity decreases at 1375 cm^{-1} observed with increasing elemental carbon content and coalification in addition to progressive deoxygenation of the whole coals studied.

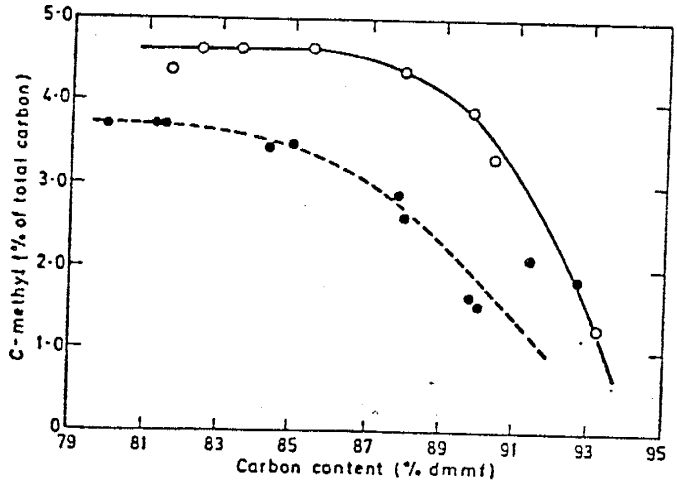

Figure 50. Variation of the true methyl content of coal with rank and its comparison with the Kuhn–Roth estimate
● values by Kuhn–Roth method, O values derived from pyrolysis (Reproduced from Mazumdar *et al*[8])

(From: Mazumdar, 1972.)

Absorptivity at 1250 cm^{-1} versus Carbon Content

Figure 51 is the plot of absorptivity at 1250 cm^{-1} as a function of elemental carbon on a dry, ash-free basis. A linear best-fit correlation line, defined by $a = 0.915 - 9.80X10^{-3}$ (%C, daf) with a 0.864 correlation coefficient, in Figure 51 shows absorptivity rapidly decreases with correspondingly small elemental carbon (daf) increases attending coalification. Extrapolation of the linear correlation line to the abscissa yields 93.3% C (daf) suggesting no distinguishable absorbance at 1250 cm^{-1} occurs in whole coals with more than or equal to 93% C (daf), i.e. anthracites. Provided the 1250 cm^{-1} absorption band primarly results from -C-O- stretching vibrations of phenolic structures in whole coals (Painter and Coleman, 1979; Murchison, 1976; Siskov and Petrova, 1974; Brown, 1955), then the extrapolated value of approximately 93% C (daf) for zero absorbance at 1250 cm^{-1} is consistent with unoxidized anthracites containing more than 93% C (daf) being characterized by rather low elemental oxygen (daf) contents and virtually devoid of phenolic structures. Because of the intense background absorption characteristic of anthracites, zero absorbance at 1375 cm^{-1} is not observed for whole coals with more than 93% C (daf).

Absorptivity at 1250 cm^{-1} versus Hydrogen Content

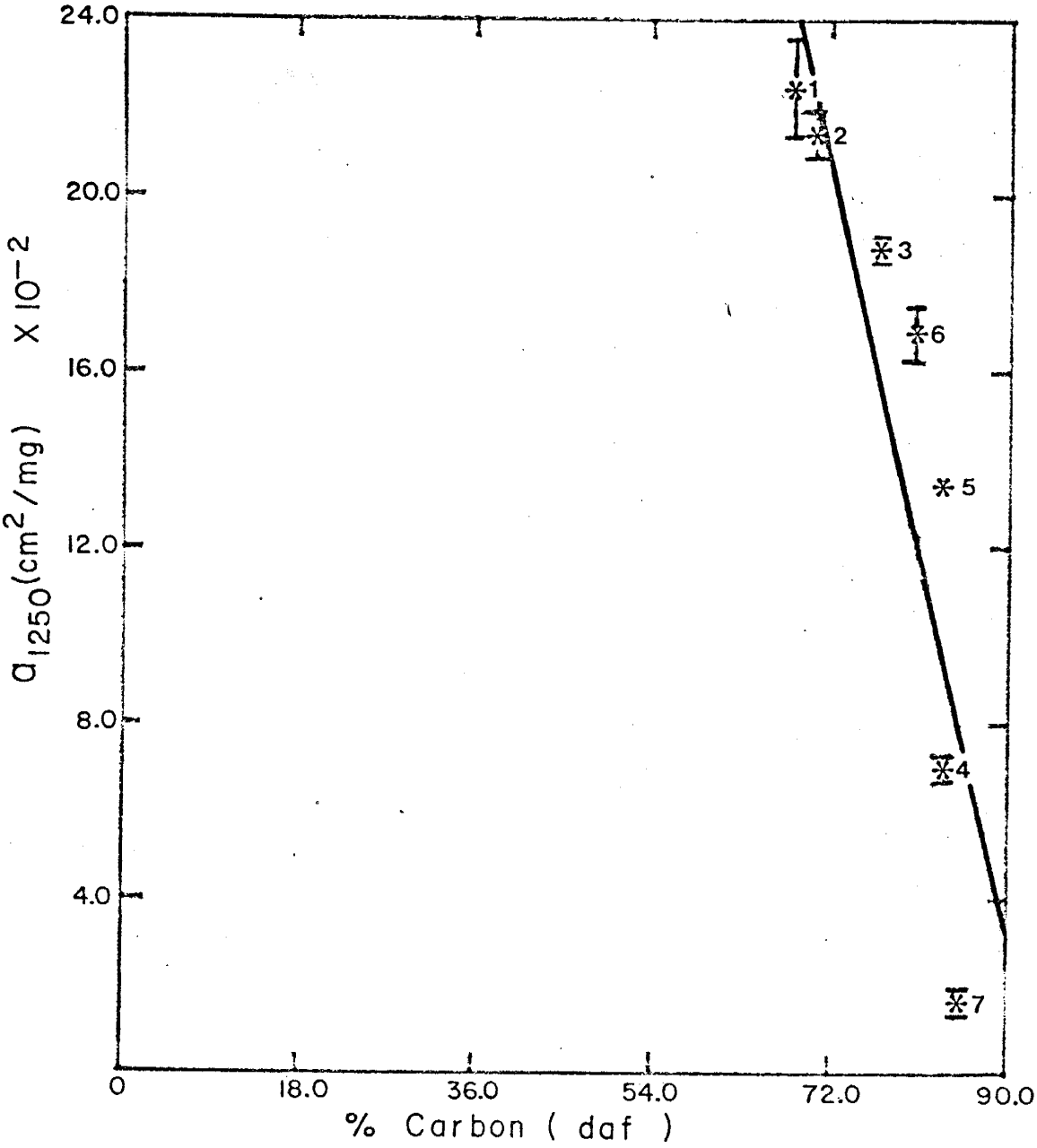

Figure 51. Plot of mean absorptivity values at 1250 cm-1 versus carbon concentration on a dry, ash-free basis for Coals 1-7. Vertical bars represent the sample standard deviation.

Plotting absorptivity at 1250 cm^{-1} as a function of elemental hydrogen on a dry, ash-free basis, Figure 52, illustrates that a curvilinear (crudely parabolic) trend describes the relationship between absorptivity at 1250 cm^{-1} and elemental hydrogen content. The curvilinear trend in Figure 52 demonstrates that, in general, absorptivity decreases correspond to increasing elemental hydrogen in lower rank whole coals (less than 84% C, daf) and decreasing elemental hydrogen in high-rank whole coals (more than or equal to 84% C, daf). Recalling that whole coals of vastly different rank may have similar elemental hydrogen contents, the decreasing absorptivity trend in Figure 52 corresponds remarkably well to the trend shown in Figure 41. Thus high-rank whole coals (more than or equal to 84% C, daf) typically have low absorptivities whereas lower rank whole coals (less than 84% C, daf) are characterized by high absorptivities. The correlation between absorptivity at 1250 cm^{-1} and elemental hydrogen (daf) in Figure 52, and elemental hydrogen (daf) and carbon (daf) content, Figure 41, suggest that hydrogen-containing functionalities, possibly hydrogen-bonded phenolic structures (Elofson, 1957; Colthump, 1964; Murchison, 1976; Painter and Coleman, 1979), influence the absorption character of the 1250 cm^{-1} region.

Absorptivity at 1250 cm^{-1} versus Oxygen Content

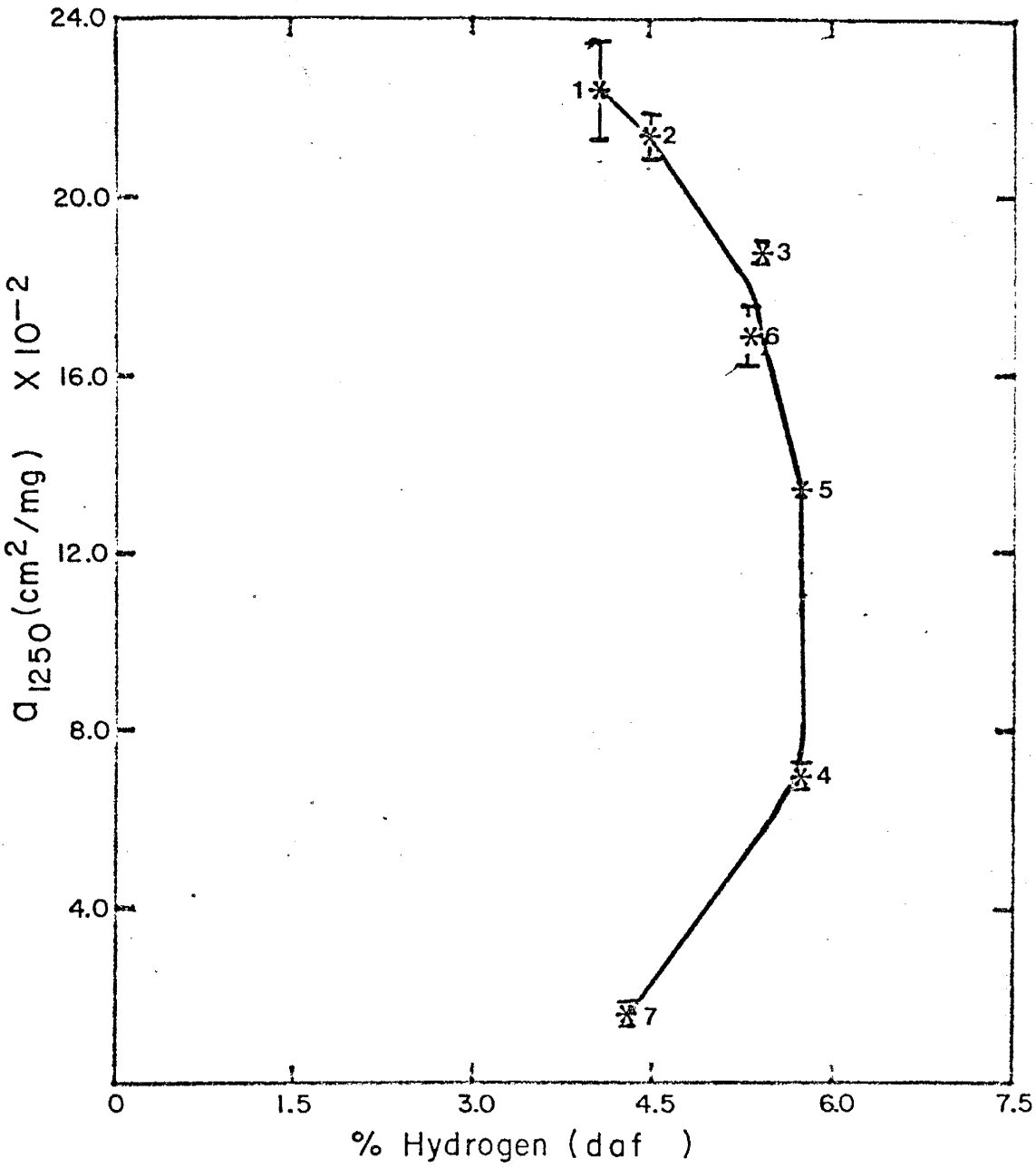

Figure 52. Mean absorptivity values at 1250 cm-1 plotted against hydrogen concentration on a dry, ash-free basis for Coals 1-7. Vertical bars indicate the sample standard deviation.

A curvilinear trend appears when absorptivity at 1250 cm^{-1} is plotted as a function of elemental oxygen on a dry, ash-free basis, Figure 53. The curvilinear trend in Figure 53 demonstrates absorptivity decreases with decreasing elemental oxygen and increasing rank. Correspondingly gradual absorptivity decreases attend decreasing elemental oxygen for the whole coals in this study having between 25.4% and approximately 10% O (daf). Whole coals with less than 10% O (daf) show very rapid absorptivity decreases occur with small decreases in elemental oxygen accompanying coalification. Extrapolation of the linear correlation line to the abscissa yields approximately 6% O (daf) suggesting whole coals with less than 6% O (daf) should not show any discernible 1250 cm^{-1} absorbance. This does not make sense in terms of what is known of the structure of coal. The absorption at 1250 cm^{-1} in anthracites is about 100% and is attributed to a high degree of condensation of aromatic clusters (Brown, 1955).

Elemental oxygen from minerals contained in whole coals with reported high ash contents significantly contributes to elemental oxygen values (determined by difference) reported in the ultimate analysis of whole coals, Table 3II, thus yielding abnormally high elemental oxygen values. Oxygen-containing groups in most minerals ⅓e.g. phyllosilicates (-OH), carbonates ($-CO_3$), sulfates ($-SO_4$), common to whole coals apparently do not significantly enhance the 1250 cm^{-1} absorbance -- compare whole coal spectra, Figure 3, with demineralized coal spectra, Figure 5. Inferred from these considerations is that if

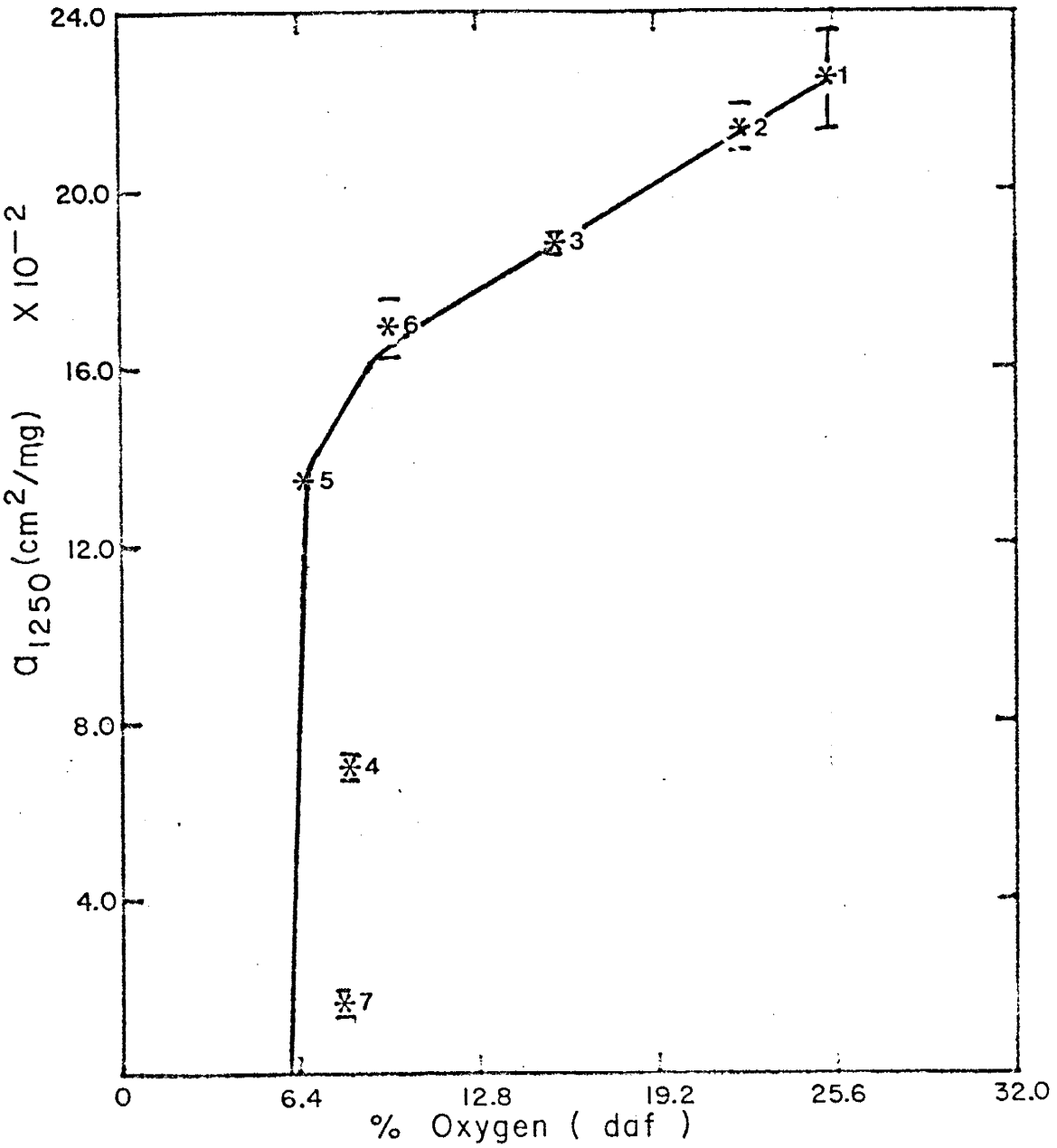

Figure 53. Mean absorptivity values at 1250 cm-1 plotted as a function of oxygen concentration on a dry, ash-free basis for Coals 1-7. Vertical bars represent the sample standard deviation.

whole Coals 4 and 7 contained ash contents similar to the other whole coals studied, i.e. less than or equal to 11% ash, then absorptivities should remain unchanged to slightly lowered from the absorptivites shown in Figure 53, although the data points for whole Coals 4 and 7 would shift toward lower oxygen contents, i.e. toward the ordinate.

Absorptivity at 870 cm^{-1} versus Carbon Content

Figure 54, absorptivity at 870 cm^{-1} versus elemental carbon on a dry, ash-free basis, demonstrates that the whole coals studied containing more than 80% C (daf) show a distinct absorbance at 870 cm^{-1}. Coal 7, the highest rank whole coal studied, has the highest absorptivity. Coals 4 and 5 have very simi lar elemental carbon (daf) contents although the absorptivity for Coal 4 ($a = 0.0138$ cm^2/mg) is approximately half that for Coal 5 ($a = 0.0259$ cm^2/mg). This disparity in absorptivities for whole coals with similar elemental carbon contents and hence similar rank probably reflects the relative abundance of highly substituted aromatic structures occurring even in whole coals of the same rank. A single spectrum out of 6 spectral scans of Coal 1 yielded a weak but measureable absorption at 870 cm^{-1}. Correlation of absorptivity at 870 cm^{-1} with elemental carbon (daf) was expected to be high since the 870 cm^{-1} band is attributed to aryl C-H out-of-plane bending and aryl skeleton vibrational modes. Figure 54 shows this is not the case for the whole coals studied.

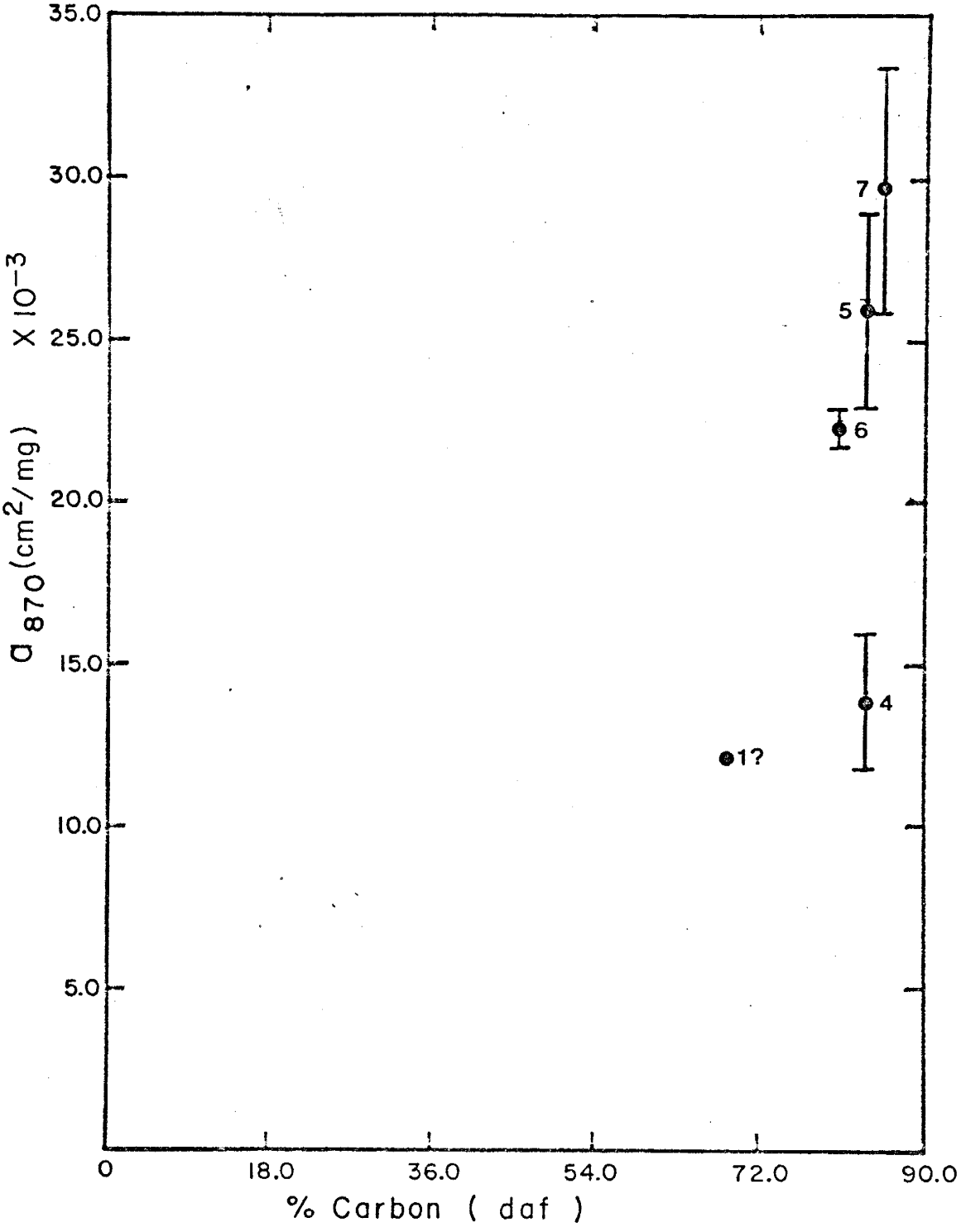

Figure 54. Plot of mean absorptivity values at 870 cm-1 against carbon concentration on a dry, ash-free basis for Coals 1 and 4-7. Vertical bars indicate the sample standard deviation. ? means not confident of mean absorptivity value due to insufficient data.

Absorptivity at 870 cm^{-1} versus Hydrogen Content

Plotting absorptivity at 870 cm^{-1} as a function of elemental hydrogen on a dry, ash-free basis, Figure 55, suggests absorptivity generally decreases with elemental hydrogen (daf) increases. The apparent absorptivity decrease attending increasing elemental hydrogen (daf) in high-rank whole coals (80% , %C , 95%) roughly corresponds to decreasing rank as measured by elemental carbon (daf) contents, Figure 41. These data are consistent with what is known of the structure of coal, whereby absorption intensity increases correspond to rank increases in the region between 900-700 cm^{-1}, the aryl C-H out-of-plane bending and aryl skeleton vibrational modes. Coals 4 and 5 are whole coals with similar elemental hydrogen (daf) contents and significantly different absorption intensity at 870 cm^{-1}, Figure 55, indicating significant differences occur in the number of highly substituted aromatic structures in whole coals with similar rank parameters.

Absorptivity at 795 cm^{-1} versus Carbon Content

Plotting absorptivity at 795 cm^{-1} as a function of elemental carbon on a dry, ash-free basis reveals a linear trend demonstrating absorptivity increases with increasing elemental carbon and coalification, Figure 56. The linear correlation line in Figure 56 is defined by $a = 1.65X10^{-3}$ (%C, daf) - 0.103 with a 0.956 correlation coefficient. Extrapolation of the linear correlation line to the

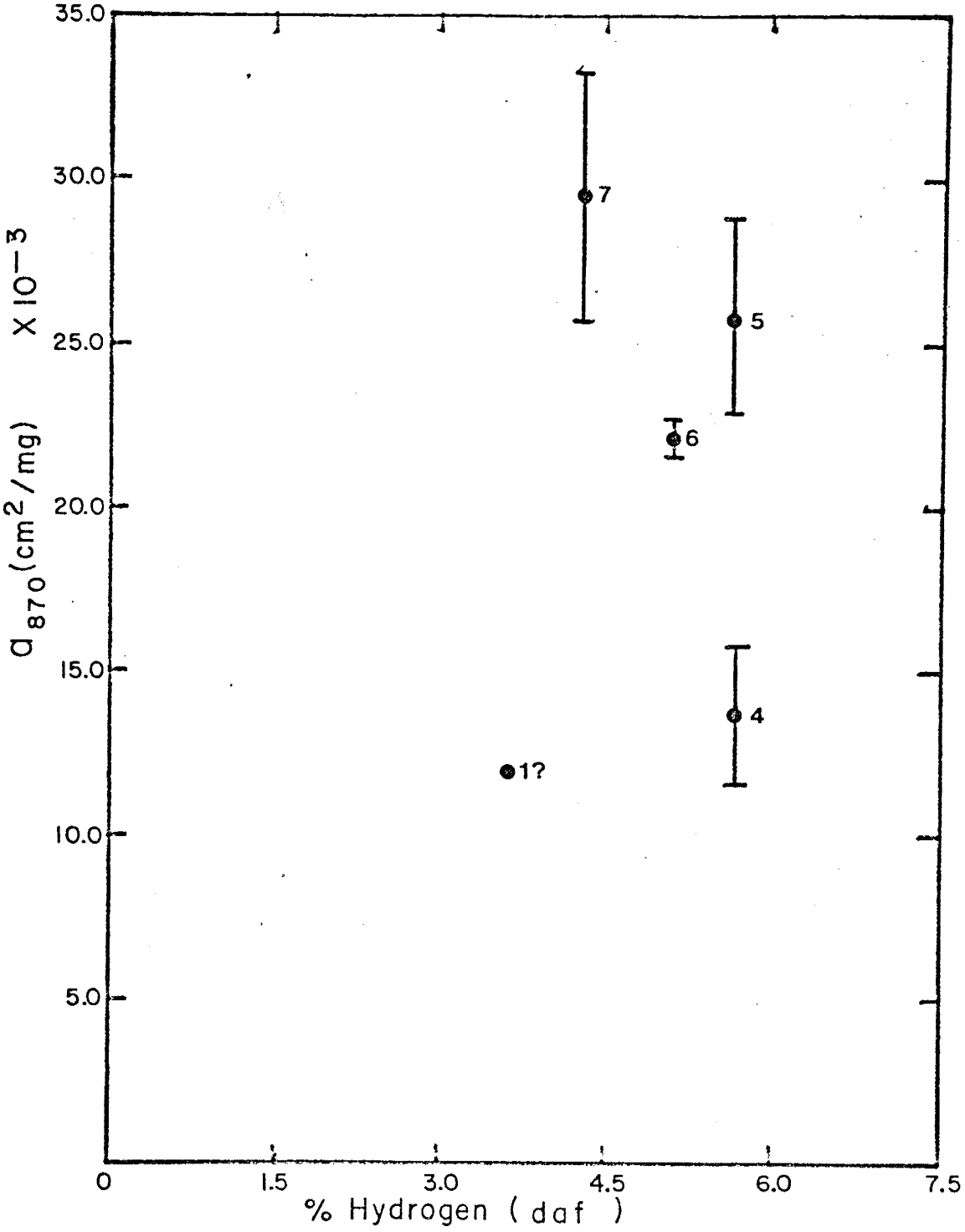

Figure 55. Mean absorptivity values at 870 cm-1 plotted against hydrogen concentration on a dry, ash-free basis for Coals 1 and 4-7. Vertical bars represent the sample standard deviation. ? means not confident of mean absorptivity value due to insufficient data.

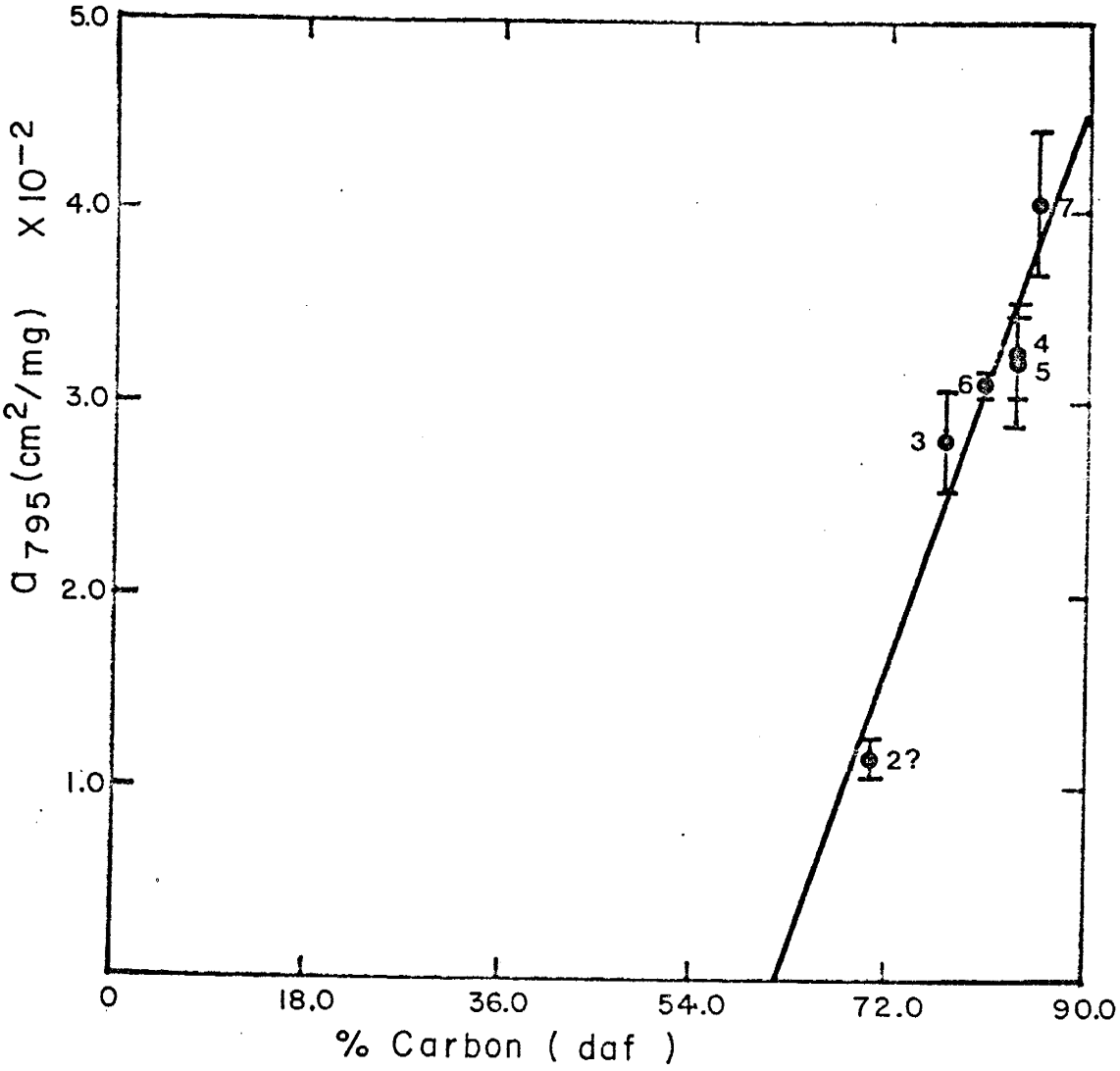

Figure 56. Mean absorptivity values at 795 cm-1 plotted as a function of carbon concentration on a dry, ash-free basis for Coals 2-7. Vertical bars indicate the sample standard deviation. ? means not confident of mean absorptivity value due to insufficient data.

abscissa, a = 0.000 cm^2/mg, yields 62.4% C (daf), suggesting whole coals containing less than 63% C (daf) show no distinguishable absorbance at 795 cm^{-1}. Absorptivity increases at 795 cm^{-1} corresponding to increasing elemental carbon is compatible with increasing aromaticity attending coalification in high-rank whole coals. This progressive increase in absorptivity at 795 cm^{-1} attending coalification may reflect decreasing substitution of aromatic molecules in addition to contemporaneous condensation of these aromatic units into polycyclic aromatic clusters (graphitic structures). Van Vucht et al. (1955, p. 57) noted, " . . . these bands (900-700 cm^{-1}) are not yet present in the spectra of young coal, nor in those of lignin and brown coal. At a carbon content above 81 per cent these bands become clearly percept ible, but vanish again when the carbon content increases beyond 94 per cent, probably because they become masked by the gradually increasing electronic absorption."

Absorptivity at 795 cm^{-1} versus Oxygen Content

Absorptivity at 795 cm^{-1} plotted as a function of elemental oxygen on a dry, ash-free basis, Figure 57, reveals that absorptivity increases correspond to elemental oxygen decreases generally attending increasing rank. The linear best-fit correlation line, defined by a = 0.046 - $1.44X10^{-3}$ (%O, daf) with a -0.904 correlation coefficient, describes the inverse relationship between absorptivity at 795 cm^{-1} and elemental oxygen in Figure 57. Extrapolation of the linear correlation line to

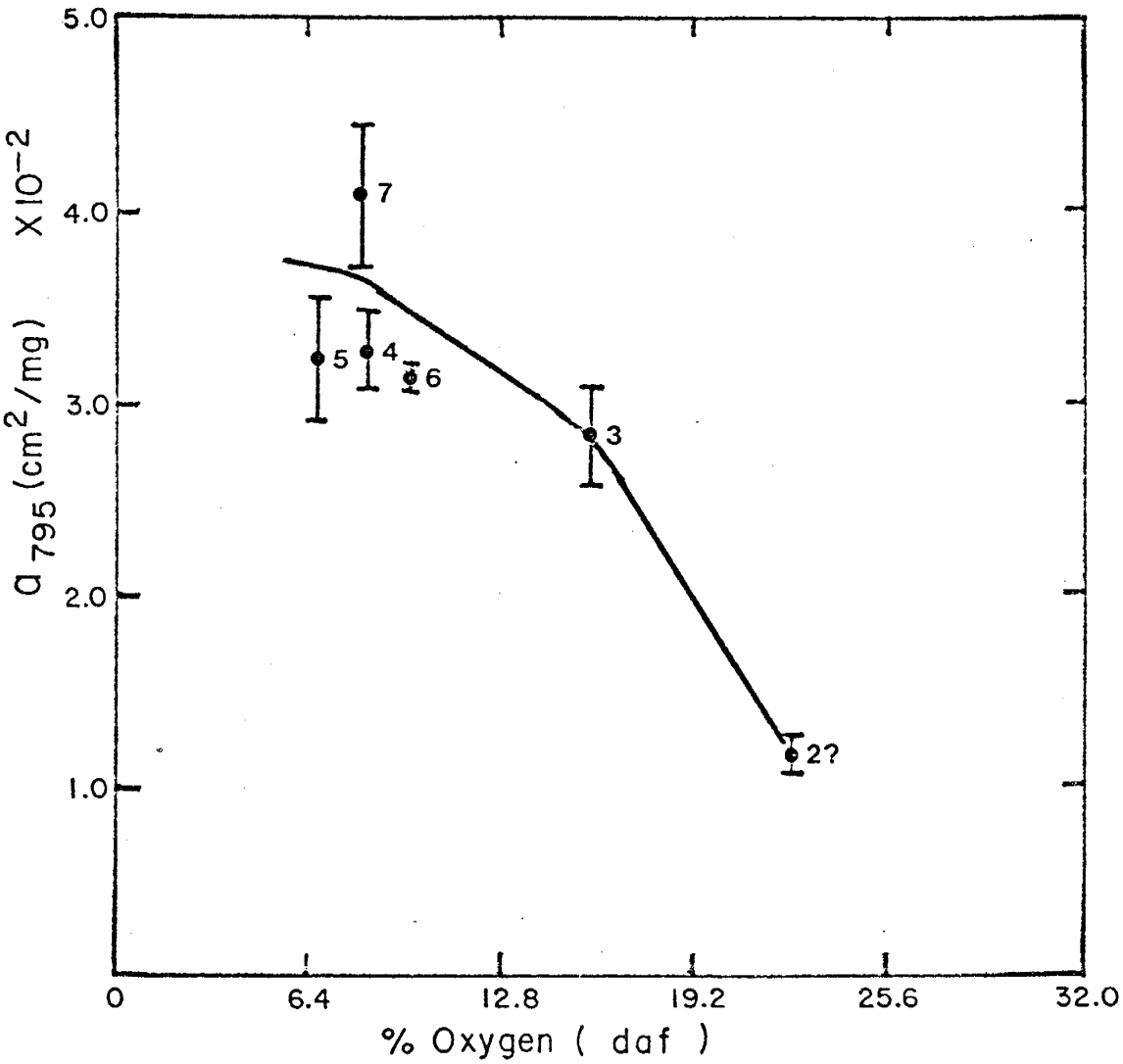

Figure 57. Plot of mean absorptivity values at 795 cm-1 versus oxygen concentration on a dry, ash-free basis for Coals 2-7. Vertical bars indicate the sample standard deviation. ? means not confident of mean absorptivity value due to insufficient data.

the abscissa yields 32% O (daf) suggesting no perceptible absorbance at 795 cm^{-1} occurs in whole coals containing more than 32% O (daf). The weak absorption intensity at 795 cm^{-1} characterizing lowrank whole coals is attributed to highly substituted aromatic molecules, principally phenolic. As coalification proceeds, these highly substituted aromatic molecules become less substituted, in addition to contemporaneous condensation of these aromatic units into polycyclic aromatic clusters, resulting in a stronger, but still weak, absorption intensity at 795 cm^{-1} in high-rank whole coals. Recalling whole coals with high mineral (ash) contents (see discussion for a_{1250} vs oxygen content, pages 150 - 154), it is reasonable to infer that of the total elemental oxygen reported, the elemental oxygen associated with organic structures in whole coals would displace the data points to the left, i.e. toward lower oxygen values. Furthermore, the data points representing whole coals with lower mineral (ash) contents would slightly shift toward the ordinate as a function of the quantity of oxygen-bearing minerals present in the whole coal. The result of shifting the data points toward the ordinate is a linear trend similar to the linear trend in Figure 57.

It is interesting to note that the 795 cm^{-1} absorption band is not generally assigned to oxygen-containing functionalities.

Absorptivity at 740 cm^{-1} versus Carbon Content

Figure 58, the plot of absorptivity at 740 cm^{-1} as a function of elemental carbon on a dry, ash-free basis, illustrates that as elemental carbon content and rank gradually increase absorptivities rapidly increase. The linear correlation line in Figure 58, defined by $a = 2.86X10^{-3}$ (%C, daf) - 0.203, describes the positive relationship between absorptivity at 740 cm^{-1} and elemental carbon (daf). Extrapolation of the linear correlation line to the abscissa yields approximately 70% C (daf) suggesting no absorbance will be discernible in whole coals containing less than or equal to 70% C (daf). This interpretation is consistent with what is known of the structure of coal.

The absorptivity for Coal 6 appears to be rather low relative to the absorptivities for the other whole coals studied. This may be indicative of the relative scarcity of this substituted aromatic moiety in Coal 6. Actually Coal 6 has a relatively high absorptivity for the 870 cm^{-1} absorption band suggesting that these more highly substituted aromatic functionalities are more abundant (dominant) relative to the less substituted aromatic functionalities absorbing near 740 cm^{-1}. This inference assumes negligible differences exist in the magnitude of the absorption coefficients (a_k) for the 870 and 740 cm^{-1} regions in whole coals.

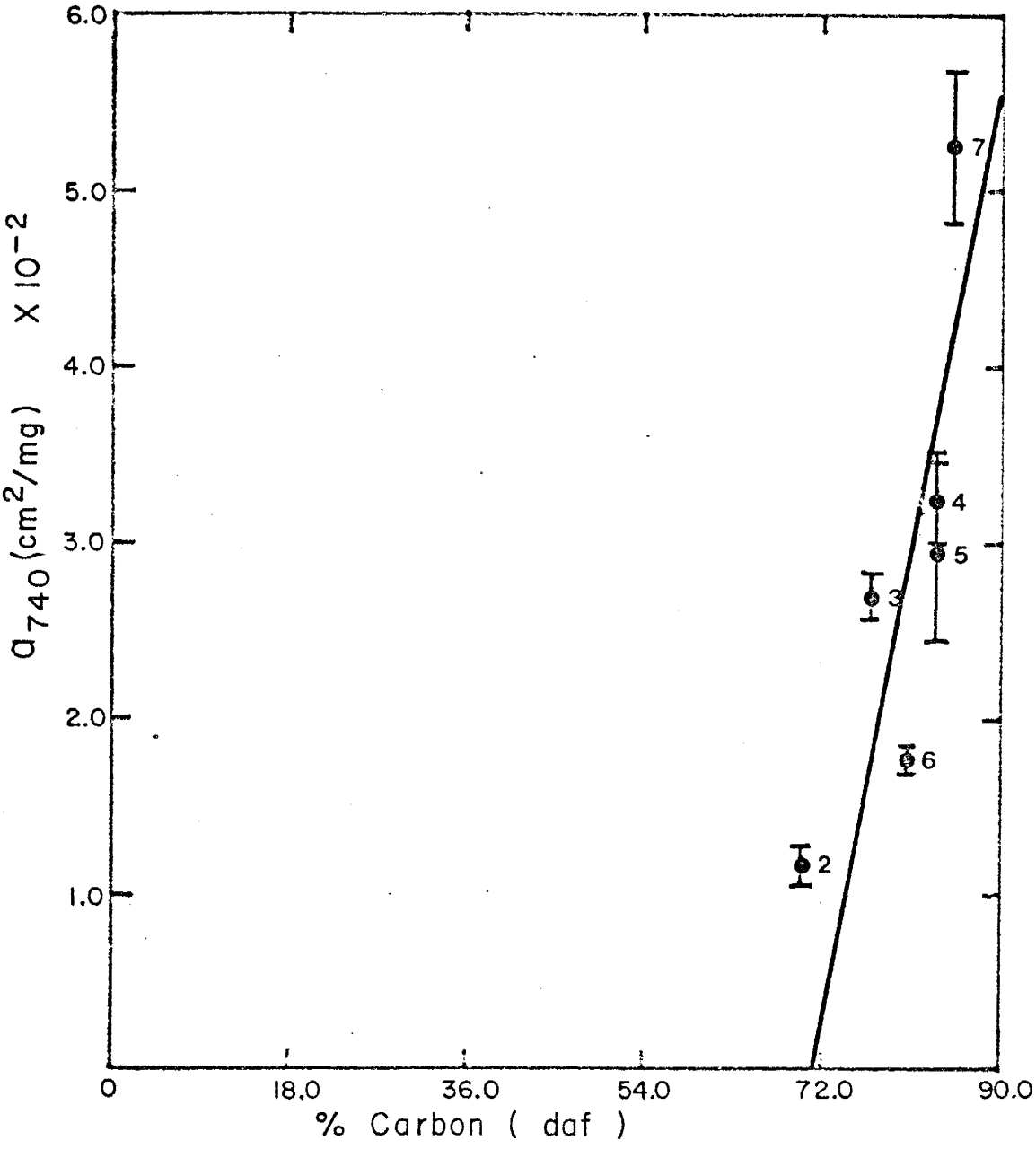

Figure 58. Mean absorptivity values at 740 cm-1 plotted against carbon concentration on a dry, ash-free basis for Coals 2-7. Vertical bars represent the sample standard deviation.

Absorptivity at 740 cm^{-1} versus Hydrogen Content

The plot of absorptivity at 740 cm^{-1} as a function of elemental hydrogen on a dry, ash-free basis, Figure 59, demonstrates that, in general, absorptivity increases correspond to increasing elemental hydrogen contents in whole coals with less than 84% C (daf) and decreasing elemental hydrogen contents in whole coals with more than or equal to 84% C (daf). Here again, the curvilinear (crudely parabolic) trend used to describe the relationship between absorptivity at 740 cm^{-1} and elemental hydrogen (daf) perhaps is a reflection of the linear trend shown in Figure 41. Coals 2 and 7 have similar elemental hydrogen contents although Coal 7, a dominantly polycyclic aromatic coal, has a high absorptivity whereas Coal 2, a more aliphatic coal, has a relatively low absorptivity. Indeed comparing Figure 59 with graphs of elemental hydrogen plotted as a function of alkyl functionalities, e.g. 1440 cm^{-1} (Figure 48), phenoxy and alkoxy functionalities, e.g. 1250 cm^{-1} (Figure 52), and other functional groups, e.g. 3400 cm^{-1} (Figure 28) and 1590 cm^{-1} (Figure 44), reveals a trend for whole coals with high degrees of aromaticity that is antithetical to that for whole coals with low degrees of aromaticity, i.e. principally aliphatic/alicyclic whole coals. Stated differently, apparently highly aliphatic and alicyclic whole coals are characterized by very low absorptivities for the 870, 795 and 740 cm^{-1} bands and high absorptivities for absorption bands generally characteristic of non-aromatic functionalities; the opposite trend is observed for relatively highly aromatic whole coals. This

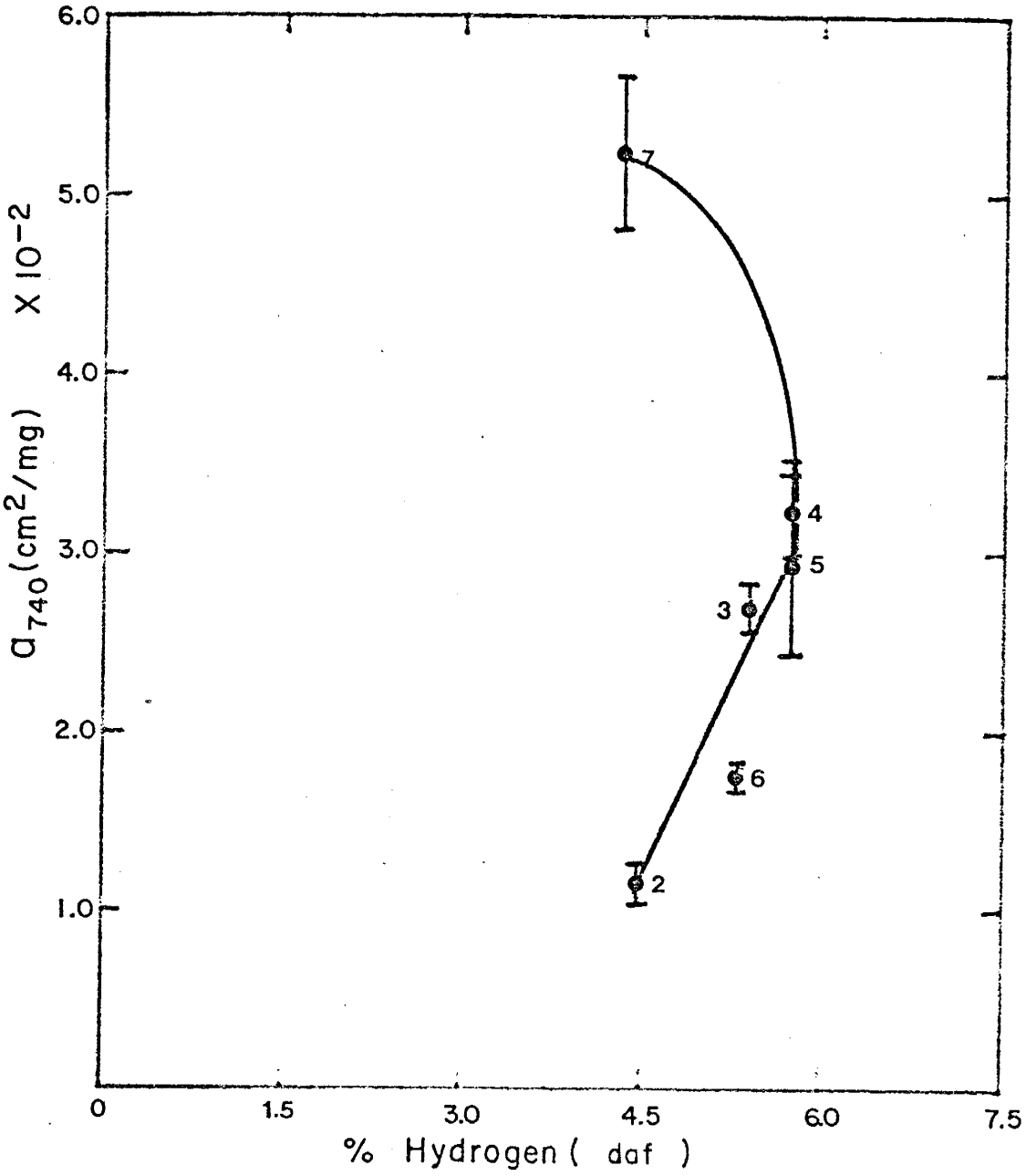

Figure 59. Mean absorptivity values at 740 cm-1 plotted as a function of hydrogen concentration on a dry, ash-free basis for Coals 2-7. Vertical bars indicate the sample standard deviation.

trend becomes more obvious when the 1440 cm^{-1} absorptivities are plotted against the 740 cm^{-1} absorptivities, Figure 70.

QUANTITATIVE ANALYSIS OF ABSORPTIVITIES AT A GIVEN FREQUENCY PLOTTED AGAINST ABSORPTIVITIES AT A DIFFERENT FREQUENCY

Introduction

Plotting absorptivity at a given frequency against absorptivity at a different frequency illustrates that systematic changes in absorptivities occur over a range of rank in whole coals. As a result of inadequate knowledge of the nature of change, if changes occur, in the absorption coefficient with rank, it is not clear whether the apparent relationships between the absorptivities at different wavelengths reflect changes in the absorption coefficient, the concentration of the absorbing species, or both. The graphs of absorptivity at a given wavelength poltted as a function of absorptivity at a different wavelength, Figures 60-71, tend to suggest that many modes vary in a systematic fashion with rank. The systematic variation of absorptivities with rank demonstrates that much of the data set is not independent but related in some fashion.

Absorptivity at 3400 cm^{-1} versus Absorptivity at 1700 cm^{-1}

Plotting absorptivity at 3400 cm^{-1} as a function of the absorptivity at 1700 cm^{-1}, Figure 60, demonstrates that decreasing absorptivity at 1700 cm^{-1} attend absorptivity decreases at 3400 cm^{-1} as rank increases. The exponential correlation line in Figure 60 is

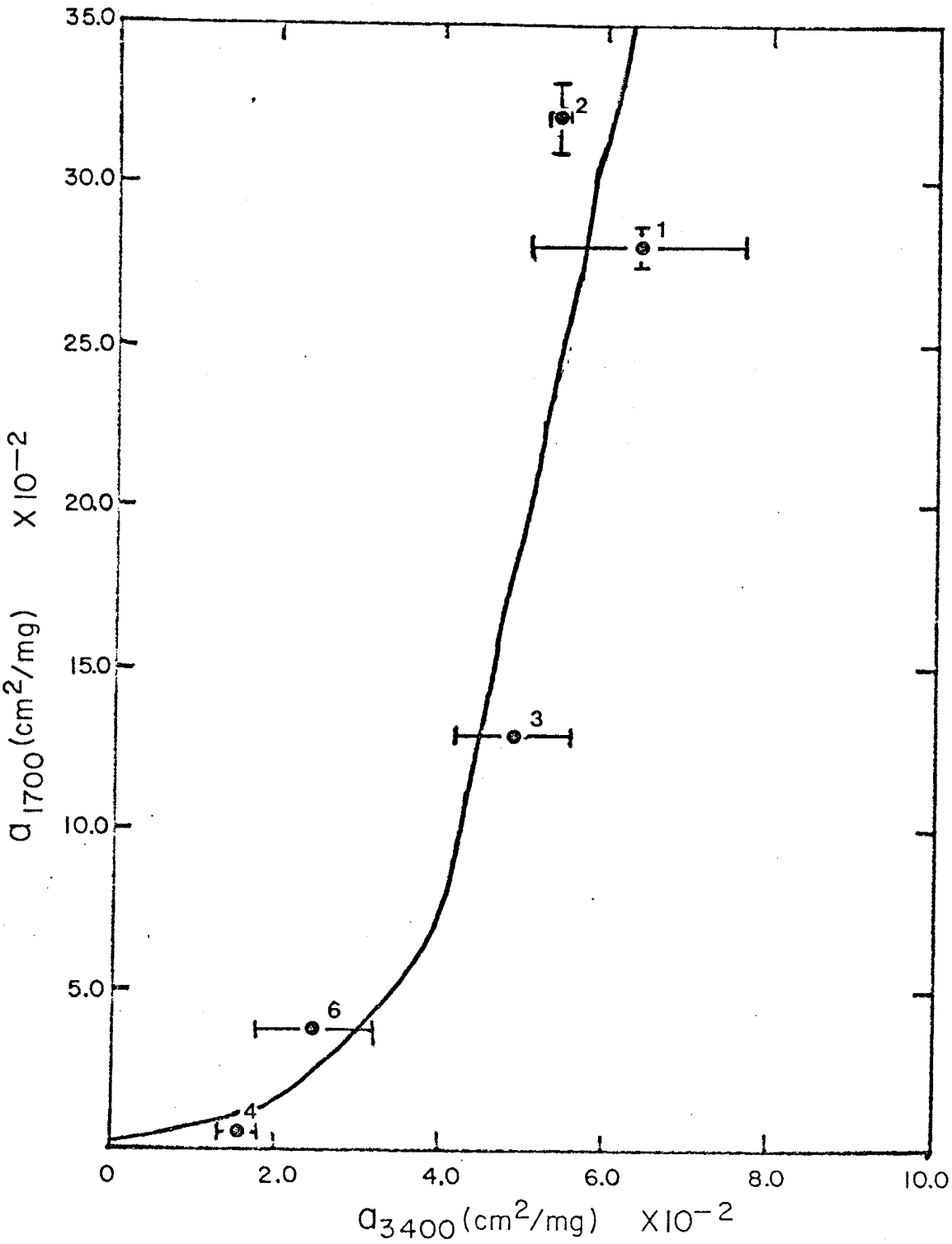

Figure 60. Mean absorptivity values at 1700 cm-1 plotted against mean absorptivity values at 3400 cm-1 measured according to the 3700-3000 cm-1 measurement method for Coals 1-4 and 6. Vertical and horizontal bars indicate the sample standard deviation.

defined by $\ln a_{1700} = 74.88(a_{3400}) - 5.65$ with a 0.953 correlation coefficient. Extrapolation of the correlation line to the ordinate yields an absorptivity value of 0.0035 cm^2/mg for the 1700 cm^{-1} band. This value is inconsistent with the results of pyrolysis experiments on kerogens (Rouxhet and Robin, 1978; Rouxhet et al., 1979) and infrared studies of the catagenesis of kerogens (Brown, 1955; Rouxhet and Robin, 1978). These studies revealed that the 3400 cm^{-1} absorption band persists long after the disappearance of the 1700 cm^{-1} band, unless these materials have strongly oxidized. Alternatively, linear regression analysis on the data reveals that a rectilinear relation, defined by $a_{1700} = 6.234(a_{3400}) - 0.130$ with a 0.909 correlation coefficient, describes the relationship between the absorptivities at 3400 and 1700 cm^{-1}. The rectilinear correlation line extrapolated to the abscissa, i.e. absorptivity at 1700 cm^{-1} = 0.0000 cm^2/mg, yields a 0.0165 cm^2/mg absorptivity for the 3400 cm^{-1} band. This values is more compatible with the results of other studies, e.g. Rouxhet et al. (1979). This observed relationship between the absorptivities at 3400 and 1700 cm^{-1} suggests that these data are not independent. Note: Coals 5 and 7 exhibit no distinct absorption band at 1700 cm^{-1} (see Fig. 3 and Appendix 3).

Absorptivity at 3400 cm^{-1} versus Absorptivity at 1660 cm^{-1}

Figure 61, absorptivity at 3400 cm^{-1} plotted as a function of the absorptivity at 1660 cm^{-1}, demonstrates that absorptivity decreases at 1660 cm^{-1} correspond to absorptivity decreases at 3400 cm^{-1} attending rank increases. This apparent relationship between the absorptivities at 3400 and 1660 cm^{-1} may be described by an exponential correlation line, defined by $\ln a_{1600} = 51.90\ (a_{3400}) - 4.14$ with a 0.972 correlation coefficient, shown in Figure 61. Extrapolation of this correlation line to the ordinate, i.e. absorptivity at 3400 cm^{-1} = 0.0000 cm^2/mg, yields a 0.0159 cm^2/mg absorptivity for the 1660 cm^{-1} band. This is not consistent with what is known of the structure of whole coal. A rectilinear correlation line, defined by $a_{1600} = 5.696(a_{3400}) - 0.045$ with a 0.906 correlation coefficient, can be used to describe the relationship between absorptivities at 3400 and 1660 cm^{-1}. The rectilinear correlation line extrapolated to the abscissa, i.e. absorptivity at 1660 cm^{-1} = 0.0000 cm^2/mg, yields a 0.0079 cm^2/mg absorptivity for the 3400 cm^{-1} band. This value is more consistent with what is known of the structure of whole coal. This relationship between absorptivities at 3400 and 1660 cm^{-1} suggests that this data set is not independent but related in some fashion. Note: Coals 1 and 6 exhibited no distinct absorption band at 1660 cm^{-1}.

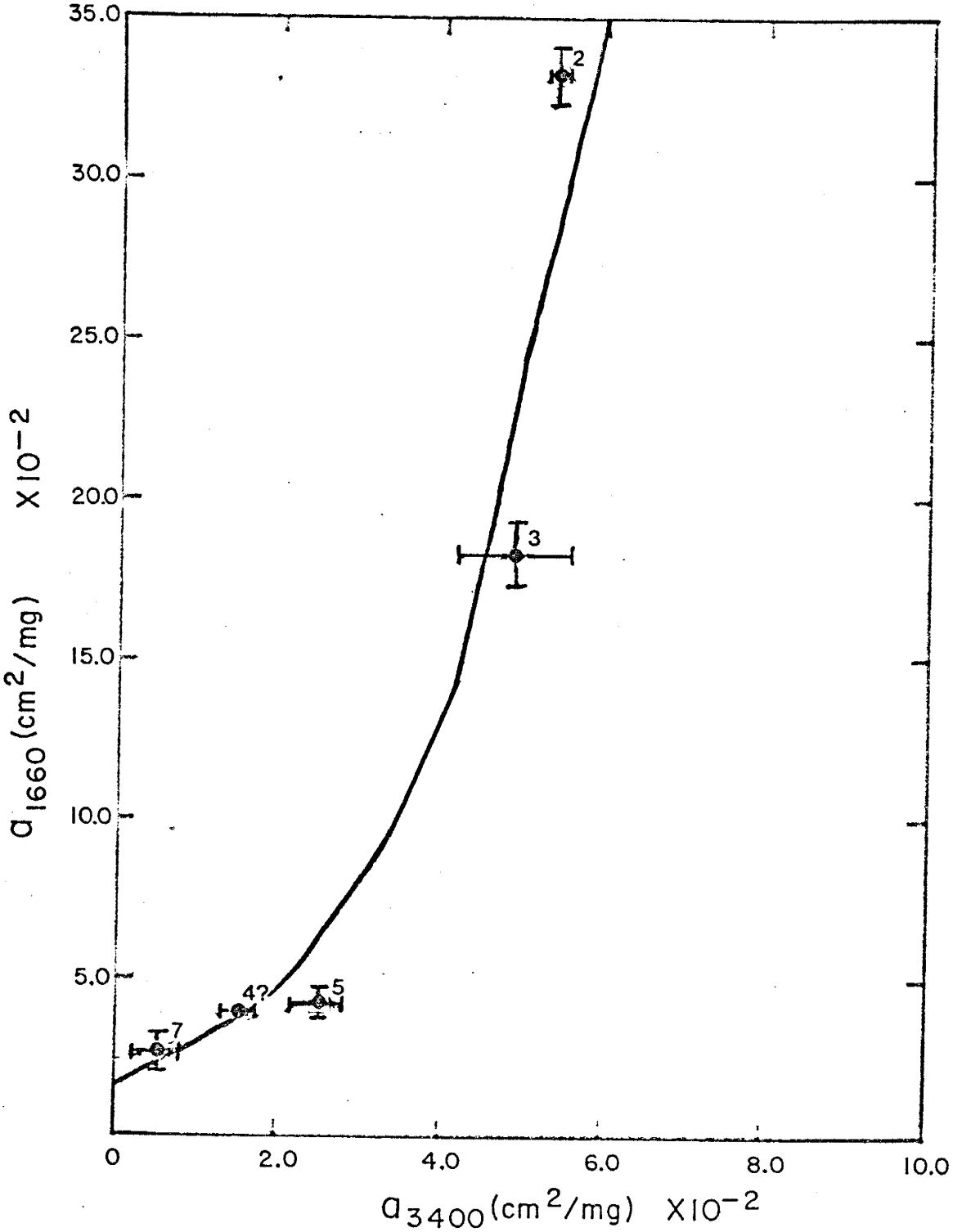

Figure 61. Mean absorptivity values at 1660 cm-1 plotted as a function of mean absorptivity values at 3400 cm-1 measured according to the 3700-3000 cm-1 measurement method for Coals 2-5 and 7. Vertical and horizontal bars represent the sample standard deviation. ? means not confident of mean absorptivity value due to insufficient data.

Absorptivity at 3400 cm^{-1} versus Absorptivity at 1590 cm^{-1}

The plot of absorptivity at 3400 cm^{-1} as a function of absorptivity at 1590 cm^{-1}, Figure 62, reveals a linear relation defined by $a_{1590} = 6.141(a_{3400}) + 0.076$ with a correlation coefficient of 0.975. The correlation line in Figure 62 demonstrates that absorptivities at 1590 cm^{-1} show corresponding decreases as absorptivities at 3400 cm^{-1} decrease with increasing rank. Extrapolation of the correlation line to the ordinate yields a 0.076 cm^2/mg absorptivity for the 1590 cm^{-1} band. This value seems reasonable when considering that the 1590 cm^{-1} band is for many whole coals the most prominent spectral feature. It is inferred from this that highly-conjugated phenolic hydroxyl and NH groups enhance the absorption intensity of the 1590 cm^{-1} band. This inference is compatible with the conclusions reached by Painter et al. (1981a,b). The approximately 0.076 cm^2/mg absorptivity for the 1590 cm^{-1} band in high-rank whole coals that exhibit no distinguishable absorbance at 3400 cm^{-1}, i.e. whole coals with more than or equal to 89% C (daf) ¼see Fig. 27₁, suggests that the 1590 cm^{-1} absorption band in high-rank whole coals is a result of other functionalities, e.g. aromatic >C=C< stretching modes and highly-conjugated hydrogen-bonded carbonyl groups (>C=O...HO-). This linear relationship between absorptivities at 3400 and 1590 cm^{-1} suggests that these data are related in some way.

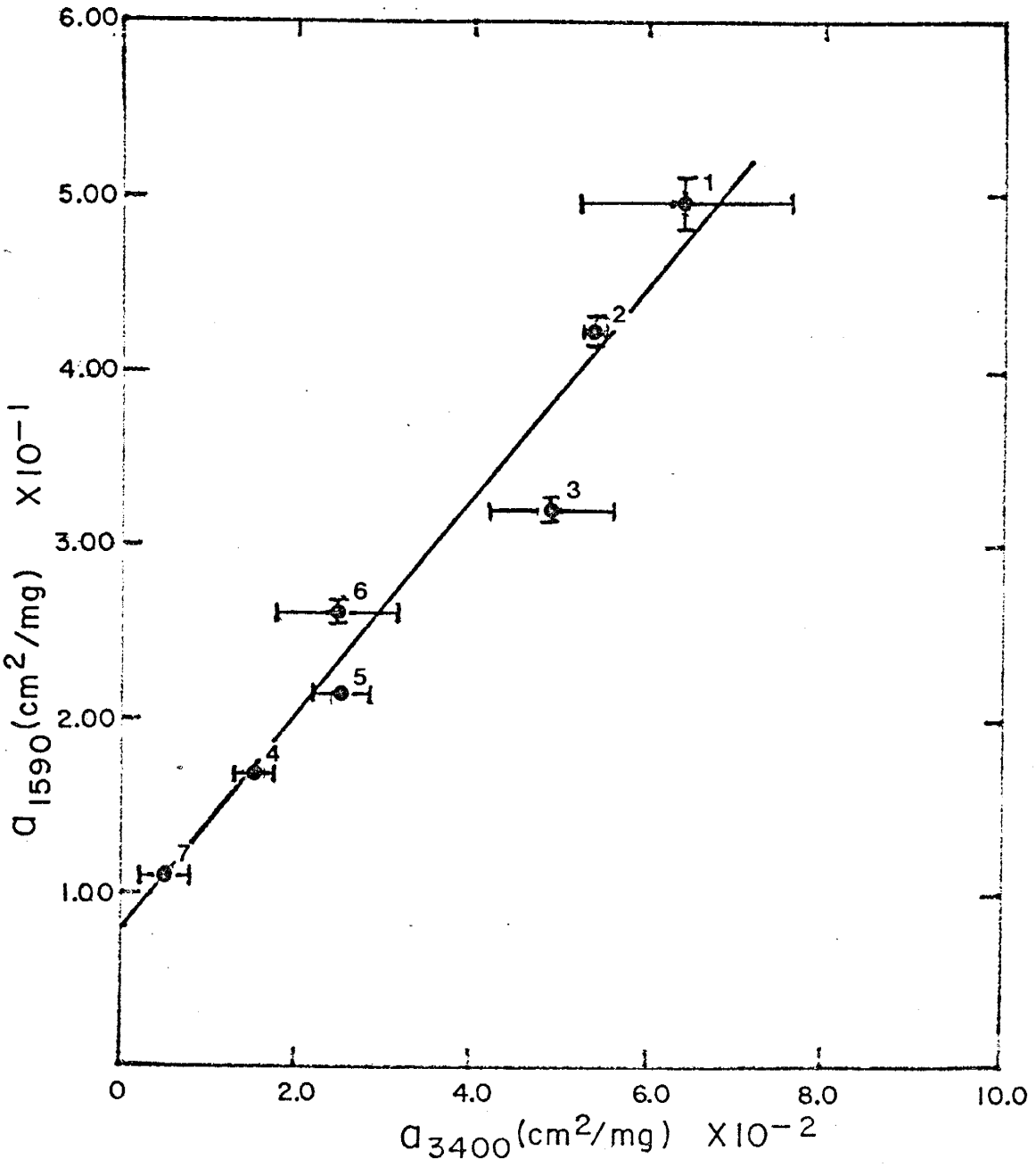

Figure 62. Plot of mean absorptivity values at 1590 cm-1 versus mean absorptivity values at 3400 cm-1 measured according to the 3700-3000 cm-1 measurement method for Coals 1-7. Vertical and horizontal bars indicate the sample standard deviation.

Absorptivity at 3400 cm^{-1} versus Absorptivity at 1250 cm^{-1}

Figure 63 shows that a logarithmic correlation line can describe the relationship between absorptivities at 3400 cm^{-1} and those at 1250 cm^{-1}. The logarithmic correlation line in Figure 63, defined by $a_{1250} = 0.086\ln(a_{3400}) + 0.459$ with a 0.972 correlation coefficient, demonstrates that decreases in absorptivity at 1250 cm^{-1} correspond to decreases in absorptivity at 3400 cm^{-1} with increasing rank. Extrapolation of the correlation line to the abscissa suggests that the 3400 cm^{-1} absorptivity approaches 0.0049 cm^2/mg as the 1250 cm^{-1} absorptivity approaches zero. The 0.0049 cm^2/mg value is not compatible with what is known of the structure of whole coal for the following reason. Both the 3400 and 1250 cm^{-1} absorption bands principally arise from hydrogen-bonded phenolic hydroxyls (Painter and Coleman, 1979; Murchison, 1976; Siskov and Petrova, 1974; Brown, 1955), although the 1250 cm^{-1} band is intensity enhanced by ether functionalities, presumably aryl-aryl ethers (Rouxhet et al., 1980). Therefore, as the 3400 cm^{-1} absorptivity approaches zero the 1250 cm^{-1} absorptivity should show a corresponding decrease, although the 1250 cm^{-1} absorptivity should not be zero since ether groups are believed to exist even in anthracites.

Linear regression analysis on the data reveals that a rectilinear relation, defined by $a_{1250} = 3.2817(a_{3400}) + 0.0336$ with a 0.925 correlation coefficient, can describe the relationship between the

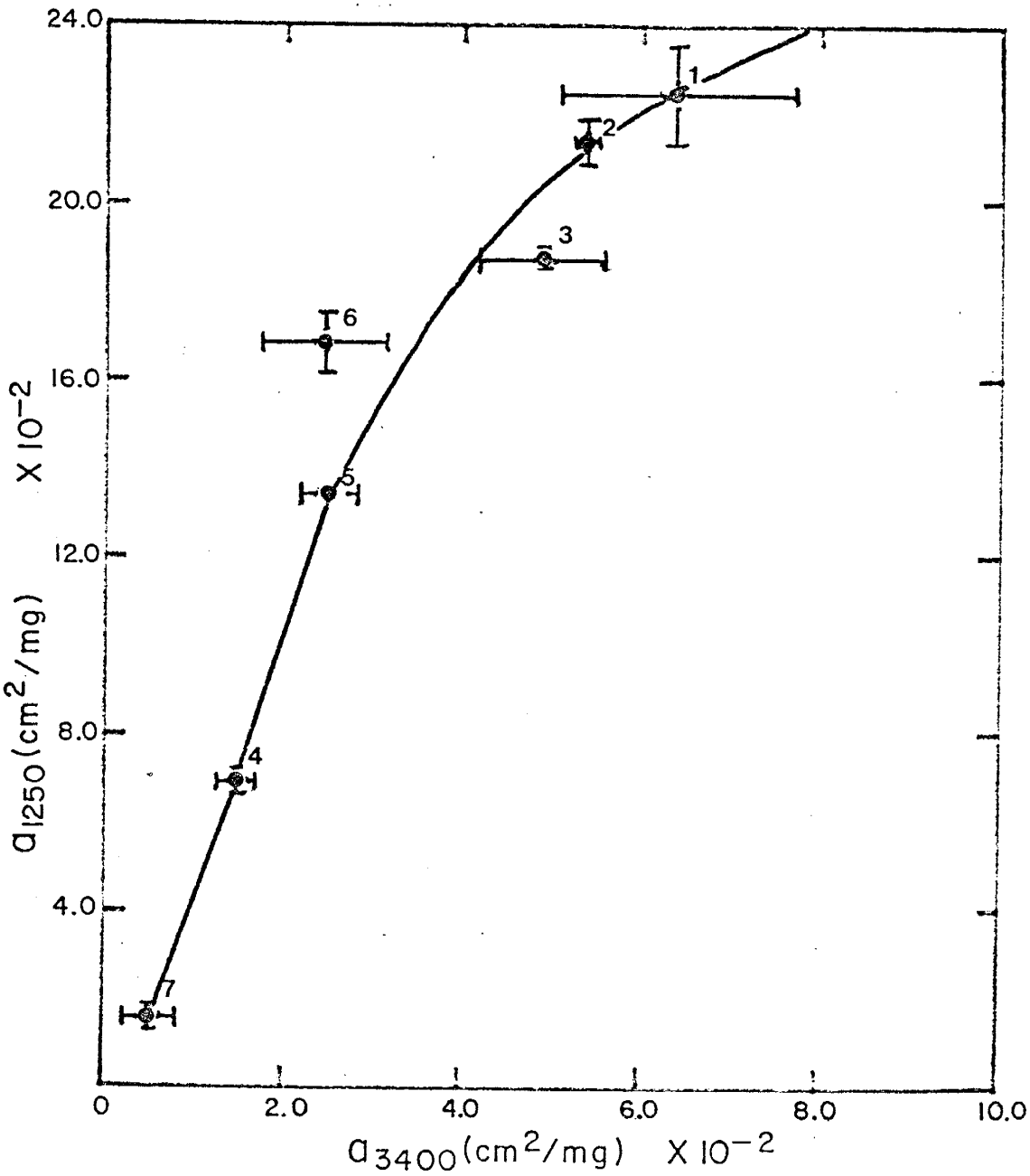

Figure 63. Mean absorptivity values at 1250 cm-1 plotted against mean absorptivity values at 3400 cm-1 measured according to the 3700-3000 cm-1 measurement method for Coals 1-7. Vertical and horizontal bars represent the sample standard deviation.

absorptivities at 3400 and 1250 cm^{-1}. The rectilinear correlation line extrapolated to the ordinate yields an absorptivity of 0.0336 cm^2/mg for the 1250 cm^{-1} band. This appears to be more compatible with what is known of the structure of whole coal than the logarithmic correlation value. The existence of a correlation between absorptivities at 3400 and 1250 cm^{-1}, regardless of the correlation used, suggests that the data are not independent.

Absorptivity at 1590 cm^{-1} versus Absorptivity at 1250 cm^{-1}

Plotting the 1590 cm^{-1} absorptivity as a function of the 1250 cm^{-1} absorptivity, Figure 64, demonstrates that decreases in the absorptivity at 1250 cm^{-1} attend decreases in the 1590 cm^{-1} absorptivity as rank increases. The exponential relationship between the 1590 and 1250 cm^{-1} absorptivities in Figure 64 is described by $\ln a_{1590} = 6.64(a_{1250}) - 2.33$ with a 0.981 correlation coefficient. Extrapolation of the correlation line to the ordinate, i.e. 1250 cm^{-1} absorptivity = 0.0000 cm^2/mg, yields a 0.0971 cm^2/mg absorptivity for the 1590 cm^{-1} band. The 1590 cm^{-1} absorptivity of 0.0971 cm^2/mg corresponding to 0.0000 cm^2/mg for the 1250 cm^{-1} absorptivity in high-rank whole coals presumably results from aromatic (>C=C<) ring stretching modes and possibly highly conjugated hydrogen-bonded >C=O groups. The excellent correlation between the 1590 and 1250 cm^{-1} absorptivities suggests that the data are not independent but related in some fashion.

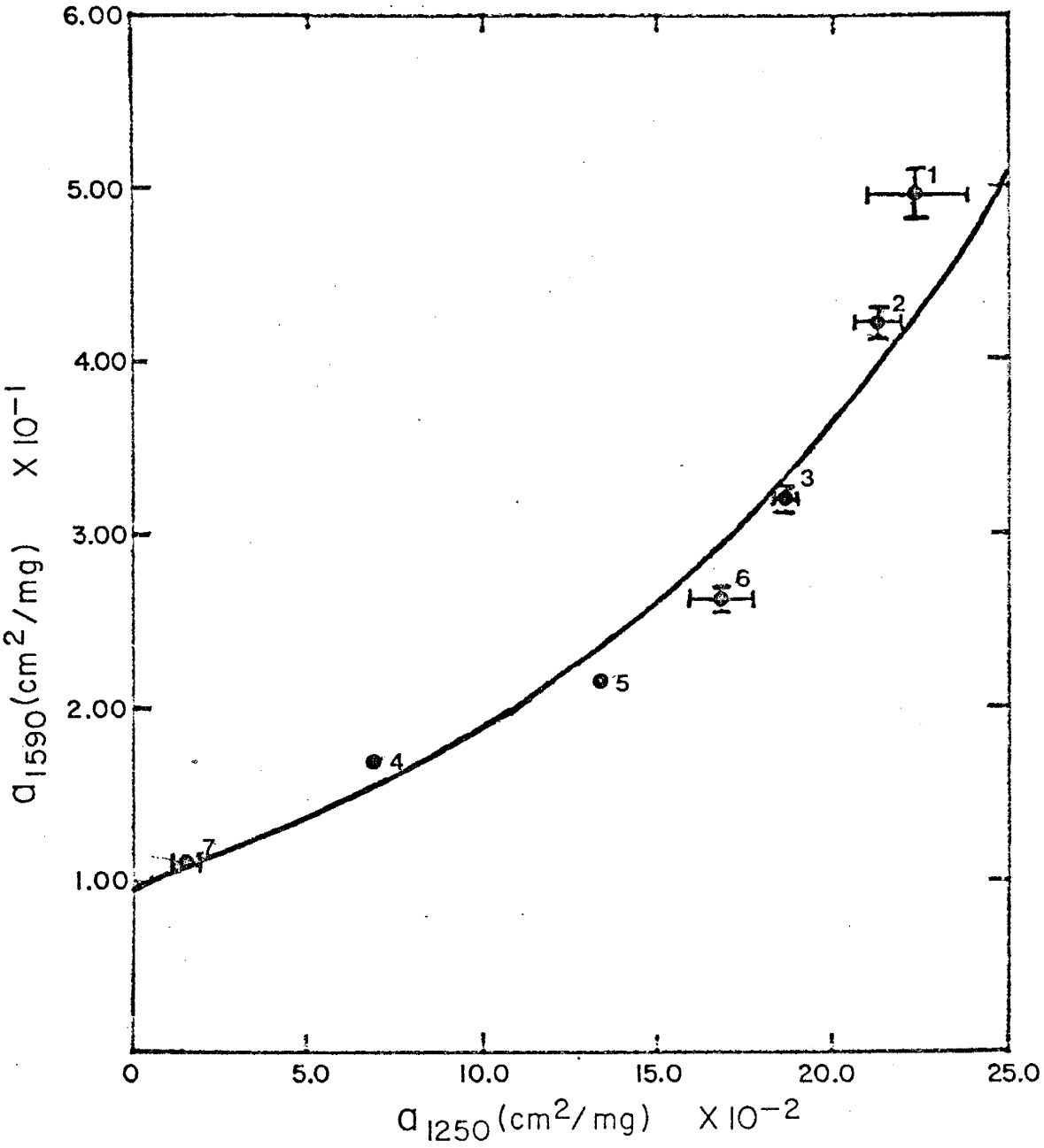

Figure 64. Plot of mean absorptivity values at 1590 cm-1 against mean absorptivity values at 1250 cm-1 for Coals 1-7. Vertical and horizontal bars indicate the sample standard deviation.

Absorptivity at 1700 cm^{-1} versus Absorptivity at 1590 cm^{-1}

The plot of absorptivity at 1700 cm^{-1} as a function of absorptivity at 1590 cm^{-1}, Figure 65, shows that the 1590 cm^{-1} absorptivity decreases correspond to decreasing absorptivity at 1700 cm^{-1} as rank increases. The rectilinear correlation line describing the relationship between the 1700 and 1590 cm^{-1} absorptivities in Figure 65 is defined as $a_{1590} = 0.858(a_{1700}) + 0.200$ with a correlation coefficient of 0.937. Extrapolation of the correlation line to the ordinate, i.e. 1700 cm^{-1} absorptivity = 0.0000 cm^2/mg, yields a 0.2000 cm^2/mg absorptivity for the 1590 cm^{-1} band. As shown in Figure 65, Coal 4 has a 1590 cm^{-1} absorptivity of 0.1676 cm^2/mg, which suggests that the extrapolated value of 0.2000 cm^2/mg for the 1590 cm^{-1} band is high. It is the opinion of the author that the true value of the 1590 cm^{-1} absorptivity corresponding to zero absorbance at 1250 cm^{-1} lies between 0.1600 and 0.1000 cm^2/mg in high-rank whole coals. The weak 1700 cm^{-1} absorptivity for Coal 4 (85.77% C, daf) may indicate slight oxidation of Coal 4 has occurred. Nevertheless, the apparent correlation between the 1700 and 1590 cm^{-1} absorptivities suggests that these data are not independent. Note: Coals 5 and 7 exhibit no distinct absorption band at 1700 cm^{-1} (see Fig. 3 and Appendix 3).

Absorptivity at 2955 cm^{-1} versus Absorptivity at 2915 cm^{-1}

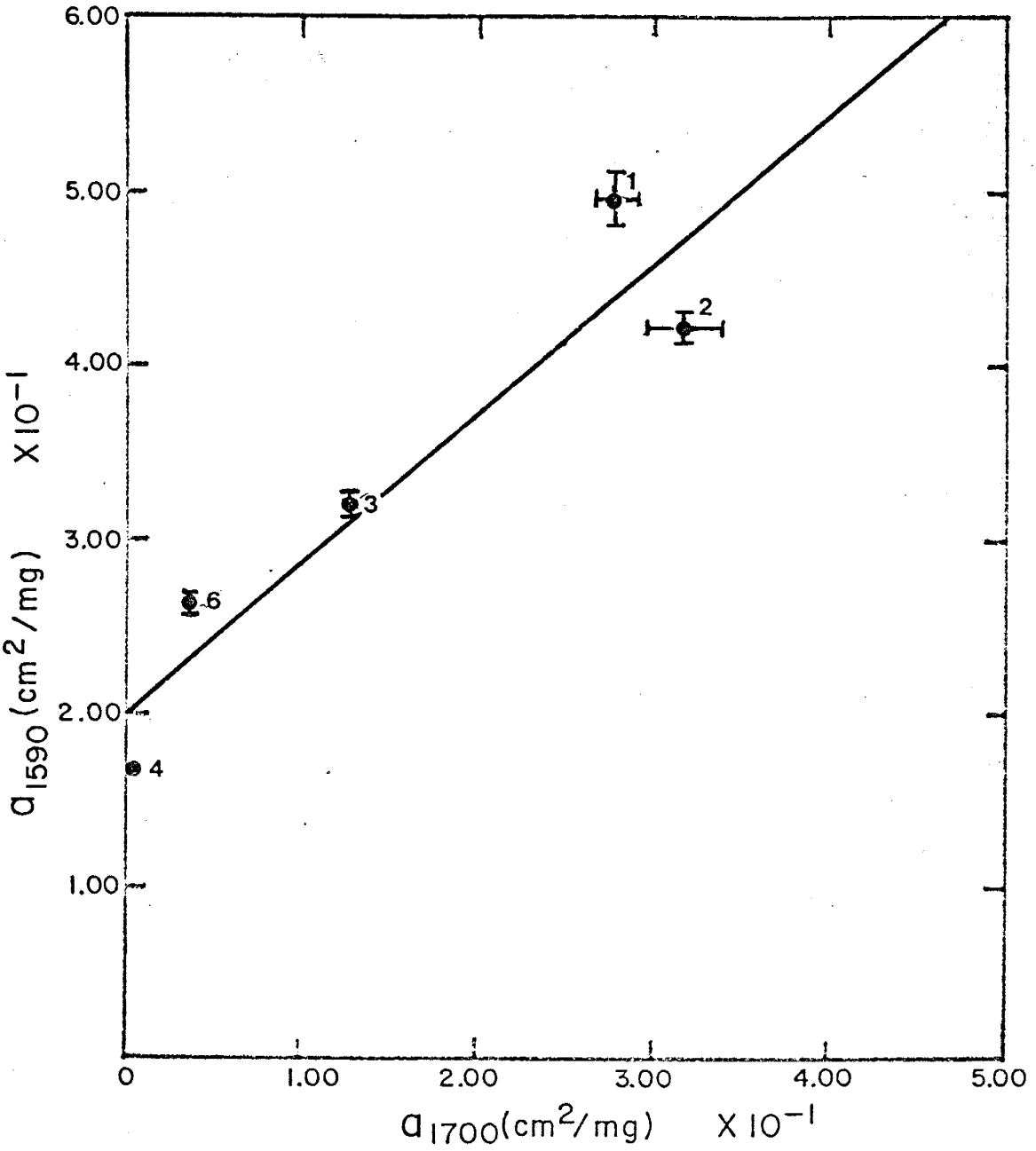

Figure 65. Mean absorptivity values at 1590 cm-1 plotted against mean absorptivity values at 1700 cm-1 for Coals 1-4 and 6. Vertical and horizontal bars represent the sample standard deviation.

The plot of absorptivity at 2955 cm^{-1} as a function of the absorptivity at 2915 cm^{-1}, Figure 66, demonstrates that decreases in absorptivity at 2955 cm^{-1} correspond to decreases in absorptivity at 2915 cm^{-1}. The correlation line in Figure 66, defined by $a_{2955} = 0.443(a_{2915}) + 3.7X10^{-4}$ with a 0.904 correlation coefficient, describes the relationship between the 2955 and 2915 cm^{-1} absorptivities. Extrapolation of the correlation line to the ordinate yields a 0.0004 cm^2/mg absorptivity for the 2955 cm^{-1} band. This value may be due to experimental errors or may reflect the methyl substituents on aromatic nuclei in high-rank whole coals (Durie, 1982). Coals 1 and 7 have similar hydrogen (daf) contents (see Table 3II) and absorptivites for the 2955 cm^{-1} band (see Appendix 4), but differ greatly in rank, i.e. Coal 1 is sub-bituminous B rank and Coal 7 is low volatile bituminous rank. This suggests then that the absorptivities plotted in Figure 66 are a function of hydrogen contents (daf) rather than a reliable indicator of rank. This observed relationship between the 2955 and 2915 cm^{-1} absorptivities suggests that these data are related in some fashion.

Absorptivity at 2955 cm^{-1} versus Absorptivity at 2850 cm^{-1}

Figure 67, the plot of the 2955 cm^{-1} absorptivity as a function of the 2850 cm^{-1} absorptivity, demonstrates that absorptivity decreases at 2850 cm^{-1} correspond to absorptivity decreases at 2955 cm^{-1}. The correlation line in Figure 67, defined by $a_{2850} = 1.382(a_{2955}) + 0.005$

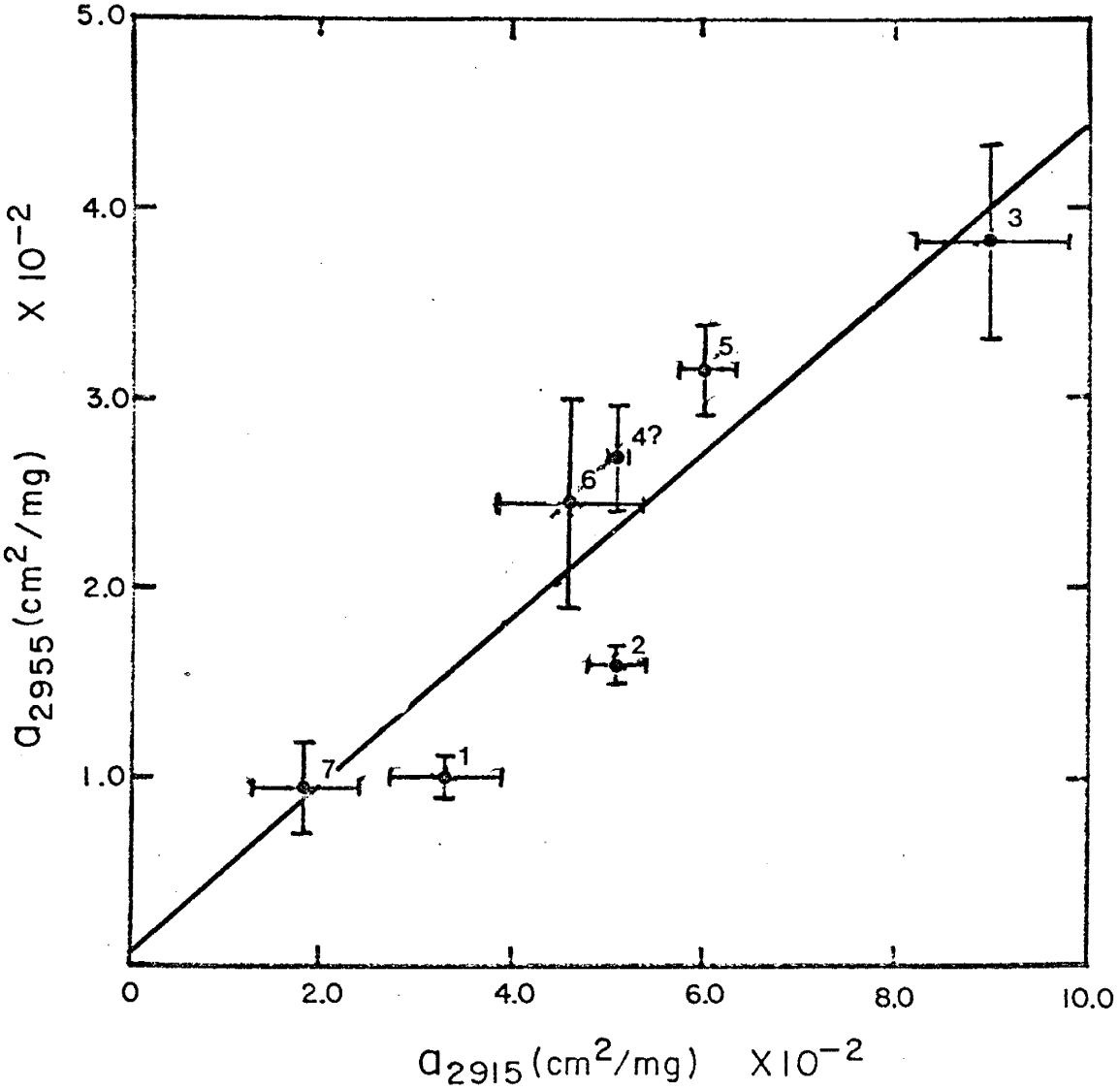

Figure 66. Plot of mean absorptivity values at 2955 cm-1 as a function of mean absorptivity values at 2915 cm-1 for Coals 1-7. Vertical and horizontal bars indicate the sample standard deviation. ? means not confident of mean absorptivity value due to insufficient data.

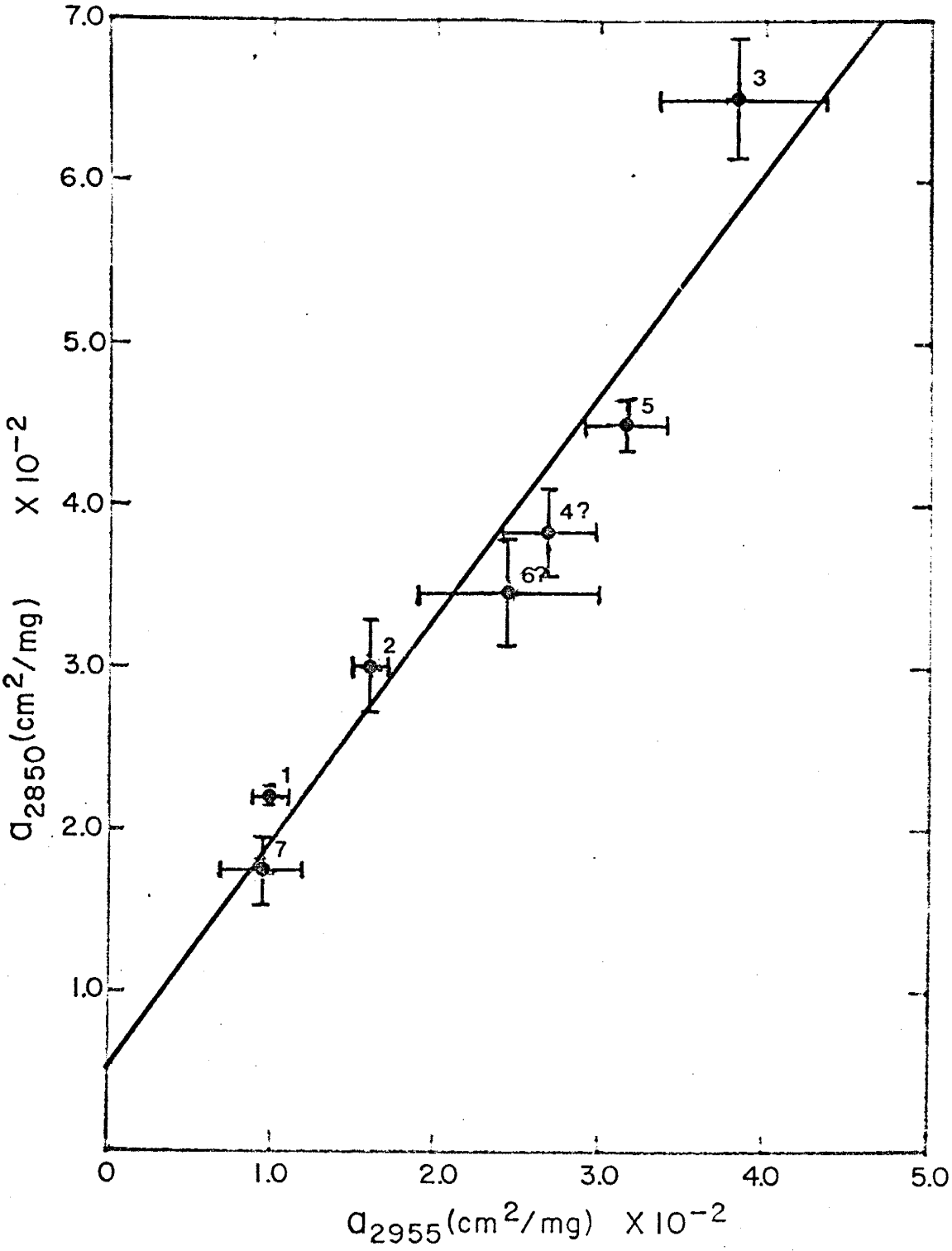

Figure 67. Mean absorptivity values at 2850 cm-1 plotted as a function of mean absorptivity values at 2955 cm-1 for Coals 1-7. Vertical and horizontal bars represent the sample standard deviation. ? means not confident of mean absorptivity value due to insufficient data.

with a 0.962 correlation coefficient, describes the relationship between the 2955 and 2850 cm^{-1} absorptivities. Extrapolation of the correlation line to the ordinate yields a 0.0050 cm^2/mg absorptivity for the 2850 cm^{-1} absorption band. The magnitude of the absorptivity value, determined by extrapolation of the correlation line to the ordinate in Figure 67, tends to suggest that the extrapolated absorptivity value of 0.0004 cm^2/mg for the plot of the 2955 cm^{-1} absorptivity against the 2915 cm^{-1} absorptivity, Figure 66, represents experimental errors. The significant absorptivity at 2850 cm^{-1} in high-rank whole coals that persists as the 2955 cm^{-1} absorptivity approaches zero suggests that the deformational modes responsible for the 2850 cm^{-1} band represent methylene and ethylene cross-linkages in the complex heterogenous cross-linked polymeric structural network of high-rank whole coals. As is the case for Figure 66, Figure 67 illustrates that the relationship between the 2955 and 2850 cm^{-1} absorptivities is a function of hydrogen content (daf) rather than rank. The good correlation between the 2955 and 2850 cm^{-1} absorptivities suggests that the data are not independent but related in some fashion.

Absorptivity at 1440 cm^{-1} versus Absorptivity at 1375 cm^{-1}

Plotting absorptivity at 1440 cm^{-1} as a function of the 1375 cm^{-1} absorptivity, Figure 68, illustrates that the 1375 cm^{-1} absorptivity decreases correspond to decreasing 1440 cm^{-1} absorptivities as rank increases. The relationship between the 1440 and 1375 cm^{-1}

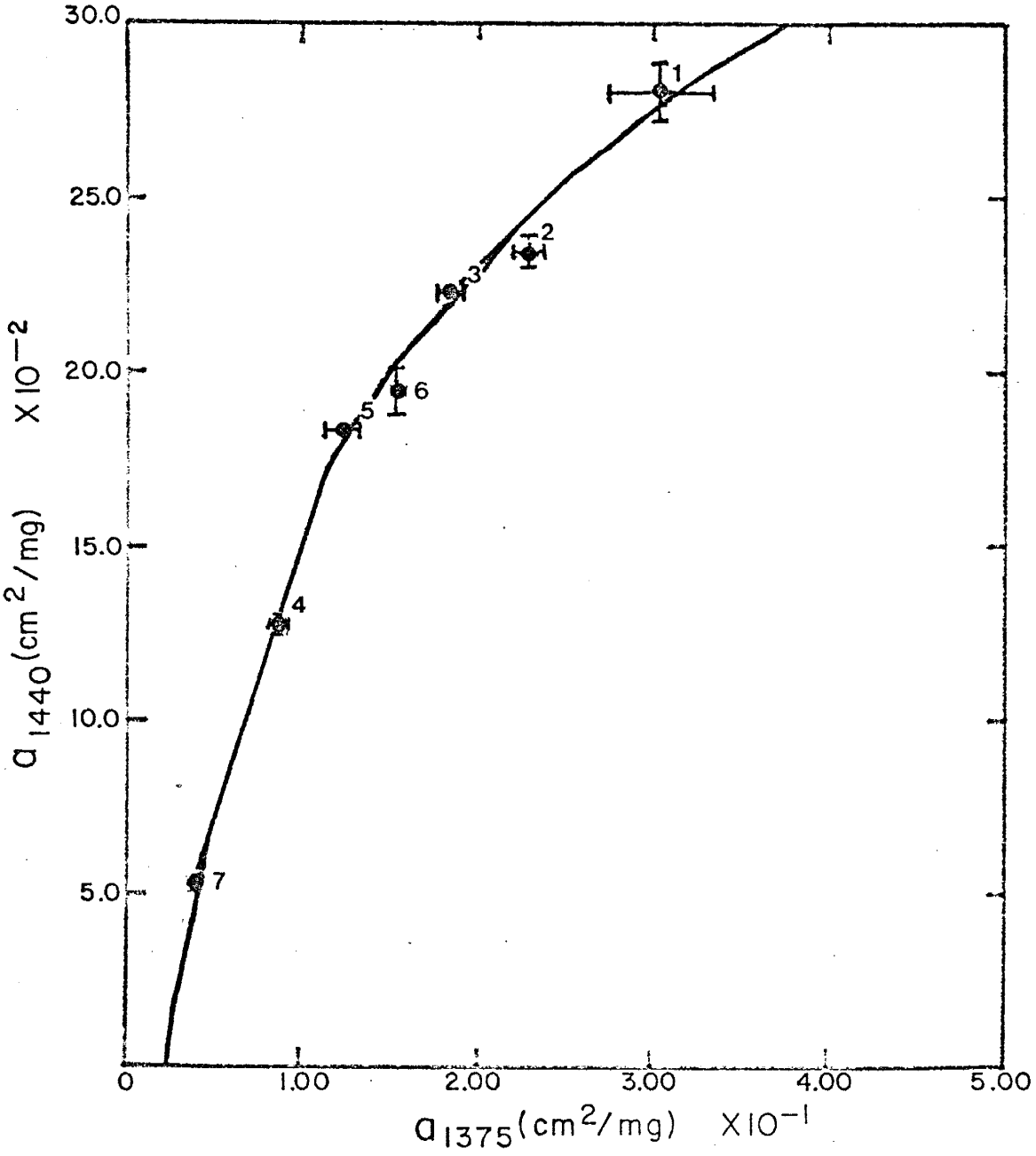

Figure 68. Mean absorptivity values at 1440 cm-1 plotted against mean absorptivity values at 1375 cm-1 for Coals 1-7. Vertical and horizontal bars represent the sample standard deviation.

absorptivities in Figure 68 is described by a logarithmic correlation line, defined by $a_{1440} = 0.1131\ln(a_{1375}) + 0.409$ with a correlation coefficient of 0.953. Extrapolation of the correlation line to the abscissa yields a 0.0267 cm^2/mg absorptivity for the 1375 cm^{-1} absorption band. This significantly high 1375 cm^{-1} absorptivity may in part represent experimental errors and in part reflect the methyl substituents on the aromatic nuclei (Durie, 1982). The correlation shown in Figure 68 suggests that not all of these data are independent.

It is interesting to note that the plot of the 1440 cm^{-1} absorptivity against the 1375 cm^{-1} absorptivity is a function of rank rather than hydrogen content (daf) as is the case for the plots of absorptivities at 2955 and 2915 cm^{-1} (Fig. 66), and 2955 and 2850 cm^{-1} (Fig. 67).

Absorptivity at 795 cm^{-1} versus Absorptivity at 740 cm^{-1}

Figure 69, the 795 cm^{-1} absorptivity plotted as a function of the 740 cm^{-1} absorptivity, illustrates that increases in the 740 cm^{-1} absorptivity correspond to increases in the 795 cm^{-1} absorptivity as rank increases. The correlation line describing the relationship between the 795 and 740 cm^{-1} absorptivities in Figure 69 is defined by $a_{1440} = 0.017\ln(a_{740}) + 0.090$ with a 0.897 correlation coefficient. Extrapolation of the correlation line to the abscissa, i.e. 795 cm^{-1} absorptivity = 0.0000 cm^2/mg, yields a 0.0044 cm^2/mg absorptivity for

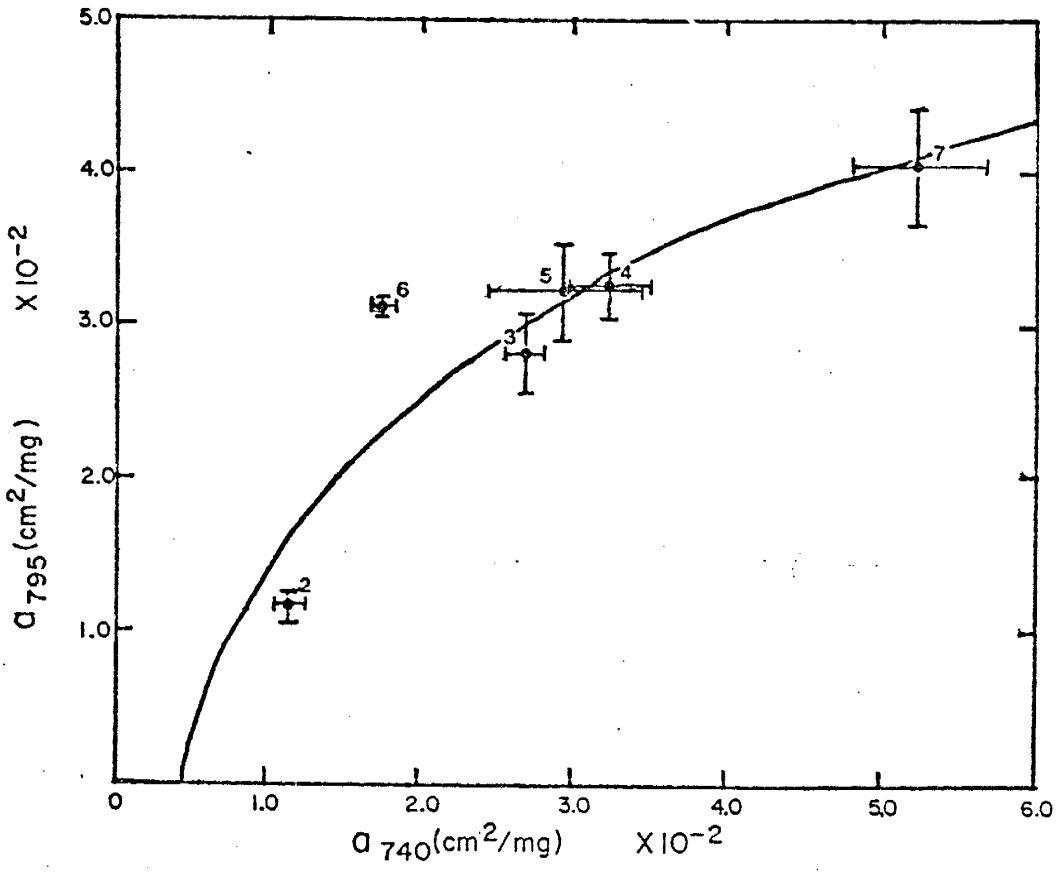

Figure 69. Mean absorptivity values at 795 cm-1 plotted as a function of mean absorptivity values at 740 cm-1 for Coals 2-7. Vertical and horizontal bars indicate the sample standard deviation.

the 740 cm^{-1} band. This observed relationship between the 795 and 740 cm^{-1} absorption bands suggest that these data are not independent but related in some fashion. Note: Coal 1 exhibits no discrete absorption band at 795 and 740 cm^{-1} (see Fig. 3 and Appendix 3).

Absorptivity at 1440 cm^{-1} versus Absorptivity at 740 cm^{-1}

Plotting the 1440 cm^{-1} absorptivity as a function of the 740 cm^{-1} absorptivity, Figure 70, demonstrates that the 1440 cm^{-1} absorptivity decreases with increases in the 740 cm^{-1} absorptivity as rank increases. The correlation line in Figure 70, defined by $a_{1440} = 0.2943 - 4.4015(a_{740})$ with a -0.915 correlation coefficient, describes the inverse relationship between the 1440 and 740 cm^{-1} absorptivities. Extrapolation of the correlation line to the ordinate, i.e. the 740 cm^{-1} absorptivity = 0.0000 cm^2/mg, yields a 0.2943 cm^2/mg absorptivity for the 1440 cm^{-1} band, whereas extrapolating the correlation line to the abscissa yields a 0.0669 cm^2/mg absorptivity for the 740 cm^{-1} band. The observed relationship between the 1440 and 740 cm^{-1} bands suggests that the data are not independent.

Absorptivity at 1590 cm^{-1} versus Absorptivity at 795 cm^{-1}

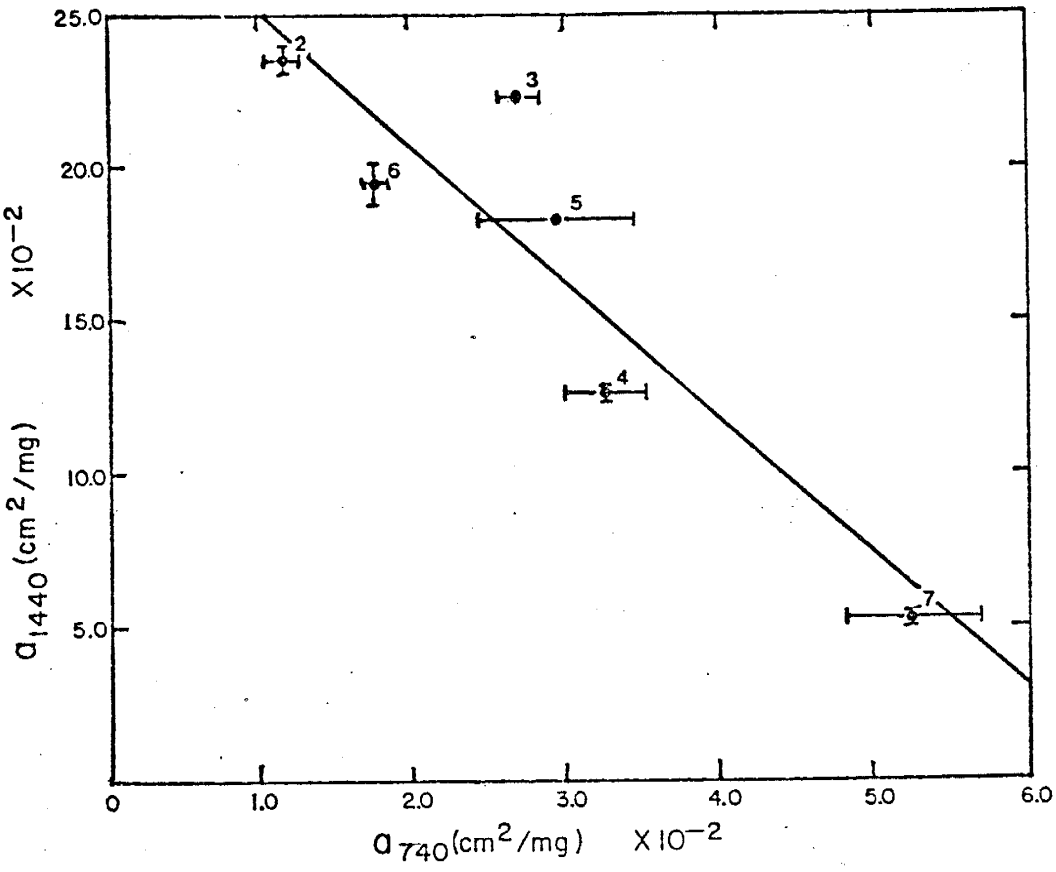

Figure 70. Plot of mean absorptivity values at 1440 cm-1 against mean absorptivity values at 740 cm-1 for Coals 2-7. Vertical and horizontal bars represent the sample standard deviation.

The plot of the 1590 cm^{-1} absorptivity as a function of the 795 cm^{-1} absorptivity, Figure 71, illustrates that decreasing 1590 cm^{-1} absorptivities correspond to increasing 795 cm^{-1} absorptivities as rank increases. The correlation line in Figure 71, defined by $a_{1590} = 0.565 - 10.808(a_{795})$ with a -0.940 correlation coefficient, characterizes the inverse relationship between the 1590 and 795 cm^{-1} absorptivities as a function of rank. Extrapolation of the correlation line to the ordinate yields a 0.5650 cm^2/mg absorptivity for the 1590 cm^{-1} band. The apparent relationship between the 1590 and 795 cm^{-1} bands suggests that these data are not independent but related in some fashion.

Painter et al. (1981b) assigned the 785 cm^{-1} band to methylene rocking modes, i.e. two-adjacent CH_2 units. If this assignment is correct for the 795 cm^{-1} band in this study, then in the context of what is known of the structure of whole coal it is difficult to explain the apparent increase in the 795 cm^{-1} intensity which attends increasing rank (see Fig. 56). Painter et al. (1981b) state, "... the intensity of the 830 cm^{-1} mode shows only a minor increase as a function of rank (as does the 785 cm^{-1} band)." The results obtained for the 795 cm^{-1} band (see Fig. 56) in this study are not consistent with those reported by Painter et al. (1981b). The data in this study illustrate that the 1590 (Fig. 43) and 740 cm^{-1} (Fig. 53) band intensity change as a function of rank (as does the 795 cm^{-1} band, Figure 56). The observed relationship between the 1590 and 795 cm^{-1} absorptivities tends to suggest that if the 795 cm^{-1} band results from aromatic CH out-of-plane

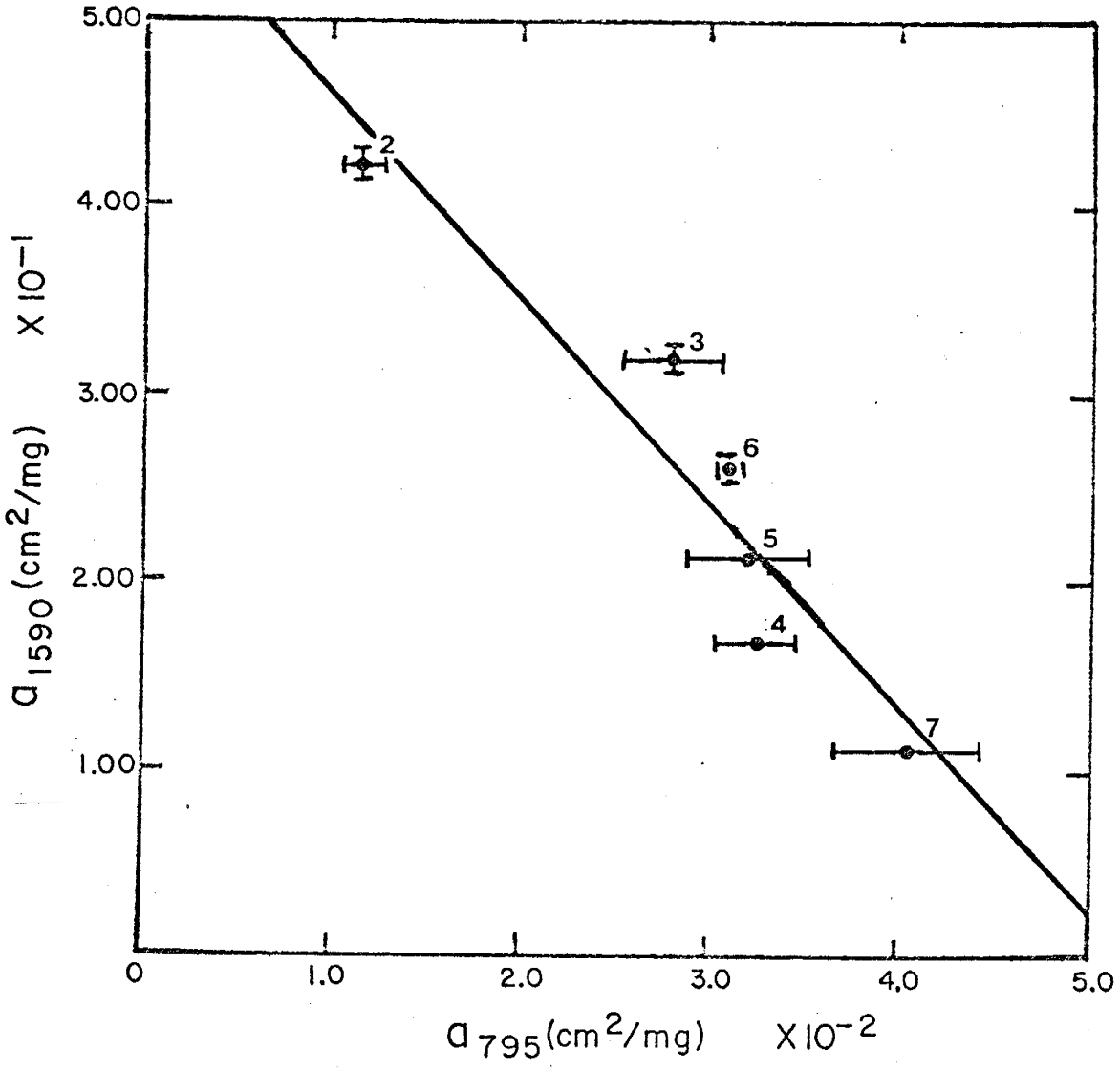

Figure 71. Mean absorptivity values at 1590 cm-1 plotted against mean absorptivity values at 795 cm-1 for Coals 2-7. Vertical and horizontal bars indicate the sample standard deviation.

bending modes, i.e. 2 and 3 neighboring aromatic hydrogen, then this would be more compatible with what is known of the structure of whole coal.

CONCLUSIONS

The observations described above confirm the usefulness of the sort of functional group analysis provided by the qualitative and quantitative interpretation of the infrared spectra of whole coals. Much information on the chemical and structural character of whole coals is gained when data provided by infrared spectrophotometry is considered as a whole for a series of whole coals. Qualitative analysis of infrared spectra provides information on the general quality of organic and mineral components of whole coal. Some of the information gained from the qualitative analysis of the infrared spectra includes structural information on the types of oxygen-containing functional groups in the whole coal. For whole coals of the same rank or different rank, the absorptivity, here defined as ac_s, provides an index of variations in the number of various chemical bonds. The change in absorptivity within the same coal bed or in the same part of a particular basin is a measure of important differences in the coal structure and composition. The results of this study show that when comparing a series of whole coal, quantitative infrared spectroscopy is a powerful tool for providing information on major functional group evolution in complex organic materials. The absorptivity at a particular frequency plotted as a function of the absorptivity at a different frequency for a series of whole coals demonstrates that many modes vary in a systematic fashion with rank. Consequently, much of the data set is not independent but related in some fashion.

The correlations shown for the plots of absorptivity at a particular frequency as a function of other parameters in this study generally are consistent with trends established for the maturation of terrestrial organic matter reported by others. Thus a study of the infrared spectra does not provide entirely new data concerning a special molecular configuration of whole coal; the results mainly confirm the findings established by other analytical methods and previous infrared work on coals.

Infrared spectroscopy is suitable for fast, on-line coal characterization. The chemical and structural information provided by the analysis of the infrared spectra of whole coals could be used by industry and government to rapidly characterize commercially important characteristics of whole coals permitting optimum utilization of each coal.

REFERENCES CITED

Alpert, N. L., Keiser, W. E., and Szymanski, H. A., 1970. IR-Theory and Practice of Infrared Spectroscopy. 2nd ed. Plenum Press, New York.

Bellamy, L. J., 1958. The Infrared Spectra of Complex Molecules. Methuen and Co. Ltd., London.

Bent, R., and Brown, J. K., 1961. The infra-red spectra of macerals. Fuel, v. 40, no. 1, pp 47-56.

Bent, R., Joy, W. K., and Ladner, W. R., 1964. An estimate of the methyl groups in coals and coal derivatives. Fuel, v. 43, no. 1, pp 5-12.

Brown, J. K., 1955. The infrared spectra of coals. J. Chem. Soc. (London), pp 744-752.

Brown, J. K., and Hirsch, P. B., 1955. Recent infra-red and X-ray studies of coal. Nature, v. 175, no. 4449, pp 229-233.

Cannon, C. G., 1953. Infra-red spectra of coals and coal products. Nature, v. 171, p. 308.

Cannon, C. G., and Sutherland, G. B. B. M., 1945. The infra-red absorption spectra of coals and coal extracts. Trans. Faraday Society, v. 41, pp 279-288.

Colthump, N. B., Daly, L. H., and Wiberley, S. E., 1964. Introduction to Infrared and Raman Spectroscopy. Academic Press, New York. 523p.

Conley, R. T., 1972. Infrared Spectroscopy. 2nd ed. Allyn and Bacon, Inc., Boston. 355p.

Czuchajowski, L., and Lawson, G. J., 1963. The infra-red spectra of some polycondensates derived from hydroxyquinones and their relation to the 1600 cm^{-1} band shown by coals. Fuel, v. 42, pp 131-140.

de Ruiter, E., and Tschamler, H., 1966. Brennstoff-Chemie, v. 47, p. 52.

Dorrence, S. M., Barbour, F. A., and Petersen, J. C., 1974. Direct evidence of ketones in oxidized asphalts. Anal. Chem., v. 46, no. 14, p. 2242.

Drushel, H. V., Ellerbe, J. S., Cox, R. C., and Lane, L. H., 1968. Monomer sequence distribution in ethylene-propylene copolymers by computer analysis of infrared spectra. Anal. Chem., v. 40, no. 2, pp 370-379.

Durand, B. (ed.), 1980. Kerogen--Insoluble Organic Matter from Sedimentary Rocks. Technip, Paris. 519p.

Durand, B., and Nicaise, G., 1980. Procedures for kerogen isolation. In: Kerogen--Insoluble Organic Matter from Sedimentary Rocks.

ed. by Bernard Durand. Technip, Paris. pp 35-54.

Durie, R. A., 1982. Coal properties and their importance in the production of liquid fuels--an overview. Fuel, v. 61, pp 883-888.

Durie, R. A., Shewchyk, Y., and Friedel, R. A., 1967. The effect of mild heating on the 1600 cm^{-1} region in the infra-red spectrum of coals. Fuel, v. 46, no. 1, pp 53-58.

Elliott, M. A. (ed.), 1981. Chemistry of Coal Utilization, Second Supplementary Volume. John Wiley and Sons, New York.

Elofson, R. M., 1957. The infrared spectra of humic acids and related materials. Can. J. Chem., v. 35, pp 926-931.

Farmer, V. C., 1974. The Infrared Spectra of Minerals. Mineral. Soc., London.

Francis, S. A., 1951. Intensities of some characteristic infrared bands of ketones and esters. J. of Chemical Physics, v. 19, no. 7, pp 942-948.

Friedel, R. A., 1958. Applied Infrared Spectra of Complex Molecules. Methuen and Co. Ltd., London.

Friedel, R. A., and Carlson, G. L., 1972. Difficult carbonaceous materials and their infrared and Raman spectra. Reassignments for coal spectra. Fuel, v. 51, pp 194-198.

Friedel, R. A., and Queiser, J. A., 1956. Infrared analysis of bituminous coals and other carbonaceous materials. Anal. Chem., v. 28, no. 1, pp 22-30.

Friedel, R. A., and Queiser, J. A., 1966. Infrared and ultraviolet spectrometric techniques and spectra-structure correlations. U.S. Bureau of Mines Bulletin 632, Washington, D.C. 32p.

Friedel, R. A., Retcofsky, H. L., and Queiser, J. A., 1967. Advances in coal spectrometry; absorption spectrometry. U.S. Bureau of Mines Bulletin 640, Washington, D. C. 48p.

Fujii, S., 1963. Infra-red spectra of coal: the absorption band at 1600 cm^{-1}. Fuel, v. 42, no. 1, pp 17-23.

Fujii, S., Osawa, Y., and Sugimura, H., 1970. Infra-red spectra of Japanese coal: the absorption bands at 3030, 2920 and 1600 cm^{-1}. Fuel, v. 49, pp 68-75.

Fujii, S., and Tsuboi, H., 1966. The absorption band at 1600 cm^{-1} in the infra-red spectra of coal--molecular orbital approach. Fuel, v. 45, pp 369-374.

Gordon, E. R., Adams, W. N., and Jenkins, G. J., 1952. Infra-red spectra of coals. Nature, v. 170, p. 317.

Kuehn, D. W., Snyder, R. W., Davis, A., and Painter, P. C., 1982. Characterization of vitrinite concentrates. 1. Fourier Transform infrared studies. Fuel, v. 61, pp 682-694.

Larsen, J. W., and Kovac, J., 1978. Polymer structure of bituminous coals. In: Organic Chemistry of Coal. ed. by John W. Larsen. Am. Chem. Soc., Symposium Series 71, Washington, D. C. pp 36-49.

Lowry, H. H. (ed.), 1963. Chemistry of Coal Utilization, Supplementary Volume. John Wiley and Sons, New York. p. 74.

Mazumdar, B. K., 1972. Hydrogen in coal: Part 1. Genetic and structural development. Fuel, v. 51, pp 284-289.

Murchison, D. G., 1966. Infrared spectra of resinites and their carbonized and oxidized products. In: Coal Science ed. by Peter H. Given. Am. Chem. Soc., Adv. Chem. Ser. 55, Washington, D. C. pp 307-331.

Murchison, D. G., 1976. Resinite: its infrared spectrum and coalification pattern. Fuel, v. 55, no. 1, pp 78-83.

Murray, J. B., and Evans, D. G., 1972. The brown-coal/water system: Part 3. Thermal dewatering of brown coal. Fuel, v. 51, no. 4, pp 290-295.

Oberlin, A., Boulmier, J. L., and Durand, B., 1974. Electron microscope investigation of the structure of naturally and artificially metamorphosed kerogen. Geochim. Cosmochim. Acta, v. 38, pp 647-650.

Oberlin, A., Boulmier, J. L., and Villey, M., 1980. Electron micro-

scopic study of kerogen microtexture. Selected criteria for determining the evolution path and evolution stage of kerogen. In: Kerogen--Insoluble Organic Matter from Sedimentary Rocks. ed. by Bernard Durand. Technip, Paris. pp 191-241.

Orchin, M., Golumbic, C., Anderson, J. E., and Storch, H. H., 1951. Studies of the extraction and coking of coal, and their significance in relation to its structure. U.S. Bureau of Mines Bulletin 505, Washington, D. C.

Oth, J. F. M., and Tschamler, H., 1963. Aliphatic hydrogen distribution in a vitrinite and its extraction products. Fuel, v. 42, pp 467-478.

Osawa, Y., and Shih, J. W., 1971. Infra-red spectra of Japanese coal: the absorption bands at 3450 and 1260 cm^{-1}. Fuel, v. 50, pp 53-57.

Painter, P. C., and Coleman, M. M., 1979. Application of Fourier transform infrared spectroscopy to the characterization of fractionated coal liquids. Fuel, v. 58, pp 301-308.

Painter, P. C., Snyder, R. W., Starsinic, M., Coleman, M. M., Kuehn, D. W., and Davis, A., 1981a. Concerning the application of FT-IR to the study of coal: A critical assessment of band assignments and the application of spectral analysis programs. Appl. Spectrosc., v. 35, no. 5, pp 475-485.

Painter, P. C. et al., 1981b. Recent FT-IR and ^{13}C NMR studies of coal structure. A joint study performed by The Pennsylvania State University and Case Western Reserve University. 88 p.

Pierron, E. D., Rees, O. W., and Clark, G. L., 1959. Plastic properties of coal. Illinois State Geol. Survey, Circ. No. 269, 36p.

Potts, Jr., W. J., 1963. Chemical Infrared Spectroscopy. John Wiley and Sons, New York.

Rao, C. N. R., 1963. Chemical Applications of Infrared Spectroscopy. Academic Press.

Rao, M. S., Gupta, P. L., Kaiser, F., and Lahiri, A., 1962. The assignment of the 1600 cm^{-1} band in the infra-red spectrum of coal. Fuel, v. 41, no. 5, pp 417-423.

Robin, P. L., and Rouxhet, P. G., 1976. Contribution of molecular water in the infrared spectra of kerogens and coals. Fuel, v. 55, no. 7, pp 177-183.

Rouxhet, P. G., and Robin, P. L., 1978. Infrared study of the evolution of kerogens of different origins during catagensis and pyrolysis. Fuel, v. 57, pp 533-540.

Rouxhet, P., Robin, P. L., and Nicaise, G., 1980. Characterization of kerogens and of their evolution by infrared spectroscopy. In: Kerogen--Insoluble Organic Matter from Sedimentary Rocks. ed. by Bernard Durand. Technip, Paris. pp 163-190.

Rouxhet, P. G., Villey, M., and Oberlin, A., 1979. Infrared study of the pyrolysis products of sporopollenin and lignite. Geochim. Cosmochim. Acta, v. 43, no.11, pp 1705-1713.

Roy, M. M., 1957. Infrared spectra of coal and coal extracts. Fuel, v. 36, no. 2, pp 249-250.

Siskov, G. D., and Petrova, R., 1974. Infrared spectra of coal macerals separated from Bulgarian lignites. Fuel, v. 53, pp 236-239.

Smith, A. L., 1979. Applied Infrared Spectroscopy. John Wiley and Sons, New York. 322p.

Smith, J. W., 1961. Ultimate composition of organic material in Green River oil shale. U.S. Bureau of Mines, Rept. of Invest. 5725, Washington, D. C.

Solomon, J. A., and Mains, G. J., 1977. A mild, protective and efficient procedure for grinding coal: cryocrushing. Fuel, v. 56, pp 302-304.

Solomon, P. R., 1981. Coal structure and thermal decomposition. In: New Approaches in Coal Chemistry. ed. by Bernard D. Blaustein, Bradley C. Bockrath, and Sidney Friedman. Am. Chem. Soc., Symposium Series 169, Washington, D. C. pp 61-71.

Solomon, P. R., and Carangelo, R. M., 1982. FTIR analysis of coal. 1. Techniques and determination of hydroxyl concentrations.

Fuel, v. 61, pp 663-669.

Solomon, P. R., and Miknis, F. P., 1980. Use of Fourier transform infrared spectroscopy for determining oil shale properties. Fuel, v. 59, pp 893-896.

Tissot, B. P., and Welte, D. H., 1978. Petroleum Formation and Occurrence. Springer-Verlag, New York. 538p.

Van der Marel, H. W., and Beutelspacher, H., 1976. Atlas of Infrared Spectroscopy of Clay Minerals and Their Admixtures. Elsevier, Amsterdam.

van Vucht, H. A., Rietveld, B. J., and van Krevelan, D. W., 1955. Chemical structure and properties of coal VIII--infrared absorption spectra. Fuel, v. 34, no. 1, pp 50-59.

Whitehurst, D. D., 1978. A primer on the chemistry and constitution of coal. In: Organic Chemistry of Coal. ed. by John W. Larsen. Am. Chem. Soc., Symposium Series 71, Washington, D. C. pp 1-35.

Appendix 1

Data for Whole Coal-$K_3Fe(CN)_6$-KBr Pellets of This Study

Sample Number	Specimen Number	Pellet Weight (mg)	Measured Pellet Thickness (cm)	Coal Weight in Pellet (mg)	K Fe(CN) Weight in Pellet (mg)	KBr Weight in Pellet (mg)	Weight Ratio KBr to Coal
Coal 1	DT 47772	103.3	0.0305	1.471	0.527	101.3	68.86
		76.2	0.0223	1.085	0.389	74.7	68.85
Coal 2	DT 42771	115.2	0.0337	1.026	0.931	113.2	110.36
		106.2	0.0319	0.946	0.858	104.4	110.36
Coal 3	DT 418771-A	71.7	0.0215	0.551	0.276	70.9	128.68
		83.8	0.0254	0.644	0.322	82.8	128.57
Coal 4	Nm-Im	107.1	0.0324	1.226	0.683	105.2	85.81
		118.2	0.0363	1.354	0.754	116.1	85.75
Coal 5	C-80	102.5	0.0296	0.939	0.616	101.0	107.56
		100.9	0.0306	0.925	0.607	99.4	107.46
Coal 6	C-16	132.2	0.0410	1.350	0.675	130.2	96.44
		93.5	0.0287	0.955	0.477	92.1	96.44
Coal 7	DT 46772	116.1	0.0348	1.214	0.580	114.3	94.15
		101.6	0.0312	1.063	0.508	100.0	94.07
		97.3	0.0298	1.018	0.486	95.8	94.11

Appendix 2

Data for Demineralized Coal-KBr Pellets of This Study

Sample Number	Specimen Number	Pellet Weight (mg)	Measured Pellet Thickness (cm)	Coal Weight in Pellet (mg)	KBr Weight in Pellet (mg)	Weight Ratio KBr to Coal
Coal 1	DT 47772	155.5	0.0437	1.491	154.0	103.29
Coal 2	DT 42771	121.4	0.0361	1.665	119.7	71.89
Coal 3	DT 418771-A	132.3	0.0392	2.228	130.1	58.39
Coal 4	Nm-Tm	94.0	0.0273	1.344	92.7	68.97
Coal 5	C-80	121.2	0.0366	1.610	119.6	74.29
Coal 6	C-16	102.9	0.0307	0.855	102.0	119.30
Coal 7	DT 46772	95.6	0.0273	0.731	94.9	129.82

Appendix 3

Measured Absorptivities (cm^2/mg) Normalized to a Common Baseline

Sample							
Coal 1	Coal 2	Coal 3	Coal 4	Coal 5	Coal 6	Coal 7	cm^{-1}
0.0527	0.0530	0.0564	0.0176	0.0269	0.0164	0.0057	
0.0527	0.0530	0.0532	0.0148	0.0222	0.0223	0.0049	
0.0754	0.0539	0.0445	0.0164	0.0230	0.0272	0.0067	
0.0754	0.0554	0.0418	0.0124	0.0286	0.0328	0.0091	
0.0501	0.0459	0.0677	0.0191	0.0390	0.0132	0.0011	3400**
0.0825	0.0594	0.0390	0.0055	0.0210	0.0375	0.0078	
						0.0027	
						0.0001	
						0.0103	
0.0784	0.1136	0.0677	0.0206	0.0322	0.0216	0.0114	
0.0778	0.1123	0.0629	0.0234	0.0287	0.0318	0.0079	
0.1111	0.1215	0.0569	0.0196	0.0278	0.0375	0.0132	
0.1083	0.1245	0.0528	0.0151	0.0314	0.0431	0.0067	
0.1207	0.1315	0.0513	0.0106	0.0400	0.0456	0.0129	3400"+
0.0771	0.1000	0.0821	0.0349	0.0257	0.0191	0.0129	
						0.0095	
						0.0043	
						0.0140	
0.0129			0.0121	0.0202	0.0179	0.0108	
0.0137			0.0107	0.0175	0.0159	0.0108	
0.0253			0.0134	0.0161	0.0172	0.0092	
			0.0142	0.0140	0.0129	0.0109	
			0.0035	0.0224	0.0243	0.0129	3040
						0.0104	
						0.0129	
						0.0150	
						0.0061	
0.0112	0.0149	0.0453	0.0302	0.0284	0.0288	0.0129	
0.0096	0.0166	0.0361	0.0252	0.0339	0.0182	0.0081	
0.0091	0.0166	0.0387	0.0254	0.0326	0.0261	0.0109	
0.0137	0.0145	0.0334		0.0316		0.0085	2955
0.0076	0.0219	0.0484		0.0261		0.0070	
		0.0322		0.0339		0.0047	
						0.0179	

0.0323	0.0489	0.0990	0.0519	0.0601	0.0458	0.0143	
0.0275	0.0506	0.0862	0.0505	0.0591	0.0359	0.0206	
0.0365	0.0502	0.0876	0.0504	0.0639	0.0460	0.0124	
0.0365	0.0540	0.0876	0.0518	0.0590	0.0488	0.0235	
0.0380	0.0463	0.0779	0.0556	0.0524	0.0516	0.0179	2915
0.0275	0.0540	0.1007	0.0483	0.0679	0.0306	0.0228	
						0.0179	
						0.0108	
						0.0245	
0.0228	0.0352	0.0703	0.0344	0.0431	0.0293	0.0122	
0.0210	0.0251	0.0687	0.0351	0.0478	0.0313	0.0171	
0.0214	0.0290	0.0614	0.0423	0.0431	0.0396	0.0202	
0.0223	0.0309	0.0587	0.0410	0.0456	0.0378	0.0164	
0.0210	0.0386	0.0521	0.0438	0.0610	0.0396	0.0164	2850
0.0246	0.0246	0.0782	0.0337	0.0409	0.0255	0.0203	
						0.0146	
						0.0102	
						0.0262	
0.2875	0.3307	0.1320	0.0074		0.0378		
0.2784	0.3180	0.1272	0.0067		0.0388		
0.2737	0.3067	0.1289	0.0061		0.0287		
0.2812	0.3269	0.1276	0.0078		0.0553		1700
0.2618	0.3321	0.1216	0.0047				
0.2941	0.3053	0.1329					
	0.3379	0.1908	0.0388	0.0384		0.0226	
	0.3255	0.1909		0.0384		0.0255	
	0.3250	0.1723		0.0428		0.0319	
	0.3419	0.1754		0.0475		0.0258	
		0.1662		0.0475		0.0321	1660
		0.1997		0.0366		0.0154	
						0.0296	
						0.0323	
						0.0109	
0.4984	0.4263	0.3262	0.1712	0.2126	0.2594	0.1104	
0.4731	0.4144	0.3221	0.1692	0.2113	0.2616	0.1069	
0.4974	0.4148	0.3164	0.1658	0.2134	0.2678	0.1156	
0.5092	0.4288	0.3092	0.1640	0.2147	0.2545	0.1061	
0.5232	0.4421	0.3073	0.2007	0.2096	0.2774	0.1110	1590+
0.4354	0.3894	0.3281	0.1596	0.2163	0.2363	0.1153	
						0.1084	
						0.1202	
						0.1005	

0.2829	0.2374	0.2231	0.1265	0.1812	0.1935	0.0494	
0.2694	0.2314	0.2195	0.1292	0.1823	0.2002	0.0502	
0.2787	0.2305	0.2244	0.1273	0.1828	0.1981	0.0554	
0.2902	0.2394	0.2228	0.1233	0.1851	0.1851	0.0548	
0.2554	0.2398	0.2269	0.1217	0.1735	0.2051	0.0531	1440
0.2902	0.2267	0.2131	0.1464	0.1872	0.1768	0.0563	
						0.0545	
						0.0358	
						0.0624	
0.3112	0.2362	0.1819	0.0914	0.1214	0.1554	0.0406	
0.2829	0.2305	0.1847	0.0914	0.1267	0.1571	0.0406	
0.3086	0.2343	0.1878	0.0849	0.1178	0.1525	0.0397	
0.3155	0.2255	0.1816	0.0871	0.1264	0.1547	0.0450	
0.3305	0.2362	0.1944	0.1021	0.1168	0.1658	0.0450	1375
0.2784	0.2207	0.1802	0.0834	0.1299	0.1418	0.0424	
						0.0399	
						0.0365	
						0.0481	
0.2199	0.2195	0.1855	0.0685	0.1353	0.1749	0.0150	
0.2112	0.2091	0.1908	0.0732	0.1353	0.1748	0.0185	
0.2302	0.2095	0.1863	0.0670	0.1329	0.1623	0.0177	
0.2361	0.2169	0.1878	0.0690	0.1340	0.1634	0.0109	
0.2397	0.2058	0.1754	0.0641	0.1264	0.1777	0.0179	1250
0.2046	0.2207	0.1908	0.0805	0.1397	0.1571	0.0147	
						0.0154	
						0.0106	
						0.0186	
0.1724	0.2057	0.1978	0.1045	0.1640	0.1879	0.0480	
0.1639	0.2047	0.1973	0.1119	0.1562	0.1916	0.0435	
0.1764	0.2023	0.1894	0.1052	0.1507	0.1957	0.0465	
0.1858	0.2011	0.1909	0.1068	0.1597	0.1851	0.0431	
0.1901	0.2000	0.1801	0.1298	0.1495	0.2051	0.0456	1165
0.1531	0.2114	0.2014	0.1036	0.1640	0.1723	0.0432	
						0.0441	
						0.0398	
						0.0506	
0.1278	0.1741	0.1732	0.1789	0.1267	0.1598	0.1747	
0.1232	0.1638	0.1692	0.1750	0.1235	0.1607	0.1719	
0.1380	0.1650	0.1723	0.1845	0.1243	0.1468	0.1716	
0.1469	0.1674	0.1740	0.1817	0.1307	0.1547	0.1622	
0.1135	0.1756		0.2045	0.1168	0.1394	0.1673	1090
	0.1616		0.1740	0.1374	0.1658	0.1726	
						0.1651	
						0.1806	
						0.1555	

0.1025	0.1327	0.1421	0.1847	0.1182	0.1189	0.2379	
0.0990	0.1338	0.1404	0.1808	0.1203	0.1173	0.2301	
0.0996	0.1278	0.1437	0.1826	0.1200	0.1224	0.2199	
0.1114	0.1310	0.1362	0.1744	0.1221	0.1215	0.2119	
0.1161	0.1396	0.1491	0.2083	0.1178	0.1287	0.2454	1030
0.0905	0.1278	0.1362	0.1702	0.1235	0.1079	0.2368	
						0.2142	
						0.1974	
						0.2503	
0.0121			0.0061	0.0070	0.0129	0.0185	
			0.0101		0.0060	0.0187	
			0.0053			0.0219	
						0.0211	940
						0.0228	
						0.0171	
						0.0155	
						0.0362	
0.0079	0.0137	0.0135	0.0115		0.0067	0.0427	
0.0079	0.0157	0.0153	0.0115		0.0068	0.0435	
0.0091	0.0130		0.0085		0.0086	0.0381	
0.0091	0.0157		0.0104			0.0356	
0.0137	0.0128		0.0134			0.0441	915
0.0072	0.0185		0.0085			0.0415	
						0.0381	
						0.0348	
						0.0447	
0.0121			0.0115	0.0302	0.0229	0.0291	
			0.0128	0.0251	0.0216	0.0312	
			0.0162	0.0232	0.0217	0.0258	
			0.0147	0.0251	0.0225	0.0235	
			0.0097	0.0321	0.0261	0.0313	870
			0.0210	0.0212	0.0210	0.0313	
						0.0347	
						0.0187	
						0.0355	
	0.0120	0.0299	0.0302	0.0358	0.0313	0.0449	
	0.0122	0.0284	0.0352	0.0302	0.0320	0.0435	
	0.0104	0.0299	0.0324	0.0288	0.0306	0.0381	
		0.0243	0.0319	0.0334	0.0306	0.0365	
		0.0231	0.0302	0.0224	0.0297	0.0424	795
		0.0309	0.0423	0.0403	0.0320	0.0432	
						0.0355	
						0.0348	
						0.0494	

0.0128	0.0256	0.0294	0.0339	0.0172	0.0509	
0.0103	0.0270	0.0352	0.0339	0.0166	0.0547	
0.0112	0.0282	0.0312	0.0251	0.0182	0.0562	
0.0122	0.0255	0.0344	0.0251	0.0182	0.0463	
0.0174	0.0316	0.0274	0.0372	0.0235	0.0506	740
0.0080		0.0352	0.0221	0.0141	0.0502	
					0.0589	
					0.0431	
					0.0589	
		0.0175	0.0158		0.0199	
		0.0155	0.0140		0.0255	
		0.0178			0.0199	
		0.0166			0.0251	
		0.0140			0.0275	685
		0.0266			0.0219	
					0.0279	
					0.0304	
					0.0186	

* = measured according to the 3700-3000 cm^{-1} method.

" = measured according to the Robin-Rouxhet method.

+ = corrected for water absorption associated with the KBr.

Note: Generally, if six absorptivities are measured for each coal sample (on 2 or 3 pellets), two (or one) of the measured absorptivities appear to be too high and/or too low. The anomolously high and/or low measured absorptivities for a particular coal at a given frequency are listed as the last two (or one) values in Appendix 3. The other (generally 4) measured absorptivity values vary slightly from each other. These rather tightly clustered, measured absorptivity values are chosen to be most representative of the coal.

Appendix 4

Arithmetic Mean($\bar{x}$) and Sample Standard Deviation(Sx) of Absorptivities (cm^2/mg) Normalized to a Common Baseline

	Sample							
	Coal 1	Coal 2	Coal 3	Coal 4	Coal 5	Coal 6	Coal 7	cm^{-1}
$\bar{x}$	0.0641	0.0538	0.0490	0.0153	0.0252	0.0247	0.0053	
Sx	0.0131	0.0011	0.0069	0.0022	0.0031	0.0070	0.0028	
$\bar{x}$	0.0648	0.0534	0.0504	0.0143	0.0268	0.0249	0.0053	3400*+
Sx	0.0145	0.0044	0.0108	0.0049	0.0067	0.0094	0.0035	
$\bar{x}$	0.0939	0.1180	0.0601	0.0197	0.0300	0.0335	0.0106	
Sx	0.0183	0.0060	0.0066	0.0034	0.0021	0.0092	0.0026	
$\bar{x}$	0.0956	0.1172	0.0623	0.0190	0.0310	0.0330	0.0103	3400"+
Sx	0.0199	0.0110	0.0115	0.0053	0.0050	0.0109	0.0034	
$\bar{x}$	0.0133			0.0121	0.0179	0.0170	0.0111	
Sx	0.0006			0.0014	0.0021	0.0010	0.0013	
$\bar{x}$	0.0173			0.0118	0.0180	0.0176	0.0110	3040
Sx	0.0069			0.0023	0.0033	0.0042	0.0025	
$\bar{x}$	0.0100	0.0160	0.0384		0.0316		0.0095	
Sx	0.0011	0.0010	0.0051		0.0023		0.0024	
$\bar{x}$	0.0102	0.0169	0.0390	0.0269	0.0311	0.0244	0.0100	2955
Sx	0.0023	0.0030	0.0065	0.0028	0.0032	0.0055	0.0044	
$\bar{x}$	0.0332	0.0509	0.0901	0.0512	0.0605	0.0441	0.0185	
Sx	0.0043	0.0022	0.0060	0.0008	0.0023	0.0057	0.0042	
$\bar{x}$	0.0331	0.0507	0.0898	0.0514	0.0604	0.0431	0.0183	2915
Sx	0.0047	0.0030	0.0086	0.0024	0.0052	0.0081	0.0050	
$\bar{x}$	0.0219	0.0301	0.0648	0.0382	0.0449	0.0345	0.0173	
Sx	0.0008	0.0042	0.0056	0.0040	0.0023	0.0050	0.0032	
$\bar{x}$	0.0222	0.0306	0.0649	0.0384	0.0469	0.0339	0.0175	2850
Sx	0.0014	0.0056	0.0093	0.0045	0.0073	0.0060	0.0049	
$\bar{x}$	0.2802	0.3206	0.1289	0.0067		0.0383		
Sx	0.0058	0.0107	0.0022	0.0007		0.0007		
$\bar{x}$	0.2795	0.3200	0.1284	0.0065		0.0402		1700
Sx	0.0112	0.0119	0.0040	0.0012		0.0111		

$\bar{x}$		0.3317	0.1824		0.0418		0.0261	
Sx		0.0088	0.0099		0.0043		0.0059	
$\bar{x}$		0.3326	0.1826		0.0419		0.0251	1660
Sx		0.0086	0.0131		0.0048		0.0077	
$\bar{x}$	0.4945	0.4211	0.3185	0.1676	0.2130	0.2608	0.1105	
Sx	0.0152	0.0075	0.0074	0.0033	0.0014	0.0055	0.0038	
$\bar{x}$	0.4895	0.4193	0.3182	0.1718	0.2130	0.2595	0.1105	1590+
Sx	0.0312	0.0179	0.0087	0.0148	0.0024	0.0138	0.0059	
$\bar{x}$	0.2803	0.2347	0.2225	0.1266	0.1829	0.1942	0.0534	
Sx	0.0087	0.0044	0.0021	0.0025	0.0016	0.0067	0.0026	
$\bar{x}$	0.2778	0.2342	0.2216	0.1291	0.1820	0.1931	0.0524	1440
Sx	0.0135	0.0054	0.0048	0.0089	0.0047	0.0105	0.0073	
$\bar{x}$	0.3046	0.2316	0.1840	0.0837	0.1231	0.1549	0.0419	
Sx	0.0147	0.0047	0.0029	0.0032	0.0043	0.0019	0.0023	
$\bar{x}$	0.3045	0.2306	0.1851	0.0901	0.1232	0.1546	0.0420	1375
Sx	0.0200	0.0063	0.0053	0.0068	0.0053	0.0078	0.0035	
$\bar{x}$	0.2244	0.2138	0.1876	0.0694	0.1344	0.1689	0.0157	
Sx	0.0110	0.0052	0.0023	0.0027	0.0012	0.0069	0.0026	
$\bar{x}$	0.2236	0.2136	0.1861	0.0704	0.1339	0.1684	0.0155	1250
Sx	0.0141	0.0062	0.0057	0.0058	0.0044	0.0085	0.0031	
$\bar{x}$	0.1746	0.2035	0.1940	0.1071	0.1577	0.1901	0.0449	
Sx	0.0091	0.0021	0.0045	0.0033	0.0056	0.0046	0.0019	
$\bar{x}$	0.1736	0.2042	0.1929	0.1103	0.1574	0.1896	0.0449	1165
Sx	0.0137	0.0041	0.0078	0.0100	0.0063	0.0110	0.0032	
$\bar{x}$	0.1297	0.1676		0.1800	0.1263	0.1555	0.1693	
Sx	0.0076	0.0046		0.0041	0.0032	0.0064	0.0045	
$\bar{x}$	0.1299	0.1679	0.1722	0.1831	0.1266	0.1545	0.1691	1090
Sx	0.0130	0.0057	0.0021	0.0112	0.0070	0.0098	0.0074	
$\bar{x}$	0.1031	0.1313	0.1406	0.1806	0.1202	0.1200	0.2280	
Sx	0.0057	0.0026	0.0032	0.0044	0.0016	0.0023	0.0129	
$\bar{x}$	0.1032	0.1321	0.1413	0.1835	0.1203	0.1195	0.2271	1030
Sx	0.0092	0.0044	0.0049	0.0133	0.0022	0.0069	0.0174	
$\bar{x}$							0.0200	
Sx							0.0022	
$\bar{x}$				0.0072		0.0095	0.0215	940
Sx				0.0026		0.0049	0.0064	
$\bar{x}$	0.0085	0.0145		0.0105			0.0405	
Sx	0.0007	0.0014		0.0014			0.0032	
$\bar{x}$	0.0092	0.0149	0.0144	0.0106		0.0074	0.0403	915
Sx	0.0024	0.0022	0.0013	0.0019		0.0011	0.0038	

$\bar{x}$			0.0138	0.0259	0.0222	0.0296	
Sx			0.0021	0.0030	0.0006	0.0038	
$\bar{x}$			0.0143	0.0262	0.0226	0.0290	870
Sx			0.0040	0.0042	0.0018	0.0054	
$\bar{x}$		0.0281	0.0324	0.0321	0.0311	0.0406	
Sx		0.0026	0.0021	0.0032	0.0007	0.0038	
$\bar{x}$	0.0115	0.0278	0.0337	0.0318	0.0310	0.0409	795
Sx	0.0010	0.0033	0.0046	0.0062	0.0009	0.0050	
$\bar{x}$	0.0116	0.0269	0.0326	0.0295	0.0176	0.0525	
Sx	0.0011	0.0013	0.0027	0.0051	0.0008	0.0043	
$\bar{x}$	0.0120	0.0276	0.0321	0.0296	0.0180	0.0522	740
Sx	0.0031	0.0025	0.0033	0.0062	0.0031	0.0055	
$\bar{x}$			0.0169			0.0240	
Sx			0.0010			0.0034	
$\bar{x}$			0.0180	0.0149		0.0241	685
Sx			0.0044	0.0013		0.0042	

* = measured according to the 3700-3000 cm^{-1} method.
" = measured according to the Robin-Rouxhet method.
+ = corrected for water absorption associated with the KBr.

Note: Each coal in Appendix 4 has two sets of arithmetic mean(x) and sample standard deviation. The first set contains the arithmetic mean and sample standard deviation of those values most representative of the measured absorptivities for a given absorption band in a particular coal. The second set contains the arithmetic mean and sample standard deviation of all the measured absorptivities for a given absorption band in the same coal.

**Generally, the data show there is only a slight difference between the arithmetic mean values for a given absorption band in a particular coal. This suggests that the arithmetic mean of the tightly clustered absorptivity values may be employed to accurately represent the apparent absorptivity of a given absorption band.

$$\text{arithmetic mean} \equiv \bar{x} = \frac{\Sigma n}{n} \tag{3}$$

$$\text{sample standard deviation} \equiv S_x = \left\{\frac{n\Sigma x^2 - (\Sigma x)^2}{n(n-1)}\right\} \tag{4}$$

This formula gives the best estimates of the population standard deviations
from the sample data.